



Published in final edited form as:

*Chem Rev.* 2016 September 14; 116(17): 10035–10074. doi:10.1021/acs.chemrev.6b00018.

## Dual Catalysis Strategies in Photochemical Synthesis

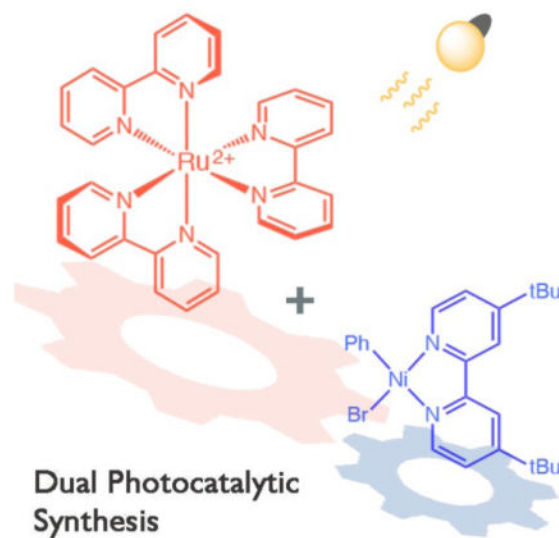
Kazimer L. Skubi, Travis R. Blum, and Tehshik P. Yoon\*

Department of Chemistry, University of Wisconsin–Madison, 1101 University Avenue, Madison, WI, 53706, USA

### Abstract

The interaction between an electronically excited photocatalyst and an organic molecule can result in the generation of a diverse array of reactive intermediates that can be manipulated in a variety of ways to result in synthetically useful bond constructions. This review summarizes dual catalyst strategies that have been applied to synthetic photochemistry. Mechanistically distinct modes of photocatalysis are discussed, including photoinduced electron transfer, hydrogen atom transfer, and energy transfer. We focus upon the cooperative interactions of photocatalysts with redox mediators, Lewis and Brønsted acids, organocatalysts, enzymes, and transition metal complexes.

### Graphical Abstract



### 1. Introduction

Catalysis has played a central role in the development of all major areas of contemporary synthetic chemistry. A remarkably diverse range of catalyst structures, both metal-based and purely organic, have been developed to increase the rate and practicality of important

Corresponding Author: tyoon@chem.wisc.edu.

The authors declare no competing financial interest.

chemical transformations. These entities are capable of providing high levels of control over the stereo- and regioselectivity of complexity-building reactions, and — perhaps most importantly — enabling novel bond constructions that can only be achieved using catalysis.

In the context of synthetic organic photochemistry, photocatalysts play a unique but no less critical role. The interaction of simple organic molecules with light is generally weak. Moreover, electronically excited states are often only available upon irradiation with quite short wavelengths of ultraviolet (UV) light. These high-energy photons can cause uncontrolled photodecomposition processes to occur, a factor that has limited the broad utility of photochemical synthesis in the construction of complex organic molecules. In contrast, photocatalysts are powerfully enabling in synthetic applications because they absorb light with greater efficiency and at longer wavelengths than do simple organic small molecules. These species operate by converting the energy of an absorbed photon into chemical potential that can be used to transform organic substrates in a multitude of ways. Photocatalysis provides a direct means to access the chemistry of reactive intermediates that often cannot readily be generated using other non-photochemical strategies. Thus, many of the most practical synthetic strategies involving radical ions, diradicals, and electronically excited organic compounds rely upon the use of photocatalysts.

An intriguing synergy emerges when photocatalysis is combined with other, non-photochemical catalytic strategies. In these dual-catalyst systems, one catalyst is used to absorb light and activate organic substrates, and a second, independent catalyst species is used to further manipulate the reactivity of the resulting photogenerated intermediates. In the past several years, the synthetic chemistry community's interest in photocatalysis has enjoyed tremendous growth, and one of the most remarkable emerging features in this body of recent literature is the frequency with which dual catalysis approaches are utilized. The purpose of this review is to provide an overview of the ways in which co-catalyst strategies have been applied to synthesis, covering both contemporary developments in organic photochemistry and the important precedents that paved the way for the recent surge of renewed interest in photocatalytic synthesis.

## 1.1 Mechanisms of Photocatalysis

The interaction between an electronically excited photocatalyst and an organic molecule can result in the generation of a diverse array of reactive intermediates. By taking advantage of the distinctive chemistry of each, a wide range of powerful complexity-building synthetic transformations has been developed.<sup>1</sup> To provide a conceptual framework for discussing the impact of co-catalysis on the reactivity of these varied intermediates, we have organized this review around three common photocatalytic activation steps.

First, much of the recent renewal of interest in photochemical synthesis has been based upon the propensity of photoexcited molecules to participate in electron-transfer (or “photoredox”) processes.<sup>2</sup> A molecule in an electronically excited state is both a stronger oxidant as well as a stronger reductant than its ground state analog. Thus, one common class of photochemically initiated reactions involves activation via either a one-electron oxidation or one-electron reduction of an organic substrate by the photocatalyst (Scheme 1A). The resulting organic radical ion species can directly react in a number of different bond-forming

reactions. Alternatively, the radical ion can undergo mesolytic fragmentation to afford separate radical and ionic intermediates, either of which can be productively intercepted in synthetic transformations.

Second, radical intermediates can also result from the reaction of excited state photocatalysts via direct hydrogen atom abstraction, rather than by stepwise electron transfer and bond scission as independent processes (Scheme 1B). This is a characteristic reaction of photoexcited aromatic ketones such as benzophenone or acetophenone.<sup>3</sup> More recently, polyoxometalates have also been exploited as photocatalysts for this mechanism of photoactivation as well.<sup>4</sup> The distinction between electron and hydrogen atom transfer mechanisms is an important one for a number of reasons. Among the most critical is the identity of the thermodynamic parameters that best determine the feasibility of the activation step; while for photoredox activation the success of electron transfer is governed by the redox potentials of the substrate and excited photocatalyst, in hydrogen atom transfer reactions, the bond strength is typically more predictive.

Third, electronically excited photocatalysts can also activate an organic substrate via energy transfer (Scheme 1C).<sup>5</sup> The transfer of excited state energy from a photocatalyst to an organic substrate can occur through one of several mechanisms, but the most common in synthetic applications is Dexter energy transfer. This can be conceptualized as the bilateral electron exchange between the excited-state photocatalyst and an organic substrate, resulting in the non-radiative relaxation of the photocatalyst coupled to the simultaneous generation of an excited state substrate. For this process to be efficient, transfer of excited state energy from the photocatalyst to the substrate must be thermodynamically feasible. Photosensitization of reactions via this mode of activation is quite common in synthesis; however, the lifetime of the resulting electronically excited substrates is generally quite short. Thus strategies to use exogenous catalysts to manipulate their reactivity have been substantially more challenging to develop.

Several of the most common photocatalysts used in synthetic applications are shown in Figure 1. The structures of this family of catalysts are dominated by highly conjugated systems, as one might expect for a class of molecules designed to interact with light. Beyond this trivial similarity, however, a cursory glance at these compounds reveals their remarkable diversity. These include simple aromatic chromophores, both neutral and charged, functionalized organic dyes, inorganic clusters, and transition metal complexes whose properties can be easily tuned by ligand modification. The availability of diverse photocatalyst structures that span a broad range of triplet energies and redox potentials is an important benefit of photocatalytic synthesis; the appropriate choice of photocatalyst can be used to control the mechanistic outcome of many reactions where direct substrate photoexcitation might lead unselectively to multiple reaction pathways.

Because this diverse collection of photocatalyst structures nevertheless operate by only a few fundamentally distinct mechanisms of photoactivation, we have elected to organize the material in this review broadly based upon the mode by which the photocatalyst acts; that is, by electron transfer (Section 2), by hydrogen atom abstraction (Section 3), or by energy transfer (Section 4). However, these various photoactivation processes often lead to similar

open-shelled reactive intermediates, and because of the short lifetimes of the species involved, it is often difficult to unambiguously determine which mechanism of photoactivation is operative in a given transformation. The mechanisms provided herein reflect the best reasonable hypotheses of the publishing authors, and we present them as such. Given the understandable focus of the field on synthetic advances, experimental validation of several frequently invoked phenomena such as the persistent radical effect<sup>6–8</sup> and the relative contribution of closed catalytic versus radical propagative pathways<sup>9</sup> has not yet been performed for the majority of these reactions. Thus, certain details may be revised as the community's mechanistic understanding expands.

## 1.2 Organization and Scope of the Review

Synthetic organic photochemistry, like many interdisciplinary fields, is informed by the language and culture of several independent scholarly traditions. One significant challenge in interpreting this literature is the existence of a multitude of competing definitions of common terms such as “*catalysis*” that are used in different communities.<sup>10–13</sup> Can templating moieties that interact with the substrate only via non-covalent interactions be considered “catalysts?” Must a “catalyst” be used sub-stoichiometrically? It might be possible to mount a compelling argument that some of these definitions are more useful than others. However, for the purposes of this review, we will consider an entity a *catalyst* if it increases the macroscopic rate of the organic transformation in question while neither being formed nor consumed in the balanced reaction.

We have limited this discussion herein to the use of well-defined small-molecule photocatalysts and co-catalysts in the construction of complex organic molecules. This restriction unfortunately omits the substantial body of work involving semiconductor photocatalysis<sup>14–17</sup> as well as the study of photochemical reactions in supramolecular hosts.<sup>18–21</sup> These two themes of research within synthetic photochemistry are quite extensive, and while we cannot adequately cover them here, a number of excellent, comprehensive reviews on both fields are available. Earlier reviews covering the concept of molecular photocatalysis in synthetic applications have also been published, focusing upon carbon–carbon bond forming reactions,<sup>22–29</sup> the synthesis of natural products or complex molecular scaffolds,<sup>30–34</sup> as well as asymmetric synthesis.<sup>35–38</sup> The application of both transition metal<sup>39–43</sup> and organic photocatalysts<sup>44–46</sup> has also been discussed previously. Finally, we note that an excellent tutorial review on photochemical dual-catalyst strategies was recently published by Glorius, focusing on the revival of visible light photoredox catalysis over the past decade.<sup>47</sup>

## 2. Photoinduced Electron Transfer

The emergence of useful redox properties in the excited state is a common feature of molecular chromophores. Photoinduced promotion of an electron from the molecule's HOMO to its LUMO results in the formation of an electronically excited state that can formally be conceptualized as a charge-separated electron–hole pair. If the lifetime of this excited state is sufficiently long to engage in subsequent intermolecular reactions, it can either donate its high-energy electron to an appropriate acceptor (**A**) or fill its partially

occupied orbital from a suitable electron donor (**D**). Thus, by virtue of having an electron–hole pair, an excited photocatalyst can engage in both reductive and oxidative chemistry and is typically both a stronger reductant and a stronger oxidant than its ground state counterpart. As a result, a commonly exploited feature of a photocatalytic species is its ability to convert the energy of an incident photon into synthetically useful electrochemical potential.

Figure 2 outlines the generalized photoredox processes available to a photocatalyst. Absorption of a photon results in the generation of an electronically excited state; this can undergo relaxation back to the ground state via a number of unimolecular emissive and non-emissive pathways at relatively rapid rates. The redox properties of the excited state, however, can be exploited upon fast electron transfer *to* an electron-deficient acceptor species (**A**) or *from* an electron-rich donor species (**D**). These species are referred to as oxidative and reductive quenchers, respectively, because they result in the formation of a different oxidation state of a photocatalyst in its electronic ground state configuration. Regeneration of the photochemically active state requires a second electron-transfer process from a complementary donor or acceptor species. Thus photoredox catalysis typically results in a formal transfer of an electron from one reagent to another, which produces a pair of reactive radical ions comprising the oxidized donor (**D**<sup>•+</sup>) and reduced acceptor (**A**<sup>•-</sup>).

Both radical cations and radical anions exhibit intriguing, synthetically useful reactivity that is often not available to closed-shell organic molecules.<sup>48–57</sup> However, in photoredox catalysis, it is relatively rare for both radical ion equivalents to be simultaneously engaged in the same organic transformation. More commonly, a single synthetically relevant organic substrate is activated by photoinduced electron transfer, and a balancing redox equivalent is independently introduced to the reaction. There are two mechanistic scenarios by which this can occur. First, the substrate may directly quench the excited state of the photocatalyst, in which case the balancing redox equivalent is required to regenerate the photocatalyst (Figure 3A). This pathway is viable when electron transfer between the substrate and the excited photocatalyst is thermodynamically feasible. When it is not, however, the excited state can also be engaged by a secondary quencher (Figure 3B). This produces an oxidized or reduced ground-state catalyst that is more powerfully redox-active than the excited state and thus capable of performing a broader range of electron-transfer processes. Interaction with the substrate generates the corresponding substrate radical ion and returns the catalyst to its resting state. Prototypical oxidative quenchers include pyridinium salts, quinones, and nitroarenes. Reductive quenching is typically carried out by electron rich tertiary amines, sulfides, or phosphines. The kinetics of these quenching processes with a variety of photocatalytic species have been extensively documented.<sup>58</sup>

Co-catalysts can be used to influence photoredox transformations by mediating the electron transfer, by independently generating an intermediate species that undergoes photocatalytic activation *in situ*, or by controlling a reactive intermediate downstream of the photoinduced electron transfer process itself. The first strategy (redox mediation) constitutes the largest body of research and is treated separately (Section 2.1). The remainder of this section is organized according to the identity of the co-catalyst (Sections 2.2–2.6).

## 2.1 Redox Mediation

The feasibility of a given photoredox activation step is primarily determined by the relative half cell potentials of the photocatalyst and substrate, respectively. In general, synthetically useful photoredox reactions have been designed around exergonic electron transfer processes. However, the kinetics of electron transfer are also important; many PET processes that are thermodynamically favorable are nevertheless kinetically too slow to be useful. In addition, photoredox reactions involving modestly endergonic electron transfer are possible, although Marcus theory considerations predict slow rates of reaction for these processes. A common strategy to address either of these situations is the use of a redox mediator.

The redox mediator is a particular type of quencher that undergoes redox processes with both the photocatalyst and the substrate in separate electron transfer events (Figure 4). These co-catalysts are commonly referred to in the photochemistry literature as co-sensitizers, and occasionally as electron mediators, redox photosensitizers, redox catalysts, electron relays, or electron transfer agents.<sup>59–62</sup> There are three main mechanistic scenarios in which a redox mediator may increase the rate of a reaction. For a hypothetical oxidative reaction, these are as follows:

- I. The most straightforward use of redox mediators is for transformations in which direct oxidation of the substrate by the photocatalyst is exergonic, but inefficient rates of electron transfer result in a slow overall reaction. In this case, the appropriate choice of a redox mediator that reacts rapidly with both  $\text{PC}^*$  and the substrate can mitigate the unfavorable kinetics of the direct electron transfer process.
- II. Redox mediators can also be beneficial in reactions that involve endergonic PET. Although the electron transfer from  $\text{RM}^{*+}$  to the substrate must also be endergonic, it is kinetically more feasible than direct quenching because  $\text{RM}^{*+}$  is in its electronic ground state configuration and thus has a significantly longer lifetime than  $\text{PC}^*$ .
- III. Finally, a redox mediator may aid in generation of a solvent separated ion pair.<sup>63–66</sup> One common source of low quantum efficiency is the occurrence of back electron transfer (BET) before the intimate ion pair arising from collisional electron transfer ( $\text{PC}^{n-1}\cdot\text{sub}^{*+}$ ) can diffuse apart. A redox mediator may undergo BET more slowly and thus escape the solvent cage more efficiently. Subsequent electron transfer from the substrate to  $\text{RM}^{*+}$  results in the same reactive species but as a solvent separated ion pair ( $\text{PC}^{n-1} + \text{sub}^{*+}$ ) that is more resistant to BET.

Common photocatalyst/redox mediator pairs such as 9,10-dicyanoanthracene (DCA, **2**) and biphenyl (BP, **18**) are often employed with little discussion of which mechanistic scenario is operative.<sup>67–70</sup> As such, this section is organized by transformation, but we will attempt to highlight these mechanistic distinctions where possible.

**2.1.1 Photooxygenation**—One of the most prolific areas of study for this type of co-catalysis is the photooxygenation of cycloalkanes and small saturated heterocycles.<sup>71</sup> In the

1980s, the Schaap group discovered that biphenyl provided a dramatic rate increase to the DCA-catalyzed oxidation of cyclopropanes,<sup>72</sup> epoxides,<sup>73–76</sup> and aziridines.<sup>77</sup> For example, the photooxygenation of epoxide **19** to **20** is a slow reaction upon photocatalysis using DCA alone (Scheme 2). However, addition of 10 mol% biphenyl (BP) decreased the reaction time to 2 h, and complete conversion could be achieved in just 10 min using a stoichiometric loading of BP. The proposed explanation for this effect was in line with mechanistic situation II (Section 2.1). Substrate **19** is an ineffective quencher of DCA\*, whereas BP quenches rapidly ( $k_q = 3.1 \times 10^9 \text{ M}^{-1}\text{s}^{-1}$ ). Secondary electron transfer from BP\*+ to **19** is endergonic, but still kinetically feasible due to the long lifetime of BP\*+ relative to DCA\*.

The photooxygenation of cyclopropanes exhibited similar rate increases in the presence of biphenyl (Scheme 3), though a different mechanistic rationale was proposed.<sup>72,77</sup> Although substrate **22** quenches DCA\* at close to a diffusion-controlled rate ( $k_q = 1.1 \times 10^{10} \text{ M}^{-1}\text{s}^{-1}$ ), the rate of formation of photooxygenated products **23** and **24** are nevertheless increased 10-fold upon the addition of biphenyl. This observation is most consistent with mechanistic scenario III. Rapid PET results in the formation of a contact ion pair (DCA\*<sup>-</sup>•**22**\*+), and escape from the solvent cage is inefficient with respect to the rate of back electron transfer. In contrast, while BP quenches the photoexcited catalyst more slowly, BP\*+ can undergo more efficient dissociation. Subsequent electron transfer to this redox mediator affords the solvent separated (DCA\*<sup>-</sup> + **22**\*+) ion pair, which can more readily react with oxygen to afford the endoperoxide.

Similar effects were observed in the photooxygenation of diarylcyclopropanes,<sup>78</sup> vinylcyclopropanes,<sup>79–81</sup> and 8-methoxypsoralen.<sup>82</sup> In each case, DCA\* is quenched more efficiently by the substrate than by BP, but the addition of redox mediator nevertheless accelerates the overall rate of reaction. Tamai *et al.* quantified this effect in a study of the photoisomerization and photooxygenation of 1,2-diphenylcyclopropane **25**.<sup>83,84</sup> The addition of various polyphenylene redox mediators such as biphenyl, terphenyl, and phenanthrene was shown to result in an increase in the quantum yield for separation of RM\*+ and DCA\*<sup>-</sup> (Scheme 4).

**2.1.2 Alkene Oxidation**—Alkene radical cations have immense versatility in organic synthesis. They can readily participate in nucleophilic additions,<sup>51,85</sup> cyclizations,<sup>52,86</sup> cycloadditions,<sup>48,49,51,57</sup> fragmentations,<sup>54</sup> and rearrangement processes.<sup>53,86</sup> Photoredox catalysis offers a convenient method to generate these reactive intermediates, and redox mediation has been frequently utilized in tandem with photocatalysis to maximize the rate of reaction.

One of the earliest examples of this strategy was reported by Farid in the dimerization of phenyl vinyl ether **29** (Scheme 5) using 9-cyanoanthracene (9-CA) as a photocatalyst.<sup>87</sup> Direct quenching of [9-CA]\* by **29** is endergonic and too slow to be measured. Consistent with this inefficient electron transfer, the dimerization reaction proceeds with low quantum yield ( $\Phi = 7.3 \times 10^{-3}$ ). However, addition of redox mediators such as phenanthrene, alkylnaphthalenes or durene improved the quantum yield, up to 200-fold. This finding is consistent with the production of a long-lived arene radical cation that improves the efficiency by which the alkene radical cation can be generated.

Gassman reported that a combination of 1-cyanonaphthalene (1-CN) and biphenyl could be used to oxidize trisubstituted alkenes such as **31** (Scheme 6). The resultant radical cations could be trapped with oxygen nucleophiles in both intramolecular<sup>88,89</sup> and intermolecular<sup>90</sup> functionalization reactions. Arnold achieved similar reactivity using diphenylethene substrates.<sup>91,92</sup> Silyl enol ethers could also be oxidized and selectively desilylated in the presence of alkyl silyl ethers<sup>93</sup> and Hintz *et al.* later reported a DCA/Phen photocatalytic system for the cyclization of silyl enol ethers with pendant olefins.<sup>94</sup> The Roth laboratory observed altered chemoselectivity in the PET cyclization of geraniol, though the influence of the redox mediator was small.<sup>95</sup>

Nicewicz reported a conceptually similar strategy in for the [2+2] cycloaddition of styrenes such as **33** using 2,4,6-tris(4-methoxyphenyl)pyrylium tetrafluoroborate (*p*-MeOTPP<sup>+</sup>) as a photocatalyst (Scheme 7). Optimal yields of cycloadducts **34** required the addition of aromatic hydrocarbons such as naphthalene or anthracene.<sup>96</sup> The authors proposed that the redox mediators improve the rate of substrate oxidation compared to direct quenching.

Alkene oxidation by PET/redox mediation has also been leveraged for the rearrangement of polyunsaturated compounds such as 2-aza-1,4-dienes<sup>97,98</sup> and 1,5-hexadienes,<sup>99</sup> as well as tautomerization of styrenes,<sup>100</sup> nucleophilic addition to 1,3-dienes,<sup>101</sup> and the valence isomerization of norbornadiene.<sup>102</sup> Among the most synthetically powerful transformations in this class are the radical cation cascades developed by Warzecha, Demuth, and Görner (Scheme 8). Photocatalytic oxidation of polyene **35** by 1,4-dicyano-2,3,4,5-tetramethylbenzene (TMDCB) resulted in the formation of polycyclic scaffold **36**.<sup>103–105</sup> In these reactions, biphenyl was employed as a redox mediator, and its role is best explained by the first mechanistic scenario described in Section 2.1.<sup>106,107</sup> Stern–Volmer analysis revealed that BP is able to quench [TMDCB]\* at rates comparable to the terpene substrates. Furthermore, given its high loading and the long lifetime of BP<sup>•+</sup> relative to [TMDCB]\*, it dramatically increases the rate of substrate oxidation. Transient absorption spectroscopy also revealed the presence of BP<sup>•+</sup> under these conditions, as well as the unexpected result that TMDCB<sup>•-</sup> may reduce the substrate as well. Subsequent studies showed that other donors such as *trans*-stilbene or *N,N*-dimethylaniline were also competent as redox mediators when coupled with 2,4,6-triphenylpyrylium tetrafluoroborate (TPP<sup>+</sup> BF<sub>4</sub><sup>-</sup>).<sup>108</sup> This method was utilized in the synthesis of several steroid natural products.<sup>109,110</sup> Furthermore, a remote chiral auxiliary could be used to control the stereochemical outcome of the overall transformation.<sup>111–113</sup>

The combination of PET sensitization and redox mediation enables the facile generation of C<sub>60</sub><sup>•+</sup>, a process which has traditionally required  $\gamma$ -irradiation. Foote demonstrated that *N*-methylacridinium hexafluorophosphate (MA<sup>+</sup> PF<sub>6</sub><sup>-</sup>) could photocatalytically generate this radical cation, as observed by transient absorption spectroscopy. Addition of biphenyl increased the signal strength of C<sub>60</sub><sup>•+</sup> by an order of magnitude.<sup>114,115</sup> Subsequent work by Mattay and coworkers focused on the reaction of the C<sub>60</sub><sup>•+</sup> radical cation with alcohols, ethers, and aldehydes using DCA photocatalysis (Scheme 9).<sup>116</sup> For instance, the reaction with propionaldehyde **37** affords **38**, consistent with a process involving H-atom abstraction by C<sub>60</sub><sup>•+</sup> followed by attack of the resulting acyl radical **40** on H-C<sub>60</sub><sup>+</sup> **39**.<sup>117,118</sup>



**2.1.3 Heteroatom Oxidation**—Fagnoni and Albini reported that the photooxidation of organostannane **41** followed by mesolytic fragmentation of the C–Sn bond results in the formation of alkyl radical **44**, which subsequently can react with electron-poor acceptors such as **42** to give **43** (Scheme 10).<sup>61,119</sup> Although the process can be conducted using single photocatalysts such as 1,4-dicyanonaphthalene (DCN) or phenanthrene, the rates were increased in the presence of biphenyl as a redox mediator. Enantioselective, chiral auxiliary controlled versions of this reaction have also been reported.<sup>120</sup>

Cumpstey and Crich reported a procedure for photocatalytic glycosylation using selenosugars as donors (Scheme 11).<sup>121</sup> Photooxidation of **45** with a *N*-methylquinolinium photocatalyst (NMQ<sup>+</sup> PF<sub>6</sub><sup>-</sup>) results in elimination of the selenyl radical to give glycosyl cation **47**, which can in turn be trapped by an alcoholic acceptor moiety to form **46**. The reaction was accelerated upon addition of toluene as a co-solvent, which the authors proposed was serving as a redox mediator.

Steckhan, Blechert, and coworkers used the DCA/BP pair for the functionalization of  $\alpha$ -silyl amines,<sup>122</sup> ethers, acetals,<sup>123</sup> and carbamates.<sup>124</sup> Scheme 12 shows that following oxidation and desilylation of **48**,  $\alpha$ -alkoxy radical **51** can add to alkenes such as **49** to afford **50**. The analogous reaction with a single photocatalyst was inefficient, presumably due to rapid BET from DCA<sup>\*</sup>. As has been discussed previously, the redox mediator helps to form **48**<sup>•+</sup> free in solution and thus avoid this problem.

The Yoon laboratory reported a radical thiol–ene reaction initiated by photooxidation of sulfur-containing compounds by Ru(bpz)<sub>3</sub>(PF<sub>6</sub>)<sub>2</sub> (Scheme 13).<sup>125</sup> Several amine additives provided a dramatic rate increase, particularly those such as **54**, whose redox potentials were between that of the excited photocatalyst and the thiol substrate. As direct quenching of the photocatalyst by thiol **52** was proposed to be quite slow, the authors suggested that sequential PET events from and to the redox mediator (**54**) allowed for the increase in reaction rate. This case then falls into the first mechanistic scenario described in Section 2.1, wherein the mediator provides a more kinetically feasible pathway for electron transfer. Boyer subsequently utilized this method for the postsynthetic radical functionalization of polymers.<sup>126</sup>

In some cases, redox mediators can alter the distribution of reaction products or otherwise influence the chemoselectivity of a photocatalytic transformation. Whitten studied the oxidative fragmentation of 1,2-aminoalcohols to give aldehydes (Scheme 14) and found that redox mediation with biphenyl improved reaction rates due to its efficient quenching of DCA<sup>\*</sup>.<sup>127</sup> Moreover, while photooxidation of *syn*-**56** using DCA alone afforded higher quantum yields than *anti*-**56**, both diastereomers underwent cleavage at equivalent efficiencies in the presence of BP. The authors proposed that the former conditions involve the reaction of contact ion pairs while the latter give solvent-separated ion pairs.

**2.1.4 Oxidative Rearrangement**—Ikeda studied the rearrangement and cycloaddition of methylenecyclopropanes such as **59** under photocatalytic conditions (Scheme 15).<sup>128</sup> Transient absorption spectroscopy revealed both diradical **60** and radical cation **61** as intermediates, and their relative concentration could be controlled by photocatalyst identity.

Moreover, the addition of redox mediators such as biphenyl or toluene increased the formation of **61** relative to **60**. Although the ability of these species to undergo cycloadditions with oxygen to form **62** or with fumarate **63** to form **64** and **65** was examined, the photocatalyst/redox mediator pairs were not directly compared.

Adam and Sendelbach demonstrated that photooxidation of azoalkane **66** led to extrusion of dinitrogen, followed by ring closure to housane **67**, rearrangement to cyclopentene **68**, or intramolecular trapping of the pendant alcohol to produce spiroethers **69** and **70** (Scheme 16).<sup>129,130</sup> Addition of biphenyl as a redox mediator results in an increase in the rate of reaction and also changes the distribution of products. The authors proposed that BET from  $\text{DCA}^{\bullet-}$  to  $\mathbf{71}^{\bullet+}$  leads to 1,3-diradical **71**, which can rapidly form housane **67**. Thus, the DCA-only conditions, proposed to produce a contact radical ion pair from which back-electron transfer is rapid, generate a large amount of this product. In contrast, redox mediation with biphenyl generates  $\mathbf{71}^{\bullet+}$  as a solvent-separated ion pair with  $\text{DCA}^{\bullet-}$ . The free radical cation intermediate has a lifetime sufficient to undergo 1,2-hydrogen migration to form  $\mathbf{72}^{\bullet+}$ , which in turn leads to alkene **68** and spiroethers **69** and **70**.

Yamashita studied the rearrangement of cage ketone **73** catalyzed by 2,4,6-triphenylpyrylium perchlorate ( $\text{TPP}^+ \text{ClO}_4^-$ ).<sup>131</sup> The proposed mechanism involves oxidation of **73**, rearrangement via  $\mathbf{74}^{\bullet+}$  and  $\mathbf{75}^{\bullet+}$ , and chain-propagating electron transfer to afford **74** and **75** (Scheme 17). The addition of aromatic hydrocarbons such as biphenyl, phenanthrene, and pyrene resulted in a significant rate increase, consistent with their role as redox mediators. Furthermore, the product distribution proved to be sensitive to the structure of the mediator. Interestingly, the rate increases as the reaction progresses, and based upon quantum yield measurements, the authors suggested that the product (**75**) can also act as an autocatalytic redox mediator.

**2.1.5 Photoreduction**—While reductive redox mediators are regularly utilized in electrochemical transformations,<sup>132–136</sup> they have found relatively few applications in synthetic photoredox chemistry. An interesting example was described by Darwent and Kalyanasundaram (Scheme 18),<sup>137</sup> who found that methyl viologen ( $\text{MV}^{2+}$ ) can act as a redox mediator between a  $\text{Ru}(\text{bpy})_3\text{Cl}_2$  photocatalyst and benzoquinone **76**. Although **76** can quench the photocatalyst directly, a high concentration of superior quencher  $\text{MV}^{2+}$  results in the accumulation of  $\text{MV}^{\bullet+}$ . This in turn can reduce **76** to  $\mathbf{76}^{\bullet-}$ , which upon protonation and disproportionation affords phenol **77**. More recently, this type of redox mediation has been applied to the Meerwein–Ponndorf–Verley-type reduction of ketones, though in this case the viologen is involved in hydride transfer as well as electron transfer.<sup>138</sup>

Willner merged this approach with phase transfer catalysis in the reductive dehalogenation of vicinal dibromides (Scheme 19).<sup>139–141</sup> In his system, *N, N'*-dioctyl viologen ( $\text{C}_8\text{V}^{2+}$ ) is reduced by photoexcited  $\text{Ru}^*(\text{bpy})_3\text{Cl}_2$ . The resultant  $\text{C}_8\text{V}^{\bullet+}$  is lipophilic, and migrates to the organic phase of the reaction mixture, where it can disproportionate to  $\text{C}_8\text{V}^{2+}$  and  $\text{C}_8\text{V}$ . The former returns to the aqueous phase to reenter the catalytic cycle, and the latter carries out the two-electron reduction of dibromide **78** to **79**. Further work from this group incorporated enzymes as co-catalysts, and will be discussed later (Section 2.6).

Sawaki reported that the photoreduction and fragmentation of stilbazolium cyclobutane **80** could be carried out with 9,10-dimethoxyanthracene (DMA) as a photocatalyst and 1-CN, DCN, or DCB as redox mediators (Scheme 20).<sup>142</sup> The authors postulated that the mediator quenches DMA\* and dissociates from the solvent cage to reduce the substrate. The most dramatic increase in quantum yield was observed using 1-CN as the redox mediator, with less pronounced effects using DCN and DCB. The authors attributed this difference to an increased proclivity for the DMA\*•1-CN\*<sup>-</sup> intimate ion pair to undergo dissociation.

More recently, Tahara and Hisaeda reported a reductive dehalogenation protocol using Rose Bengal as a photocatalyst (Scheme 21).<sup>143</sup> In their proposed mechanism, the photoexcited catalyst is quenched by vitamin B12 derivative **83**, and the resulting Co<sup>I</sup> species reduces **82**.

## 2.2 Lewis Acid Catalysis

The use of Lewis acids to activate heteroatom-containing organic moieties is a ubiquitous strategy in organic synthesis that has found use in a wide variety of applications. Photochemistry is no exception, and the prevalence of ketone and enone functional groups has made this a fertile area for exploration. Coordination of a Lewis acid to heteroatom-containing substrates can impact a number of critical reactivity parameters, including electrophilicity and reduction potential. They can also impact the rate of a reaction by stabilizing a ketyl radical or other photoreduced anionic intermediate.

**2.2.1 Substrate–Lewis Acid Interactions**—Abe and Oku studied the pyrene-catalyzed PET reaction between diethyl fumarate **85** and cyclopropane **86** to give crossed product **87** and homodimer **88** (Scheme 22).<sup>144</sup> This reaction proceeds only in the presence of Mg(ClO<sub>4</sub>)<sub>2</sub> as a Lewis acidic co-catalyst. The authors proposed that stabilization of allylic ketyl radical **89** by Mg<sup>2+</sup> suppresses back electron transfer to the photocatalyst and enables the coupling with **90** to proceed efficiently. Saito and coworkers observed a similar effect of a Mg<sup>2+</sup> Lewis acid in the reductive cleavage of the benzoyloxy moiety from **91** (Scheme 23).<sup>145</sup>

Pac reported an intriguing example of a Lewis acid effect that does not require precoordination to the substrate. The rate of photoreduction of olefins by Ru(bpy)<sub>3</sub><sup>2+</sup> and a NADH analog enjoys a dramatic increase in the presence of Mg(ClO<sub>4</sub>)<sub>2</sub> (Scheme 24).<sup>146</sup> Although the Mg<sup>2+</sup> does not exhibit appreciable binding to starting alkene **93**, there is a strong stabilizing interaction with the corresponding radical anion **93**<sup>•-</sup>. This interaction thus facilitates the one-electron reduction of the substrate.<sup>147</sup>

Mizuno, Nakanishi, and Otsuji also observed that the substitution of dicyanobenzene **1** with group 14 allyl metal species such as **95** became more efficient upon addition of Mg(ClO<sub>4</sub>)<sub>2</sub> (Scheme 25).<sup>148</sup> Again, the magnesium salt was proposed to stabilize the radical anion of the substrate and inhibit back electron transfer to the photocatalyst. The resulting complex **97** can combine with an allyl radical to form **98**, which then undergoes loss of cyanide and the Lewis acid to provide **96**.

The effect of a Lewis acid on the reduction potential of organic substrates has found use in recent reports of photocatalytic methods as well. The Yoon group has applied this strategy to

a variety of photocatalytic cycloaddition reactions. For example, the intrinsic reduction potential of bis(enone) **99** is roughly  $-1.6$  V vs. SCE in DMF,<sup>149</sup> which lies outside the range accessible using  $\text{Ru}(\text{bpy})_3^{2+}$  (Scheme 26). However, coordination of  $\text{LiBF}_4$  to the substrate results in a more positive reduction potential, thereby enabling photoreduction. The resulting allylic ketyl radical **101** is able to engage with the pendant Michael acceptor to afford cyclobutane product **100**.<sup>150</sup> Intermolecular versions of this reaction have also been developed.<sup>151,152</sup>

Because the enone substrates do not absorb in the visible region, no background reaction occurs in the absence of photocatalyst or Lewis acid. Thus, a highly enantioselective [2+2] cycloaddition could be realized using a chiral  $\text{Eu}^{3+}$  Lewis acid without any competing racemic process due to direct excitation or uncatalyzed photoreduction (Scheme 27).<sup>153</sup>

Similar photoreductive conditions were applied to the [4+2] hetero-Diels–Alder cycloaddition of bis(enone) **106** (Scheme 28).<sup>154</sup> In this study, Yoon found empirically that  $\text{Mg}(\text{ClO}_4)_2$  was the optimal Lewis acid that balanced the rate of photoreductive activation of the enone substrate and that of an undesired reductive decomposition of the product.

Yoon utilized a conceptually analogous approach in the design of a [3+2] cycloaddition of acyl cyclopropanes with alkenes, where coordination of a Lewis acid to the ketone modulates the reduction potential of **108**. The resultant  $\alpha$ -cyclopropyl ketyl radical **110** can undergo ring opening followed by alkene addition and reoxidation to yield [3.3.0]bicyclooctane **109** (Scheme 29).<sup>155</sup> In this reaction,  $\text{LiBF}_4$  was insufficiently Lewis acidic to enable photoreductive activation of the cyclopropyl ketone. Instead, the more strongly Lewis acidic additive  $\text{La}(\text{OTf})_3$  was found to be the optimal Lewis acid co-catalyst for this transformation. An asymmetric intermolecular variant of this reaction was recently reported.<sup>156</sup>

Xia demonstrated that lanthanide Lewis acids are also effective in promoting the reductive dimerization of chalcones using photoredox catalysis (Scheme 30).<sup>157</sup> The authors proposed that  $\text{Sm}(\text{OTf})_3$  facilitates the reduction of **111** and stabilizes the resulting radical anion, which dimerizes to form dienolate **113**. The Lewis acid also guides the subsequent cyclization step of **114** to **112**. Importantly, this reaction is a net-reductive cyclization reaction and thus differs in an important mechanistic regard from the previous examples of  $\text{Ru}(\text{bpy})_3^{2+}$ -catalyzed cycloadditions.

Lewis acidic metal ions can also be used as templating reagents to recruit and localize Lewis basic substrates. While this strategy is common in many applications involving homogeneous catalysis, few examples related to photocatalytic transformations have been reported. Cibulka, Vasold, and König designed flavin-derived photocatalyst **119** with a tetraamine binding site.<sup>158</sup> The latter chelates  $\text{Mg}^{2+}$ , which in turn coordinates benzyl alcohol **115**. By increasing the local concentration of the substrate, the quantum efficiency of photooxidation by the flavin is increased significantly (Scheme 31).

**2.2.2 Photocatalyst–Lewis Acid Interactions**—The use of Lewis acids to activate electron-deficient organic substrates towards photocatalytic reduction is a logical co-catalyst

strategy that follows from their ability to increase the electrophilicity of a wide range of organic substrates. However, examples of Lewis acid co-catalysis of *oxidative* photochemical transformations are also known. Neither the organic substrates nor their radical cations would be expected to engage in redox-relevant interactions with a Lewis acid. On the other hand, the radical anion resulting from a reduced photocatalyst can readily be stabilized by a Lewis acid, which could serve to minimize the rate of back electron transfer. The application of this concept to photoinduced electron transfer chemistry has been a topic of investigation for several decades.<sup>66,159–161</sup>

Mizuno discovered that a range of Lewis acids increase the quantum yield for photoisomerization and oxygenation of cyclopropane **121** (Scheme 32).<sup>162</sup> One major source of inefficiency in this reaction arises from recombination of the photogenerated ion pair **123**, composed of oxidized **121**<sup>•+</sup> and reduced DCA<sup>•-</sup>. However, coordination of a Lewis acid to DCA<sup>•-</sup> is proposed to stabilize the radical anion and decrease the rate of unproductive back electron transfer. A similar strategy has been applied to a number of other transformations, including the photooxygenation of cyclopropanes,<sup>78,84,163</sup> disilenes,<sup>164</sup> biphenyls,<sup>165,166</sup> and 1,5-dienes,<sup>167</sup> as well as the addition of methanol to 1,1-diaryl alkenes.<sup>168</sup>

Lewis acids can alter the photoelectrochemical properties of photocatalysts by coordination to heteroatom binding sites in much the same way as they can change the redox potential of Lewis basic organic substrates (Section 2.2.1). Fukuzumi, Kuroda, and Tanaka showed that the excited state oxidation potential of flavin photocatalysts **126** and **127** is increased substantially upon complexation with Mg<sup>2+</sup> or Zn<sup>2+</sup> ions (Scheme 33).<sup>169</sup> Under these conditions, the oxidation of benzyl alcohol **125** to **128** was achieved in considerably shorter reaction times.<sup>170,171</sup>

**2.2.3 Lewis Acid Catalysis of Non-Redox Steps**—Lewis acid strategies that alter the redox properties of the substrate or photocatalyst or interfere with back electron transfer exert their influence primarily on the dynamics of the electron transfer process itself. These constitute the majority of synthetic applications of photoredox/Lewis acid co-catalysis to date. However, Lewis acids can also have effects on steps that are downstream of the PET step. This can be particularly important when the photogeneration of reactive intermediates is facile but their subsequent reactions are relatively inefficient. For example, Zhu and Rueping recently reported the photocatalytic  $\alpha$ -functionalization of glycol esters (Scheme 34).<sup>172</sup> After oxidation of **129**, a Zn(OAc)<sub>2</sub> co-catalyst decomposes photogenerated hemiaminal intermediate **132**; the resulting imine **133** is activated towards nucleophilic addition by indole **130** to afford **131**. Cheng and coworkers observed a similar effect, though they proposed a slightly different order of steps.<sup>173</sup>

In their study on photocatalytic radical cation cascades using Eosin Y, Yang *et al.* found that substrates such as **134** did not provide appreciable conversion, presumably due to the low nucleophilicity of the 1,3-diketone terminus. However, the addition of LiBr helped to favor the enol tautomer, allowing facile cyclization to **135** (Scheme 35).<sup>174</sup>

Ru(bpy)<sub>3</sub><sup>2+</sup> and other photoredox sensitizers can be used to photooxidatively desilylate  $\alpha$ -silylamine **136**; the chemistry of the resulting  $\alpha$ -amino radical intermediate **139** has been thoroughly investigated.<sup>175</sup> While this class of nucleophilic radical is sufficiently reactive to add to Michael acceptors unassisted,<sup>176</sup> Yoon found that the rate of the conjugate addition increases significantly upon addition of Lewis acid co-catalysts. In particular, a chiral (pybox)Sc<sup>III</sup> complex is able to accelerate the reaction and control the enantioselectivity of the conjugate addition step (Scheme 36).<sup>177</sup>

## 2.3 Brønsted Acid/Base Catalysis

Like Lewis acid coordination, the protonation of organic functional groups can have a similarly diverse range of effects on the redox properties and reactivities of organic substrates. Thus, the use of Brønsted acid co-catalysts in photocatalytic transformations has also emerged as a powerful strategy for novel synthetic methods.

**2.3.1 Proton-Coupled Electron Transfer (PCET)**—Brønsted acids can catalyze the photoreduction of organic substrates in a manner analogous to Lewis acids. However, in many cases these electron-deficient functional groups possess a pK<sub>a</sub> too low to result in a significant concentration of protonated substrate. Proton-coupled electron transfer (PCET) involves the concomitant transfer of a proton and an electron to an organic substrate in a single concerted process. This activation strategy enables the facile generation of radical intermediates that would be kinetically inaccessible via separate proton- and electron-transfer steps. This subject has been reviewed recently,<sup>178–180</sup> and we focus here on its applications to photocatalytic synthesis.

The Knowles laboratory has pioneered the development of synthetic methods that exploit PCET as a means of generating open-shell reactive intermediates. They have shown that aryl ketones are reduced and cyclized using a combination of Brønsted acid and transition metal photoredox catalysts (Scheme 37).<sup>181</sup> The authors propose a mechanism wherein photoexcited Ru(bpy)<sub>3</sub>(BArF)<sub>2</sub> is quenched by hydrogen atom donor **142** or **143** to provide Ru<sup>I</sup>; transfer of an electron from this species to the ketone substrate is assisted by a phosphoric acid co-catalyst (**141-H**) in a PCET step. The resulting ketyl radical **145** undergoes cyclization to the pendant alkene to **146**, followed by hydrogen atom transfer from **142** or **143** and lactonization to afford ester **144**. The oxidized hydrogen atom donors **142**<sup>•</sup> or **143**<sup>•</sup> can lose another electron and proton to regenerate the active Ru<sup>I</sup> reductant and the Brønsted acid co-catalyst **141-H**. Subsequently, the authors developed an enantioselective addition of photogenerated ketyl radicals to hydrazones in which chiral BINOL-derived phosphoric acid co-catalysts both activated the ketone substrate towards PCET and controlled the stereochemistry of the subsequent radical addition.<sup>182</sup>

Yoon and coworkers utilized a similar combination of Brønsted acid and photoredox catalysts in the reductive cyclization of bis(enone) **99** to **147** (Scheme 38).<sup>183</sup> The optimal activating Brønsted acid utilized in this case proved to be formic acid. While the authors did not propose that the photoreduction step involved PCET, the analogy to the ketyl radical cyclization studied by Knowles suggests that the same mechanism of activation is likely to be operative here. Notably, only the identity of the acidic co-catalyst differs from the Lewis

acid-catalyzed [2+2] method that the Yoon laboratory reported for the same bis(enone) substrates earlier.<sup>150</sup> The authors argued that the chemistry of the neutral radical intermediate generated under Brønsted acid conditions is fundamentally distinct from the reactivity of the radical anion generated under Lewis acidic conditions.

Fukuzumi and coworkers studied the effect of Brønsted acids on the reductive dehalogenation of phenacyl bromide **148** (Scheme 39).<sup>184</sup> They found that addition of HClO<sub>4</sub> substantially improves the reaction rate, and engages substrates that are otherwise unreactive, such as phenacyl chlorides. In the absence of acid, the authors propose that photoexcited [Ru\*(bpy)<sub>3</sub>]<sup>2+</sup> is reductively quenched by 9,10-dihydro-10-methylacridine (AcrH<sub>2</sub>) and the resultant Ru<sup>I</sup> species is capable of reducing the α-bromoketone substrate. Direct quenching by the substrate is not observed. In the presence of Brønsted acid, however, AcrH<sub>2</sub> is protonated to AcrH<sub>3</sub><sup>+</sup>, which is a less effective reductive quencher. Nevertheless, the rate of dehalogenation is increased, and the authors suggest a change in mechanism to explain this observation. Rather than reductive quenching by AcrH<sub>2</sub> or AcrH<sub>3</sub><sup>+</sup>, they propose direct *oxidative* quenching by the substrate, which is known to be accelerated by Brønsted acids.<sup>185,186</sup> Under these conditions, quenching rates for the ketones match or exceed those measured for AcrH<sub>2</sub> in the absence of acid. The exact nature of this acid catalysis, and the possibility of PCET, is not discussed.

Bissember and coworkers recently disclosed a reaction between maleimides and dialkylanilines that utilizes TFA as a co-catalyst.<sup>187</sup> The authors propose that the role of this Brønsted acid is to facilitate the aerobic oxidation of the photoexcited [Cu<sup>I</sup>]\* catalyst to [Cu<sup>II</sup>], although they do not comment on the exact mechanism by which this takes place. They also consider that the TFA may accelerate downstream steps as well, which is a general phenomenon discussed in the following section (2.3.2). PCET may also be used to *remove* a net hydrogen atom, rather than add one. For example, Knowles showed that amides could be oxidized to amidyl radicals and cyclized onto tethered alkenes (Scheme 40).<sup>188</sup> The key PCET step is thought to involve simultaneous deprotonation of **150** by a catalytic phosphate base and electron transfer to photoexcited [Ir<sup>III</sup>]\*. Following cyclization, alkyl radical **152** can either add to **149** and gain a net hydrogen atom to form **151**,<sup>188</sup> or directly abstract a hydrogen atom from an appropriate donor (hydrogen atom transfer co-catalysis is discussed further in Section 2.4.2).<sup>189</sup>

**2.3.2 Brønsted Acid Catalysis of Non-Redox Steps**—Brønsted acids can control non-photochemical processes downstream of the photoactivation step in a manner analogous to Lewis acid co-catalysts. For example, the Yoon group studied the addition of photocatalytically generated α-amino radical **155** to methyl vinyl ketone (Scheme 41).<sup>190</sup> This reaction was accelerated by acidic additives such as TFA, which the authors proposed could increase the net electrophilicity of the Michael acceptor.

Ooi recently disclosed a highly enantioselective radical coupling based on the idea of ion pairing.<sup>191</sup> In their proposed mechanism (Scheme 42), amine **157** quenches the photoexcited iridium catalyst, which can then reduce imine **156** to the corresponding radical anion. Hydrogen bond donor **158**<sup>+</sup> undergoes counterion exchange with this species to form chiral

ion pair **160**. At the same time, oxidized **157**<sup>+</sup> is deprotonated to form  $\alpha$ -amino radical **161** which adds to **160** to form **159**.

The Yoon laboratory reported the photocatalytic reduction of nitroarenes such as **162** (Scheme 43).<sup>192</sup> The addition of a catalytic amount of camphorsulphonic acid (CSA) was required for the formation of cyclized hydroxamic acid **165**; in its absence of this co-catalyst, only hydroxylamine **164** was observed.

Brønsted acid additives have been empirically shown to be beneficial in a number of other photoredox transformations as well, although the precise nature of their effect is not always clear. For example, Maity and Zheng reported a photocatalytic oxidative indole synthesis that is accelerated by the addition of silica gel.<sup>193</sup> Yu employed a catalytic amount of *p*-chlorobenzenesulfonic acid in the photocatalytic synthesis of azaarenes, presumably to facilitate formation of an acyl oxime precursor rather than to influence PET.<sup>194</sup> Qi and Zhang found that catalytic TsOH improved their synthesis of  $\alpha$ -alkoxybenzamides.<sup>195</sup> König observed improved performance of photocatalytic amine deprotection at low pH, though the mechanistic basis of this effect was not determined.<sup>196</sup>

## 2.4 Organocatalysis

Over the past two decades, organocatalysis has evolved into a robust and diverse theme of contemporary synthetic research. A wide range of organocatalytic activation modes have been used in conjunction with photoredox catalysis. The majority of these co-catalysts influence the photocatalytic activation step itself, either by facilitating electron transfer or by catalytically generating a transient species that participates directly in the PET process. Other co-catalysts impact the rate of downstream steps by interacting with a reactive intermediate produced by photoactivation but not with the photocatalyst itself. The organization of this section will be based upon the class of organocatalyst utilized.

**2.4.1 Enamine/Iminium Catalysis**—Some of the earliest applications of organocatalysis to photoredox reactions were developed by MacMillan, who reported several protocols for the  $\alpha$ -functionalization of aldehydes. The general mechanism for these reactions is exemplified by Scheme 44, and is proposed to be operative for the addition of  $\alpha$ -carbonyl,<sup>197</sup> fluoroalkyl,<sup>198</sup>  $\alpha$ -cyanoalkyl,<sup>199</sup> benzyl,<sup>200</sup> and carbamoyl groups.<sup>201</sup>

The condensation of chiral secondary amine **168** with aldehyde **166** provides enamine **170**. A sacrificial quantity of this species quenches the photoexcited Ru(bpy)<sub>3</sub><sup>2+</sup> catalyst, forming Ru(bpy)<sub>3</sub><sup>+</sup>. This reduces alkyl halide **167** to **167**<sup>•-</sup>, which then undergoes dehalogenation to afford electron deficient  $\alpha$ -keto radical **171**. The SOMOphilic enamine **170** undergoes radical addition to **171**, and the resulting  $\alpha$ -amino radical can either be oxidized by photoexcited Ru(bpy)<sub>3</sub><sup>2+</sup> or another equivalent of the alkyl halide in a chain propagative manner.<sup>9</sup> Finally, the iminium ion can be hydrolyzed to release the  $\alpha$ -functionalized product and regenerate the amine organocatalyst. In addition to high yields under mild conditions, these reactions produce highly enantioenriched products due to the exquisite facial selectivity afforded by this class of organocatalysts in the radical addition step.



Following MacMillan's initial report, several other research groups have merged enamine organocatalysis with photoredox catalysis. For example, Luo developed a highly enantioselective photoredox alkylation protocol that was able to construct a variety of acyclic, cyclic, and spirocyclic quaternary stereocenters using a secondary amine organocatalyst.<sup>202</sup> Koike and Akita demonstrated that organocatalytically generated chiral enamines could be oxidized and trapped with TEMPO,<sup>203</sup> and the Jang group showed that the chiral enamine intermediate for this  $\alpha$ -oxygenation could be accessed via chiral iminium catalyzed conjugate addition.<sup>204</sup> Gualandi reported that an inexpensive Fe(bpy)<sub>3</sub>Br<sub>2</sub> catalyst could be used in place of a Ru photocatalyst,<sup>205</sup> while the Zeitler<sup>206,207</sup> and Ferroud<sup>208</sup> groups independently showed that transition metal photocatalysts could often be replaced by photoredox-active organic dyes such as Eosin Y and Rose Bengal.

MacMillan also demonstrated that selective  $\beta$ -functionalization of aldehydes and ketones could be accomplished using a related co-catalytic system (Scheme 45). Photoexcited Ir(ppy)<sub>3</sub> can reduce electron-poor cyanoarenes such as **1** to **1**<sup>•-</sup>. Concomitantly, aldehyde **166** can condense with secondary amine **172** to afford enamine **174**, which is then oxidized by Ir(ppy)<sub>3</sub><sup>+</sup> and deprotonated to form the  $5\pi e^-$   $\beta$ -enamine radical **175**. The authors propose these two radical species undergo heterocoupling, and upon loss of cyanide and hydrolysis this affords  $\beta$ -arylated product **173**.<sup>209</sup>

MacMillan also developed a similar reaction that utilized ketones<sup>210</sup> and imines<sup>211</sup> in place of cyanoarenes (Scheme 46). In this case, formation of  $\alpha$ -amino radical **179** was proposed to be facilitated by a catalytic amount of acid, presumably via PCET activation. These protocols also employ 1,4-diazabicyclo[2.2.2]octane (DABCO) as a redox mediator. This base quenches the Ir\*(ppy)<sub>2</sub>(dtbbpy)PF<sub>6</sub> photocatalyst more rapidly than either substrate, and the resultant DABCO<sup>•+</sup> can oxidize enamine **180**. The mediator is also able to shift the reaction selectivity, as it generates exclusively  $\beta$ -Mannich product **178**, while the reaction intrinsically gives a mixture of  $\alpha$ - and  $\beta$ -products in its absence. In the case of ketones, LiAsF<sub>6</sub> proved to be important in minimizing the occurrence of ketyl radical dimerization by stabilizing this intermediate. Thus, in addition to the iridium photocatalyst, this reaction is influenced by an organocatalyst, a redox mediator, a Brønsted and Lewis acid catalyst.

The MacMillan laboratory developed an analogous coupling with electron-deficient alkenes (Scheme 47).<sup>212</sup> In this case, however, oxidation of the enamine was proposed to be from direct quenching of the excited photocatalyst, Ir(dmppy)<sub>2</sub>(dtbbpy)PF<sub>6</sub>. The  $\beta$ -enamine radical could then add to Michael acceptors such as **181** and be further reduced to afford the  $\beta$ -alkylated product **183**.

The photooxidation of amines constitutes a major theme of research in synthetic photochemistry. Many classical<sup>213,214</sup> and contemporary<sup>215,216</sup> methods have exploited the photogeneration of iminium ions via amine oxidation and subsequently trapped them using a range of nucleophiles. Among the most thoroughly studied transformations in this context involve the oxidation of *N*-phenyltetrahydroisoquinoline (THIQ) **153**, which is particularly susceptible towards oxidative functionalization. Several reports of tandem photocatalytic/organocatalytic Mannich reactions have been published based upon this reactivity. For example, Rueping and coworkers demonstrated that iminium ion **185** could be coupled with

ketones using proline as an organocatalyst (Scheme 48).<sup>217</sup> Zeitler expanded this method to other amine scaffolds and also improved throughput by carrying out the reactions in a flow photoreactor.<sup>207</sup> Organic photoredox sensitizers have also been utilized for these reactions. For example, Tan accomplished the amine oxidation/organocatalytic coupling with Rose Bengal,<sup>218</sup> while Zhao employed a variety of BODIPY photocatalysts.<sup>219</sup>

**2.4.2 Hydrogen Atom Transfer (HAT) Catalysis**—Photoinduced electron transfer processes result in the formation of open-shelled intermediates, and production of closed-shell products via efficient termination of open-shell reaction manifolds often proves to be somewhat challenging. One strategy that has proven to be particularly important in photoredox chemistry has been the use of organic hydrogen atom transfer (HAT) co-catalysts.

Nicewicz has exploited this strategy extensively to develop high-yielding anti-Markovnikov alkene functionalization reactions (Scheme 49).<sup>220</sup> Photoexcitation of 9-mesityl-10-methylacridinium perchlorate (Mes-Acr<sup>+</sup> ClO<sub>4</sub><sup>-</sup>) and quenching by alkene **186** gives radical cation **186**<sup>•+</sup>. Alkene radical cations are susceptible to attack by a range of nucleophiles;<sup>51–53,85–86</sup> intramolecular cyclization of the pendant alcohol in this case affords **189**. This tertiary alkyl radical is insufficiently oxidizing to directly react with **186** in chain propagating electron transfer or with the reduced photocatalyst to regenerate the photochemically active acridinium. With no co-catalyst, therefore, the rate of product formation is relatively slow. However, the introduction of 2-phenylmalononitrile **187** as a hydrogen atom shuttle that reacts with **189** affords the closed shell product **188**. This HAT co-catalyst is then regenerated by electron transfer from the reduced Mes-Acr photocatalyst. In addition to **187**, subsequent work from this laboratory showed that methylthiosalicylate,<sup>221</sup> thiophenol,<sup>222</sup> and phenylsulfonic acid<sup>223</sup> could also act as HAT catalysts. Thiophenol in particular could be generated *in situ* from operationally benign phenyldisulfide.<sup>224</sup>

Using a similar strategy, Nicewicz has also achieved anti-Markovnikov functionalization of alkenes with ethers,<sup>220,225,226</sup> amines,<sup>222,224</sup> trifluoromethyl groups,<sup>221</sup> halogens,<sup>227</sup> carboxylic acids,<sup>223</sup> amides, and thioamides.<sup>228</sup> Complex heterocyclic scaffolds are accessible using an intermolecular coupling partner with an additional  $\pi$  system (Scheme 50). Initial addition of **191** to radical cation **190**<sup>•+</sup> affords radical **193**, which can cyclize on a pendant alkene<sup>229,230</sup> or oxime<sup>231</sup> before being trapped by the HAT catalyst to afford **192**.

Thiyl HAT co-catalysts can also be used to terminate radical intermediates that are photogenerated in other ways. For example, the photooxidation of carboxylic acids is a well-established method to produce carbon-centered radicals via decarboxylation.<sup>232</sup> Nicewicz demonstrated that these radicals could be productively intercepted by thiyl HAT co-catalysts; in their absence, these radicals primarily undergo homodimerization.<sup>233–235</sup>

Nicewicz has also recently reported a protocol for C–H amination of arenes with nitrogen nucleophiles.<sup>236</sup> In the proposed mechanism (Scheme 51), [Mes-Acr<sup>+</sup>]<sup>\*</sup> oxidizes arene **194**, which can be attacked by an amine nucleophile **195**. Following deprotonation to neutral

radical **197**, TEMPO is used to abstract a hydrogen atom, affording the closed shell product. The HAT co-catalyst can then be regenerated by a reactive oxygen species.

MacMillan has also developed several reactions that employ thiols as HAT co-catalysts (Scheme 52). In an early example, methyl 2-mercaptoacetate **199** was deprotonated and oxidized by  $\text{Ir}(\text{ppy})_3^+$  to afford thiyl radical **201**; this intermediate can abstract a hydrogen atom from benzylic ethers such as **198**. The resulting radical **202** can add to both cyanoarenes<sup>237</sup> and imines.<sup>238</sup> The Tan group carried out benzylic bromination using a similar strategy with morpholine as the HAT catalyst.<sup>239</sup> Li reported the oxidation of primary alcohols using tandem photoredox/TEMPO catalysis.<sup>240</sup> The authors proposed a mechanism in which photoexcited  $\text{Ru}(\text{bpy})_3(\text{PF}_6)_2$  oxidizes TEMPO to the corresponding oxammonium, a known reagent for alcohol oxidation.

This method has been expanded to include the activation of other compounds with weak C–H bonds. The direct allylic coupling of simple alkenes such as **203** with cyanoarenes was achieved using HAT organocatalyst **204** (Scheme 53).<sup>241</sup> Primary alcohols can also be used, and their coupling with heteroarenes was followed by an intriguing spin-center shift rearrangement.<sup>242</sup> The presence of a base proved advantageous for these reactions, presumably by facilitating sulfur oxidation through a PCET process (see Section 2.3.1).

This Brønsted acid/base synergy was further exploited for the site selective activation of aliphatic alcohols (Scheme 54).<sup>243</sup> In these reactions, the radical cation of the catalytic quinuclidine is proposed to abstract a hydrogen atom adjacent to the alcohol. The phosphate co-catalyst in this process forms a hydrogen bond with the hydroxyl functionality; the resulting increase in hydricity facilitates the HAT process.

**2.4.3 Other Modes of Organocatalysis**—Rovis demonstrated that photoredox chemistry can also be merged with the use of chiral *N*-heterocyclic carbene (NHC) organocatalysis (Scheme 55).<sup>244</sup> Addition of NHC **209** to propionaldehyde **208** results in the formation of Breslow intermediate **212**. This nucleophilic species was used to trap THIQ iminium ion **185**, which was generated by photoquenched  $\text{Ru}^{\text{III}}$ .<sup>245–247</sup> The resulting amino alcohol **213** could fragment to form  $\alpha$ -amino ketone **211** in good enantioselectivity and regenerate the NHC catalyst.

Stephenson reported a procedure for the synthesis of symmetric anhydrides from carboxylic acids using photocatalysis (Scheme 56).<sup>248</sup> Their reaction is carried out in DMF, which is proposed to catalyze the dehydration by formation of the Vilsmeier reagent **216** *in situ*. The authors propose a mechanism in which photoexcited  $\text{Ru}(\text{bpy})_3\text{Cl}_2$  promotes reductive dehalogenation of  $\text{CBr}_4$  to form  $\cdot\text{CBr}_3$ . Addition of this radical to DMF, followed by oxidation and bromide exchange forms **216**. This can in turn act as an acyl transfer reagent for the formation of anhydride **215** from **214** with concomitant regeneration of DMF.

Finally, Hopkinson, Glorius, and coworkers merged a typical photoredox cycle with a catalytic halide salt in order to achieve the oxidative trifluoromethylthiolation of styrenes (Scheme 57).<sup>249</sup> In the mechanism proposed by these authors, the bromide additive reacts with *N*-(trifluoromethylthio)phthalimide **218** to afford highly reactive trifluoromethylsufenyl

bromide **220** *in situ*. This species undergoes photoreduction and mesolytic cleavage to form  $\cdot\text{SCF}_3$  and to regenerate  $\text{Br}^-$ . Addition of the sulfur-centered radical to styrene **217** followed by radical-polar crossover affords product **219**. Lu and Xiao proposed a conceptually similar application of halide catalysis in order to generate allyl iodides *in situ*, which could then be coupled with *N*-aryltetrahydroisoquinolines.<sup>250</sup>

## 2.5 Transition Metal Catalysis

Transition metal catalysis has become an indispensable tool in all areas of synthetic chemistry, for a variety of reasons. Among the most important features in the design of new organometallic transformations is the ability of a transition metal center to exist in multiple oxidation states, each of which can access distinct reactivity patterns. Thus, the combination of transition metal catalysis and photoredox catalysis offers unique opportunities for the innovative design of powerful synthetic transformations. Because the use of transition metal catalysts in tandem with photoredox catalysts is a relatively recent development, few of these reactions have been subject to detailed mechanistic interrogation, and there is still considerable ambiguity regarding many mechanistic subtleties in these processes. Broadly speaking, however, there are a handful of dominant reaction modes that effectively describe most current examples of photoredox/transition metal dual catalysis.

The following section is organized according to the manner in which the transition metal catalyst and the photocatalyst interact in the mechanisms proposed by the authors. First, we will discuss transition metal catalyzed reactions where photocatalysis produces an oxidation state change that facilitates an otherwise sluggish organometallic step (Figure 6A). These can occur either by direct electron transfer between the organometallic complex and the photocatalyst or be mediated by a photogenerated reactive intermediate such as superoxide. Second, we will discuss reactions in which a photogenerated reactive intermediate is intercepted by an organometallic complex (Figure 6B). In these reactions, the redox balance is often proposed to be maintained by a secondary back electron transfer between the organometallic fragment and the photocatalyst; however, the principal role of the photocatalyst in these methods is the independent production of the key reactive intermediate.

**2.5.1 Catalysis of Redox Steps**—Catalyst turnover by reoxidation of a reduced transition metal is often the rate-limiting process in oxidative organometallic transformations. To address this challenge, Rueping developed an indole synthesis based upon the intramolecular oxidative C–H arylation of enamides (Scheme 58).<sup>251</sup> The authors proposed a mechanism in which the organometallic steps are rapid but where aerobic oxidation of the  $\text{Pd}^0$  catalyst is slow. The authors hypothesized that a photocatalyst could facilitate this reoxidation process. The details of the oxidation have not yet been elucidated, but given the two-electron oxidation state change required, the mechanism must presumably be somewhat more complicated than a simple bimolecular photoinduced single electron transfer. Rueping has utilized a similar design strategy in oxidative Heck reactions of aryl amides<sup>252</sup> and phenols<sup>253</sup> catalyzed by rhodium and ruthenium, respectively.

Photocatalysts may also be used to enable novel or unusual reactivity by accessing higher metal oxidation states. The MacMillan laboratory demonstrated this concept in the coupling of simple alcohols with aryl bromides (Scheme 59).<sup>254</sup> Nickel-catalyzed cross couplings of this type are difficult due because C–O reductive elimination from Ni<sup>II</sup> is predicted to be thermodynamically uphill. However, oxidation to Ni<sup>III</sup> by photoexcited Ir(dF(CF<sub>3</sub>)ppy)<sub>2</sub>(dtbbpy)(PF<sub>6</sub>) renders this step energetically favorable. In the proposed catalytic cycle, Ni<sup>I</sup> is returned to Ni<sup>0</sup> by the reduced Ir<sup>II</sup> photocatalyst. A similar mechanism was invoked for the decarboxylative coupling of acids and acid chlorides,<sup>255</sup> as well as the oxidative coupling of anilines with alkenes reported by Jamison.<sup>256</sup>

A limited number of examples utilizing this strategy have been reported using other transition metal co-catalysts. Kobayashi disclosed a copper-catalyzed Chan–Lam protocol that employs Ir(ppy)<sub>3</sub> as a co-catalyst.<sup>257</sup> The key bond forming step is postulated to require reductive elimination from Cu<sup>III</sup>, which can be accessed either by PET to the photoexcited [Ir<sup>III</sup>]\* or by superoxide. You, Cho, and coworkers reported a Pd/Ir-dual catalysis strategy for the formation of carbazoles.<sup>258</sup> The photocatalyst is proposed to oxidize the intermediate complexes to either Pd<sup>III</sup> or Pd<sup>IV</sup> to facilitate the transformation.

Tunge developed a method for the decarboxylative allylation of alkanolic esters using a combination of Pd(PPh<sub>3</sub>)<sub>4</sub> and Ir(ppy)<sub>2</sub>(bpy)(BF<sub>4</sub>).<sup>259</sup> In their proposed mechanism (Scheme 60), reaction of allylic ester **225** with Pd<sup>0</sup> affords π-allyl complex **227**. Subsequent photooxidation of the aniline triggers radical decarboxylation. Palladium complex **228** may undergo reductive elimination and SET from Ir<sup>II</sup> to form product **226**, which has been suggested in related systems.<sup>260</sup> Alternatively, liberation and heterodimerization of *p*-aminobenzyl radical **229** with allyl radical **230** could also give rise to **226**. This pathway was postulated based on the observation of side products consistent with homodimerization of **229** and **230**, as well as stereochemical probe experiments.<sup>261</sup> A similar transformation was reported by Lu, Xiao, and coworkers using an allyl phosphate in place of the ester.<sup>262</sup> In both cases, the extent to which palladium is involved in the bond-forming step seems to depend on the stability of the possible radical intermediate, with more stable species favoring the latter pathway, and less stable radicals favoring the former.

**2.5.2 Catalysis of Downstream Steps**—The facile photooxidation of tetrahydroisoquinoline **153** to the corresponding iminium ion **185** has become a relatively common means to test the compatibility of photoredox catalysis with complementary activation modes. As such, several recent reports have described the reaction of the photogenerated iminium electrophile with organometallic nucleophiles. Stephenson<sup>263</sup> and Rueping<sup>264</sup> independently reported that metal acetylides are good nucleophiles in this context. These groups reported cross dehydrogenative coupling reactions in which silver or copper salts activate terminal alkyne **231** and the resulting metal acetylide **233** adds to iminium ion **185** (Scheme 61). An asymmetric adaptation of this method was reported by Li and coworkers using (*R*)-QUINAP as a chiral ligand for copper.<sup>265</sup> Zhao demonstrated that BODIPY photocatalysts could also be used to perform the amine oxidation in place of ruthenium or iridium species.<sup>266</sup>

Sanford reported an early example of photoredox/transition metal dual catalysis (Scheme 62).<sup>267,268</sup> Her laboratory's detailed mechanistic studies of the Pd-catalyzed oxidative C–H arylation of phenylpyridines had revealed that the metallation of the C–H bond is relatively facile but that oxidation of the resulting cyclometallated Pd<sup>II</sup> intermediate **237** by hypervalent iodoarene oxidants is inefficient and rate-limiting. Thus, Sanford developed a strategy to utilize photogenerated aryl radicals as more reactive oxidants in these reactions. Taking advantage of an insight reported by Cano-Yelo and Deronzier,<sup>269</sup> Sanford generated aryl radical **238** by the photocatalytic reduction of aryl diazonium salt **235**. This species reacts rapidly at room temperature with cyclometallated intermediate **237** to generate arylated Pd complex **239** at a higher oxidation state, which is poised to undergo rapid reductive elimination. This dual catalyst strategy enabled the Pd-catalyzed C–H arylation reaction to be conducted at room temperature under conditions considerably milder than previously reported.

Gold complexes have become recognized as synthetically powerful soft Lewis acidic catalysts for the activation of carbon–carbon multiple bonds. Several reactions involving the interception of photogenerated aryl radicals with organometallic gold complexes have recently been described. Glorius reported a strategy for combining gold and photoredox catalysis to effect the alkoxyarylation of alkenes (Scheme 63).<sup>270,271</sup> In this process, the role of the  $\pi$ -acidic catalyst (Ph<sub>3</sub>PAu)NTf<sub>2</sub> is to activate the alkene of substrate **240** toward alcohol addition. The authors proposed that the resulting alkyl gold species **242** is attacked by a photocatalytically generated aryl radical **238**. This combination would produce a high-valent organogold species that is poised to undergo facile reductive elimination, in conceptual analogy to the photocatalytic Pd-catalyzed arylation developed by Sanford (Scheme 62).<sup>267</sup>

Toste suggested a slightly different mechanism for the gold-catalyzed arylative ring expansion of vinyl cyclobutanol **243** (Scheme 64).<sup>272,273</sup> In his proposal, Au<sup>I</sup> first adds to photochemically generated aryl radical **238**, before alkene coordination and oxidation. The resultant high-valent intermediate **245** is well-suited to catalyze the ring expansion and reductive elimination giving rise to product **244**. This strategy has since been utilized for a variety of methods, including the coupling of arenes with terminal alkynes<sup>274,275</sup> and propargyl alcohols,<sup>276,277</sup> as well as the hydroarylation of alkynes<sup>277</sup> and the formation of sp<sup>2</sup> C–P bonds.<sup>278</sup>

First-row transition metals are particularly promising partners for dual catalytic systems involving photoredox catalysis due to the relative ease by which they undergo one-electron redox changes. Molander exploited this behavior in several examples of organoboron cross coupling using nickel chemistry in tandem with photoredox catalysis.<sup>279</sup> The initial studies investigating this combination involved the reaction of trifluoroborate **246** and aryl bromide **247** (Scheme 65). Oxidation of **246** by the photoexcited iridium catalyst generates benzylic radical **249**. Concomitantly, the aryl bromide substrate undergoes oxidative addition to Ni<sup>0</sup>. The resulting Ni<sup>II</sup> complex **250** then intercepts the benzylic radical to afford Ni<sup>III</sup> **251**. Reductive elimination from this species releases cross-coupled product **248**, along with Ni<sup>I</sup>, which can be reduced by Ir<sup>II</sup>. Alternatively, computational studies suggest that benzylic radical **249** may instead add directly to Ni<sup>0</sup> to form Ni<sup>I</sup> complex **252**, and that the oxidative

addition of aryl bromide **247** and subsequent reductive elimination occur after this step.<sup>280</sup> Interestingly, the dissociation of benzyl radical from Ni<sup>III</sup> complex **251** is facile, meaning that there is a rapid equilibrium between **250** and **251** prior to reductive elimination, even if initial formation of **251** proceeds through Ni<sup>I</sup> complex **252**. This has important ramifications for stereoinduction in this system (*vide infra*).

This strategy has been applied to benzylic,<sup>279,281</sup> secondary alkyl,<sup>282</sup> alkoxyethyl,<sup>283,284</sup> and  $\alpha$ -amino<sup>285</sup> boron nucleophiles. Notably, the mild conditions utilized for the photooxidation of the trifluoroborate salts do not affect other organoboron species. Thus, Molander has described conditions for the use of aryl halides bearing boronate esters and other less reactive boron functional groups in photoredox reactions, affording products poised for further elaboration by cross-coupling.<sup>286</sup> Finally, preliminary reports have demonstrated asymmetric induction using chiral ligands on the nickel catalyst, although enantioselectivities reported to date are moderate.<sup>279,280</sup> The facile dissociation of benzylic radical from Ni<sup>III</sup> scrambles the stereocenter, thereby rendering the transformation stereoconvergent. Moreover, the rapid equilibration between Ni<sup>II</sup> and both diastereomers of Ni<sup>III</sup> creates a dynamic kinetic resolution in which the stereoselectivity is determined in the final reductive elimination.<sup>280</sup>

MacMillan and Doyle published a concurrent report of a similar Ir/Ni dual catalytic system that employs carboxylic acids in place of organoboron reagents (Scheme 66).<sup>287</sup> Photooxidative decarboxylation of **253** affords  $\alpha$ -amino radical **255**. The authors proposed that this radical serves the same function as the benzylic radical in the Molander system; addition to Ni<sup>II</sup> adduct **256** affords a high-valent Ni<sup>III</sup> complex **257** that is prone towards reductive elimination, resulting in the formation of product **254**. This method was employed for the cross-coupling of aryl and vinyl halides to radicals derived from  $\alpha$ -amino,  $\alpha$ -oxy, and alkyl carboxylic acids.<sup>288</sup> Acyl radicals, generated from  $\alpha$ -keto acids, can be added to indoles<sup>289</sup> and aryl halides.<sup>290</sup> The latter intermediates can also participate in palladium-catalyzed cross coupling to afford direct C–H acylation of acetamides.<sup>291</sup> Furthermore, Luo and Zhang showed that organic donor-acceptor fluorophores are effective photocatalysts for these transformations.<sup>292</sup> Lastly, MacMillan and Fu recently developed an asymmetric variant of the  $\alpha$ -amino acid/aryl halide coupling using semicorrin-type bis(oxazoline) ligands for nickel.<sup>293</sup> The reaction is stereoconvergent and dictated entirely by nickel, as the radical intermediate following decarboxylation is achiral.

Several other noteworthy developments have been reported recently in this area. Investigators at AstraZeneca demonstrated that both Molander and MacMillan's protocols can be carried out using Ni<sup>II</sup> salts under aerobic conditions.<sup>294</sup> Independently, Molander<sup>295,296</sup> and Fensterbank<sup>297,298</sup> showed that hypervalent silicon compounds can be oxidized and fragment to alkyl radicals, which can engage in nickel-catalyzed cross-coupling as previously described. In addition to C–C bonds, this dual catalyst system is capable of forging C–S bonds by reacting with thiyl radicals, which can be generated from thiols either by oxidation/deprotonation<sup>299</sup> or by HAT to an alkyl radical.<sup>300</sup> Analogously, Lu, Xiao, and coworkers were able to achieve C–P cross-couplings using phosphorus-centered radicals, generated by oxidation/deprotonation of the phosphine oxide.<sup>301</sup>

Copper has also been utilized in dual catalytic systems of this type. Sanford reported the trifluoromethylation of boronic acids using  $\text{Ru}(\text{bpy})_3\text{Cl}_2$  and  $\text{CuOAc}$  (Scheme 67).<sup>302</sup> Photocatalytic reductive dehalogenation of trifluoromethyl iodide **259** affords trifluoromethyl radical **261**, which can be intercepted by  $\text{Cu}^{\text{II}}$ . Transmetalation with the arylboronic acid and reductive elimination provides product **260** along with  $\text{Cu}^{\text{I}}$ , which is proposed to undergo photooxidation to generate  $\text{Cu}^{\text{II}}$ .

A conceptually distinct photocatalytic system was reported by Saito, who performed the oxidation of adamantane and cyclododecane **257** using  $N,N'$ -dimethyl-2,7-diazapyrenium ( $\text{MDAP}^{2+}$ ) and iron co-catalysts (Scheme 68).<sup>303</sup> The mechanism of this process is likely to be a Fenton-type alkane oxidation by hydroxyl radical.<sup>304</sup> The role of the photocatalyst would thus be to photoreduce dioxygen in situ, and the Fe catalyst would result in subsequent homolytic production of hydroxyl radical.

Wu has reported several examples of acceptorless dehydrogenative reactions that use  $\text{Co}(\text{dmgH})_2(\text{DMAP})\text{Cl}$  in tandem with a photocatalyst such as  $\text{Ru}(\text{bpy})_3(\text{PF}_6)_2$ <sup>305,306</sup> or Eosin Y.<sup>307</sup> The proposed mechanism of one representative example is depicted in Scheme 69. Photooxidation and deprotonation<sup>308</sup> of **265** affords thioamidyl radical **267**, which undergo cyclization to afford **268**.<sup>309</sup> The  $\text{Co}^{\text{III}}$  catalyst is then proposed to be sequentially reduced by  $\text{Ru}^{\text{I}}$  and by radical **268**. Proton transfer from the pentadienyl cation to the  $\text{Co}^{\text{I}}$  complex results in the formation of rearomatized benzothiazole **266** and regenerates the  $\text{Co}^{\text{III}}$  catalyst with evolution of hydrogen gas. Wu has exploited a similar design strategy for the addition of  $\beta$ -keto esters to photocatalytically generated oxocarbenium ions.<sup>310</sup>

## 2.6. Enzymatic Catalysis

Enzymes can offer several attractive features in synthetic applications, including high chemo-, regio- and stereoselectivity, as well as the ability to use environmentally benign terminal oxidants and reductants. However, relatively few reports have described strategies to couple the catalytic reactivity of enzymes to photocatalytic reactions to date. Willner developed several systems for reductive enzymatic processes that utilize these cooperative effects (Scheme 70).  $\text{Ru}(\text{bpy})_3^{2+}$  transfers reducing equivalents from a terminal reductant (EDTA) to a redox mediator ( $\text{MV}^{2+}$ ), which then proceeds to turn over enzymatic reduction of  $\text{NADP}^+$  to NADPH. The resulting NADPH is subsequently utilized in enzymatic ketone reductions<sup>141,311</sup> and reductive aminations.<sup>312,313</sup> Park used a similar strategy for the enzymatic conversion of  $\alpha$ -ketoglutarate to L-glutamate. In these studies,  $[\text{Cp}^*\text{Rh}(\text{bpy})(\text{H}_2\text{O})]^{2+}$  was employed as a redox mediator to facilitate enzymatic reduction of  $\text{NADP}^+$ .<sup>314,315</sup> In other cases, these cofactors were proposed to turn over the photocatalyst directly.<sup>316</sup>

Oxidative transformations have also been carried out using enzymatic co-catalysis, including the oxidation of alcohols,<sup>317</sup> hydroxylation of C–H bonds, epoxidation of alkenes,<sup>318</sup> oxidative decarboxylation of fatty acids,<sup>319</sup> and Baeyer–Villiger reactions of ketones.<sup>320</sup> These processes typically involve the photochemical generation of oxidants such as  $\text{H}_2\text{O}_2$  or  $\text{NADP}^+$ , which then participate in downstream enzyme catalysis.



### 3. Photoinduced Hydrogen Atom Transfer

A second important mechanism of photocatalytic activation involves production of radical intermediates via the transfer of a hydrogen atom from an organic substrate directly to a photoexcited chromophore. The previous section discussed several examples of transformations that involve two discrete photooxidation and deprotonation steps, which can produce similar reactive radical intermediates. However, the feasibility of concerted hydrogen atom transfer is largely determined by C–H bond strength, while redox potential is the relevant thermodynamic parameter in photoinduced electron transfer processes. The previous section also discussed C–H abstraction using HAT co-catalysts as a strategy for photoredox catalysis (Section 2.4.2). The transformations discussed in the following section, however, involve direct cleavage of a C–H bond by the photocatalyst and thus do not require a secondary catalyst to generate the key radical intermediate.

Jones, Edwards, and Parr reported an example using benzophenone in conjunction with Cu<sup>II</sup> to perform the aerobic dehydration of alkanes (Scheme 71).<sup>321</sup> The authors proposed a mechanism in which photoexcited benzophenone abstracts H• from cyclohexane to generate alkyl radical **272**. Cu<sup>II</sup> subsequently serves to both oxidize this radical and regenerate the photocatalyst, and Cu<sup>I</sup> can be reoxidized by oxygen.

More recently, Sorensen reported similar reactivity using polyoxotungstate TBADT and a cobaloxime co-catalyst.<sup>322</sup> This dual catalytic system was effective for the dehydrogenation of both alkanes and alcohols (Scheme 72). After excitation, the polyoxometalate photocatalyst can abstract a hydrogen atom from **273**, and the resulting radical can undergo a second HAT step with the cobalt catalyst, generating oxidized product **3**. The tandem catalytic cycle is turned over by evolution of H<sub>2</sub> from the cobaloxime complex.

### 4. Photoinduced Energy Transfer

A third major mechanism of photocatalytic activation involves the sensitization of organic substrates via energy transfer. In the context of organic synthesis, the predominant mechanism for activation of substrates by this method has been the Dexter electron exchange mechanism.<sup>5</sup> This process can be conceptualized as simultaneous photoinduced electron transfer both to and from the excited state of the photocatalyst. This results in the generation of an electronically excited substrate molecule and concomitant relaxation of the photocatalyst to its electronic ground state (Scheme 73). Importantly, the electron exchange process results in no net redox chemistry. Thus electrochemical potentials are not typically useful predictors of reactivity for these reactions. Instead, the relative triplet state energies for both photocatalyst and substrate are more important determinants in the feasibility of energy transfer.

Photosensitization by energy transfer thus provides a means to access the distinctive reactivity of electronically excited molecules, with several important advantages over direct photoexcitation of the substrate. First, direct irradiation of ground-state, closed-shell organic molecules leads to the formation of excited singlets; these often do not undergo efficient intersystem crossing to longer-lived triplet states and thus relax rapidly to the ground state

before useful bimolecular reactions can occur. Useful triplet sensitizers, on the other hand, generally undergo rapid intersystem crossing and provide a more efficient route for the production of triplet state organic compounds. Additionally, direct photoexcitation of most organic compounds requires relatively high-energy UV light that can be incompatible with common organic functional groups such as organohalides and nitroarenes. Most common photocatalytic chromophores, however, typically absorb at longer wavelengths that are more compatible with the densely functionalized, complex organic structures common in synthetic applications.

On the other hand, the use of co-catalysts to modulate the reactivity of photocatalytically generated excited state intermediates presents unique challenges. The lifetimes of the open-shell radical intermediates generated through electron transfer or hydrogen atom transfer photocatalysis, though short, are nevertheless substantially longer than the lifetimes of electronically excited intermediates. A variety of distinctive deactivation modes are available to photoexcited compounds, including unimolecular emissive and vibrational relaxation pathways that are generally fast. As such, the ability of a second molecular catalyst to intercept the electronically excited substrate and impact its reactivity is limited.

Nevertheless, several reports of dual catalyst systems have proposed that the photocatalytic component engages in an energy transfer process. Many of these reactions involve the photochemical generation of singlet oxygen, the lifetime of which is on the order of several hundreds of microseconds,<sup>323</sup> much longer than the lifetimes of simple excited state organic compounds. This section covers the use of energy transfer photocatalysis in conjunction with a second organic, transition metal, or Brønsted acid co-catalyst.

#### 4.1 Transition Metal Catalysis

Adam reported an early example in which a transition metal catalyst is used to activate the ground-state product of a photosensitization reaction. Tetraphenylporphyrin (H<sub>2</sub>TPP) is a common photocatalyst for the production of singlet oxygen via energy transfer. Reaction of <sup>1</sup>O<sub>2</sub> with alkene **275** affords allylic hydroperoxide **277**, which subsequently reacts with a Ti<sup>IV</sup> alkoxide catalyst (Scheme 74). This results in O-atom transfer to the alkene to generate  $\alpha$ -epoxy alcohol **276**.<sup>324</sup>

The scope for this transformation is remarkably broad, and the primary competing reactions are reduction of the allylic hydroperoxide for electron deficient substrates in which the epoxidation step is slow. Additionally, the authors demonstrate that the use of (+)-diethyl tartrate (DET) as a chiral element in the epoxidation generates enantioenriched products in good yields and moderate enantioselectivities (Scheme 75).

Campestrini recently demonstrated a similar transformation using Mo(CO)<sub>6</sub> as a catalyst.<sup>325</sup> However, because the molybdenum catalyst consumes two equivalents of hydroperoxide for each epoxide formed, a maximum theoretical yield of 50% is possible for each olefin substrate. Nevertheless, yields of up to 38% (77% of theoretical maximum) were obtained under the optimized conditions.

Krief developed a multi-catalytic cascade process exploiting singlet oxygen sensitization for olefin dihydroxylation (Scheme 76).<sup>326</sup> Earlier work by this group had shown that photochemically generated singlet oxygen can oxidize selenides such as **282**.<sup>327</sup> The resulting selenoxide **283** is capable of oxidizing Os<sup>VI</sup> to Os<sup>VIII</sup>.<sup>328</sup> Thus, by combining Rose Bengal as a photocatalyst for singlet oxygen generation, benzyl phenyl selenide **282**, and catalytic K<sub>2</sub>OsO<sub>2</sub>(OH)<sub>4</sub>, the authors were able to develop a high-yielding protocol for an aerobic version of the Sharpless asymmetric dihydroxylation<sup>329</sup> of **280** to **281**.

The use of photocatalysts to directly interact with a second catalytic transition metal species can be considered a conceptually different strategy from the preceding examples. Kobayashi proposed such a mechanism<sup>330</sup> to rationalize the observation that the addition of Ir(ppy)<sub>3</sub> accelerates the rate of a photochemical Ullman coupling developed recently by Fu and Peters (Scheme 77).<sup>331–333</sup> The key step of the original, single-catalyst system involves photoinduced electron transfer between Cu<sup>I</sup> bis(carbazole) complex **287** and iodoarene **285**; this process results in the formation of aryl radical **238** that recombines with the oxidized Cu<sup>II</sup> complex to furnish a product featuring a new C–N bond. Kobayashi<sup>330</sup> suggests that the formation of excited [Cu<sup>I</sup>]\* complex **288** can arise from sensitization of **287** by <sup>3</sup>[Ir]\*. The main benefit of the dual-catalyst system is the ability to excite the Ir complex at longer wavelengths than the Cu<sup>I</sup> carbazole complex.

## 4.2. Organocatalysis

A pioneering example of the use of chiral amines to influence energy transfer photoreactions was reported by Shioiri,<sup>334</sup> who investigated the enantioselective photooxygenation of *N*-Moc tryptamine **289** using photogenerated singlet oxygen and (–)-nicotine (Scheme 78). Although the mechanism of stereoinduction was not proposed, experimentally significant levels of enantiomeric excess were reported.

Subsequent work by Córdova also utilized chiral amine co-catalysts in asymmetric photooxygenation reactions (Scheme 79). This work took advantage of the enantiocontrol offered by amino acids and derivatives such as the Jørgensen–Hayashi diarylprolinol<sup>335</sup> in a range of aldehyde<sup>336,337</sup> and ketone<sup>338</sup> functionalization reactions. Reaction of the transient chiral enamine intermediate with photogenerated singlet oxygen was proposed to furnish hydroperoxide **292** *in situ*, which was reduced to diol **293** upon workup with NaBH<sub>4</sub>. Gryko has reported that the formation of trace <sup>1</sup>O<sub>2</sub>-derived oxidative byproducts can be observed by GC-MS to support the intermediacy of both enamine and singlet oxygen in this reaction.<sup>339</sup>

Meng demonstrated that asymmetric phase transfer catalysis could also be used to control the stereochemistry of photocatalytic enolate oxidation reactions (Scheme 80).<sup>340</sup> The optimal system utilized quaternized cinchona alkaloid salt **295**<sup>+</sup> Br<sup>–</sup> as the phase transfer catalyst and H<sub>2</sub>TPP as the sensitizer for singlet oxygen generation. Upon deprotonation, β-ketoester **294** was converted to enolate **297**, and the addition of <sup>1</sup>O<sub>2</sub> was controlled by chiral counterion **295**<sup>+</sup>. The activation of oxygen by energy transfer was validated using experiments showing that the reaction rate was retarded in the presence of a singlet oxygen trap (DABCO)<sup>341</sup> but not in the presence of a trap for superoxide (*p*-benzoquinone).<sup>342</sup>

### 4.3 Brønsted Acid Catalysis

König has studied the photocatalytic amination of electron-rich heteroarenes with benzoyl azides and reported that the use of a Brønsted acid co-catalyst is necessary for optimal reactivity (Scheme 81).<sup>343</sup> The authors propose photocatalytic activation of benzoyl azide **298** using Ru(bpy)<sub>3</sub>Cl<sub>2</sub> as a triplet sensitizer, which liberates dinitrogen to generate free nitrene **301**. Under neutral reaction conditions, this intermediate can undergo rapid unimolecular Curtius rearrangement to a phenyl isocyanate **302** or perform a C–H abstraction to yield benzamide **303**. However, under the strongly acidic reaction conditions, the authors suggest that protonation of the nitrene minimizes these side reactions and promotes electrophilic attack onto electron rich aromatic systems to afford C–H amination product **300**.

Hanson has reported that excited state proton transfer chemistry can be sensitized using transition metal chromophores (Scheme 82).<sup>344</sup> The hydroxyl moiety of an excited state naphthol **307** is significantly acidified relative to the ground state **306** and is capable of protonating silyl enol ethers. While this reaction can be accessed directly by UV irradiation of appropriate naphthols, the authors show that the addition of an Ir sensitizer enables longer wavelengths of light to be used.

## 5. Conclusion and Outlook

There has recently been an increasing awareness among synthetic chemists that the use of two catalysts in a single chemical reaction is a powerful design strategy that can effect transformations that are either difficult or impossible to achieve otherwise. It is interesting to reflect on the observation that dual catalyst strategies have been a major theme of research in organic photochemistry for many decades, long predating the recent renewal of interest in synthetic photoredox catalysis. Non-photoactive co-catalysts have been used to alter the rate of all aspects of photocatalytic reactions. They can be used to impact the properties of the photocatalyst or the rate of the photoactivation steps; they can be used to transiently generate intermediates that intersect with the excited state of the photocatalyst; or they can be used to control the rate and selectivity of steps that occur downstream of the photoactivation step itself.

One might rationalize the uniquely enabling impact of dual catalyst strategies in photochemistry as a consequence of the ways in which photocatalysis differs from other modes of catalysis. The ability to absorb and convert the energy of a photon into useful chemical potential does not necessarily require strongly bonding interactions with the substrate. Thus photocatalysts often do not need to possess potentially reactive binding sites, and the range of co-catalysts that consequently have been shown to be compatible with photocatalysis spans a remarkably broad range, from simple protic additives to enzymes and structurally complex transition metal assemblies. As photochemistry becomes an increasingly common tool for synthesis, the development of new dual catalytic approaches will surely continue to be a powerfully enabling strategy for the photochemical construction of complex organic molecules.

## Acknowledgments

We are grateful to the NIH (GM09888) and the Sloan Foundation for financial support.

## References

1. Albini, A.; Fagnoni, M. *Photochemically Generated Intermediates in Synthesis*. Wiley & Sons; Hoboken: 2013.
2. Kavarnos GJ, Turro NJ. Photosensitization by Reversible Electron Transfer: Theories, Experimental Evidence, and Examples. *Chem Rev.* 1986; 86:401–449.
3. Scaiano JC. Intermolecular Photoreductions of Ketones. *J Photochem.* 1973; 2:81–118.
4. Tzirakis MD, Lykakis IN, Orfanopoulos M. Decatungstate as an Efficient Photocatalyst in Organic Chemistry. *Chem Soc Rev.* 2009; 38:2609–2621. [PubMed: 19690741]
5. Turro NJ. Energy Transfer Processes. *Pure Appl Chem.* 1977; 49:405–429.
6. Studer A. The Persistent Radical Effect in Organic Synthesis. *Chem Eur J.* 2001; 7:1159–1164. [PubMed: 11322540]
7. Fischer H. The Persistent Radical Effect: A Principle for Selective Radical Reactions and Living Radical Polymerizations. *Chem Rev.* 2001; 101:3581–3610. [PubMed: 11740916]
8. Studer A. Tin-Free Radical Chemistry using the Persistent Radical Effect: Alkoxyamine Isomerization, Addition Reactions and Polymerizations. *Chem Soc Rev.* 2004; 33:267–273. [PubMed: 15272366]
9. Cismesia MA, Yoon TP. Characterizing Chain Processes in Visible Light Photoredox Catalysis. *Chem Sci.* 2015; 6:5426–5434. [PubMed: 26668708]
10. Laidler KJ. A Glossary of Terms Used in Chemical Kinetics, Including Reaction Dynamics (IUPAC Recommendations 1996). *Pure Appl Chem.* 1996; 68:149–192.
11. Wubbels GG. Catalysis of Photochemical Reactions. *Acc Chem Res.* 1983; 16:285–292.
12. Parmon V, Emeline AV, Serpone N. Suggested Terms and Definitions in Photocatalysis and Radiocatalysis. *Int J Photoenergy.* 2002; 4:91–131.
13. Studer A, Curran DP. Catalysis of Radical Reactions: A Radical Chemistry Perspective. *Angew Chem Int Ed.* 2016; 55:58–102.
14. Fox MA, Dulay MT. Heterogeneous Photocatalysis. *Chem Rev.* 1993; 93:341–357.
15. Shiraishi Y, Hirai T. Selective Organic Transformations on Titanium Oxide-Based Photocatalysts. *J Photochem Photobiol C.* 2008; 9:157–170.
16. Kisch H. Semiconductor Photocatalysis—Mechanistic and Synthetic Aspects. *Angew Chem Int Ed.* 2013; 52:812–847.
17. Zou X, Tao Z, Asefa T. Semiconductor and Plasmonic Photocatalysis for Selective Organic Transformations. *Curr Org Chem.* 2013; 17:1274–1287.
18. Vallavoju N, Sivaguru J. Supramolecular Photocatalysis: Combining Confinement and Non-Covalent Interactions to Control Light Initiated Reactions. *Chem Soc Rev.* 2014; 43:4084–4101. [PubMed: 24705505]
19. Bibal B, Mongin C, Bassani DM. Template Effects and Supramolecular Control of Photoreactions in Solution. *Chem Soc Rev.* 2014; 43:4179–4198. [PubMed: 24480895]
20. Ramamurthy V, Mondal B. Supramolecular Photochemistry Concepts Highlighted with Select Examples. *J Photochem Photobiol C.* 2015; 23:68–102.
21. Yang C, Inoue Y. Supramolecular Photochirogenesis. *Chem Soc Rev.* 2014; 43:4123–4143. [PubMed: 24292117]
22. Fagnoni M, Dondi D, Ravelli D, Albini A. Photocatalysis for the Formation of the C–C Bond. *Chem Rev.* 2007; 107:2725–2756. [PubMed: 17530909]
23. Hoffmann N. Efficient Photochemical Electron Transfer Sensitization of Homogeneous Organic Reactions. *J Photochem Photobiol C.* 2008; 9:43–60.
24. Narayanam JMR, Stephenson CRJ. Visible Light Photoredox Catalysis: Applications in Organic Synthesis. *Chem Soc Rev.* 2011; 40:102–113. [PubMed: 20532341]

25. Tucker JW, Stephenson CRJ. Shining Light on Photoredox Catalysis: Theory and Synthetic Applications. *J Org Chem.* 2012; 77:1617–1622. [PubMed: 22283525]
26. Xuan J, Xiao WJ. Visible-Light Photoredox Catalysis. *Angew Chem Int Ed.* 2012; 51:6828–6838.
27. Reckenthäler M, Griesbeck AG. Photoredox Catalysis for Organic Syntheses. *Adv Synth Catal.* 2013; 355:2727–2744.
28. Xi Y, Yi H, Lei A. Synthetic Applications of Photoredox Catalysis with Visible Light. *Org Biomol Chem.* 2013; 11:2387–2403. [PubMed: 23426621]
29. Schultz DM, Yoon TP. Solar Synthesis: Prospects in Visible Light Photocatalysis. *Science.* 2014; 343:1239176-1–1239176-8. [PubMed: 24578578]
30. Mattay, J.; Griesbeck, A., editors. *Photochemical Key Steps in Organic Synthesis: An Experimental Course Book.* VCH; Weinheim: 1994.
31. Iriondo-Alberdi J, Greaney MF. Photocycloaddition in Natural Product Synthesis. *Eur J Org Chem.* 2007:4801–4815.
32. Hoffmann N. Photochemical Reactions as Key Steps in Organic Synthesis. *Chem Rev.* 2008; 108:1052–1103. [PubMed: 18302419]
33. Bach T, Hehn JP. Photochemical Reactions as Key Steps in Natural Product Synthesis. *Angew Chem Int Ed.* 2011; 50:1000–1046.
34. Beatty JW, Stephenson CRJ. Amine Functionalization via Oxidative Photoredox Catalysis: Methodology Development and Complex Molecule Synthesis. *Acc Chem Res.* 2015; 48:1474–1484. [PubMed: 25951291]
35. Rau H. Asymmetric Photochemistry in Solution. *Chem Rev.* 1983; 83:535–547.
36. Inoue Y. Asymmetric Photochemical Reactions in Solution. *Chem Rev.* 1992; 92:741–770.
37. Brimiouille R, Lenhart D, Maturi MM, Bach T. Enantioselective Catalysis of Photochemical Reactions. *Angew Chem Int Ed.* 2015; 54:3872–3890.
38. Meggers E. Asymmetric Catalysis Activated by Visible Light. *Chem Commun.* 2015; 51:3290–3301.
39. Salomon RG. Homogeneous Metal-Catalysis in Organic Photochemistry. *Tetrahedron.* 1983; 39:485–575.
40. Tepy F. Photoredox Catalysis by  $[\text{Ru}(\text{bpy})_3]^{2+}$  to Trigger Transformations of Organic Molecules. Organic Synthesis using Visible-Light Photocatalysis and its 20th Century Roots. *Collect Czech Chem Commun.* 2011; 76:859–917.
41. Hoffmann N. Homogeneous Photocatalytic Reactions with Organometallic and Coordination Compounds—Perspectives for Sustainable Chemistry. *ChemSusChem.* 2012; 5:352–371. [PubMed: 22287209]
42. Prier CK, Rankic DA, MacMillan DWC. Visible Light Photoredox Catalysis with Transition Metal Complexes: Applications in Organic Synthesis. *Chem Rev.* 2013; 113:5322–5363. [PubMed: 23509883]
43. Koike T, Akita M. Visible-Light Radical Reaction Designed by Ru- and Ir-Based Photoredox Catalysis. *Inorg Chem Front.* 2014; 1:562–576.
44. Ravelli D, Fagnoni M, Albini A. Photoorganocatalysis. What for? *Chem Soc Rev.* 2013; 42:97–113. [PubMed: 22990664]
45. Hari DP, König B. Synthetic Applications of Eosin Y in Photoredox Catalysis. *Chem Commun.* 2014; 50:6688–6699.
46. Fukuzumi S, Ohkubo K. Organic Synthetic Transformations using Organic Dyes as Photoredox Catalysts. *Org Biomol Chem.* 2014; 12:6059–6071. [PubMed: 24984977]
47. Hopkinson MN, Sahoo B, Li JL, Glorius F. Dual Catalysis Sees the Light: Combining Photoredox with Organo-, Acid, and Transition-Metal Catalysis. *Chem Eur J.* 2014; 20:3874–3886. [PubMed: 24596102]
48. Mattes SL, Farid S. Photochemical Cycloadditions via Exciplexes, Excited Complexes, and Radical Ions. *Acc Chem Res.* 1982; 15:80–86.
49. Bauld NL. Cation Radical Cycloadditions and Related Sigmatropic Reactions. *Tetrahedron.* 1989; 45:5307–5363.

50. Stirk KM, Kiminkinen LKM, Kenttämaa HI. Ion-Molecule Reactions of Distonic Radical Cations. *Chem Rev.* 1992; 92:1649–1665.
51. Mizuno K, Otsuji Y. Addition and Cycloaddition Reactions via Photoinduced Electron Transfer. *Top Curr Chem.* 1994; 169:301–346.
52. Hintz S, Heidebreder A, Mattay J. Radical Ion Cyclizations. *Top Curr Chem.* 1996; 177:77–124.
53. Schmittel M, Burghart A. Understanding Reactivity Patterns of Radical Cations. *Angew Chem Int Ed.* 1997; 36:2550–2589.
54. Mella M, Fagnoni M, Freccero M, Fasani E, Albini A. New Synthetic Methods via Radical Cation Fragmentation. *Chem Soc Rev.* 1998; 27:81–89.
55. Schmittel, M.; Ghorai, MK. Reactivity Patterns of Radical Ions-A Unifying Picture of Radical-Anion and Radical-Cation Transformations. In: Balzani, V., editor. *Electron Transfer in Chemistry.* Wiley-VCH; Weinheim: 2001. p. 5-54.
56. Cossy J, Belotti D. Generation of Ketyl Radical Anions by Photoinduced Electron Transfer (PET) between Ketones and Amines. *Synthetic Applications. Tetrahedron.* 2006; 62:6459–6470.
57. Ischay MA, Yoon TP. Accessing the Synthetic Chemistry of Radical Ions. *Eur J Org Chem.* 2012:3359–3372.
58. Hoffman MZ, Bolletta F, Moggi L, Hug GL. Rate Constants for the Quenching of Excited States of Metal Complexes in Fluid Solution. *J Phys Chem Ref Data.* 1989; 18:219–543.
59. Generally speaking, the term “cosensitizer” is commonly used in the photochemical literature while “redox mediator” is used in the electrochemical literature to describe the same concept. We prefer the latter term as it highlights the mechanistic distinction between these PET processes and energy transfer sensitization, which is discussed further in Section 4. These terms are sometimes also used to describe simple quenching processes (e.g. Ref. 60–62) which further obfuscates their meaning. See also Ref. 67.
60. Tazuke S, Kitamura N. Photoinduced Ternary Electron Transfer Reactions: a Novel Application to Electron Transfer Sensitization. *J Chem Soc, Chem Commun.* 1977:515–516.
61. Noyori R, Kurimoto I. Photoinduced Transacetalization using a Tris(bipyridine)ruthenium(II)–Methyl Viologen Cosensitizing System. *J Chem Soc, Chem Commun.* 1986:1425–1426.
62. Fagnoni M, Mella M, Albini A. Electron-Transfer-Photosensitized Conjugate Alkylation. *J Org Chem.* 1998; 63:4026–4033.
63. Masuhara H, Mataga N. Ionic Photodissociation of Electron Donor-Acceptor Systems in Solution. *Acc Chem Res.* 1981; 14:312–318.
64. Gould IR, Ege D, Moser JE, Farid S. Efficiencies of Photoinduced Electron-Transfer Reactions: Role of the Marcus Inverted Region in Return Electron Transfer within Geminate Radical-Ion Pairs. *J Am Chem Soc.* 1990; 112:4290–4301.
65. Lewis FD, Bedell AM, Dykstra RE, Elbert JE, Gould IR, Farid S. Photochemical Generation, Isomerization, and Oxygenation of Stilbene Cation Radicals. *J Am Chem Soc.* 1990; 112:8055–8064.
66. Mattay J, Vondenhof M. Contact and Solvent-Separated Radical Ion Pairs in Organic Photochemistry. *Top Curr Chem.* 1991; 159:219–255.
67. Another commonly exploited pair is phenanthrene/1,4-dicyanobenzene (Phen/DCB). For examples, see Refs. 68–70. However, the generally accepted mechanism for these reactions is excitation of Phen followed DCB quenching, and subsequent electron transfer from a substrate to Phen<sup>•+</sup>. Thus, although Phen mediates otherwise unproductive electron transfer between the substrate and DCB, this is simply a case of secondary oxidative quenching (i.e., Figure 3B). For clarity, we reserve the term “redox mediator” for scenarios described by Figure 4.
68. Pac C, Nakasone A, Sakurai H. Photochemical Reactions of Aromatic Compounds. 28. Photosensitized Electron-Transfer Reaction of Electron Donor-Acceptor Pairs by Aromatic Hydrocarbons. *J Am Chem Soc.* 1977; 99:5806–5808.
69. Majima T, Pac C, Nakasone A, Sakurai H. Redox-Photosensitized Reactions. 7. Aromatic Hydrocarbon-Photosensitized Electron-Transfer Reactions of Furan, Methylated Furans, 1,1-Diphenylethylene, and Indene with *p*-Dicyanobenzene. *J Am Chem Soc.* 1981; 103:4499–4508.
70. Borg RM, Arnold DR, Cameron TS. Radical Ions in Photochemistry. 15. The Photosubstitution Reaction between Dicyanobenzenes and Alkyl Olefins. *Can J Chem.* 1984; 62:1785–1802.

71. Lopez L. Photoinduced Electron Transfer Oxygenations. *Top Curr Chem.* 1990; 156:117–166.
72. Schaap AP, Lopez L, Anderson SD, Gagnon SD. Cosensitization by 9,10-Dicyanoanthracene and Biphenyl of the Electron-Transfer Photooxygenation of 1,1,2,2-Tetraphenylcyclopropane. *Tetrahedron Lett.* 1982; 23:5493–5496.
73. Schaap AP, Lopez L, Gagnon SD. Formation of an Ozonide by Electron-Transfer Photooxygenation of Tetraphenylloxirane. Cosensitization by 9,10-Dicyanoanthracene and Biphenyl. *J Am Chem Soc.* 1983; 105:663–664.
74. Schaap AP, Siddiqui S, Gagnon SD, Lopez L. Stereoselective Formation of *cis*-Stilbene Ozonide from the Cosensitized Electron-Transfer Photooxygenation of *cis*- and *trans*-2,3-Diphenylloxiranes. *J Am Chem Soc.* 1983; 105:5149–5150.
75. Schaap AP, Siddiqui S, Balakrishnan P, Lopez L, Gagnon SD. Cosensitized Electron-Transfer Photooxygenation of Epoxides. A New Synthesis of Ozonides. *Isr J Chem.* 1983; 23:415–419.
76. Schaap AP, Siddiqui S, Prasad G, Palomino E, Sandison M. The Photochemical Preparation of Ozonides by Electron-Transfer Photo-Oxygenation of Epoxides. *Tetrahedron.* 1985; 41:2229–2235.
77. Schaap AP, Siddiqui S, Prasad G, Palomino E, Lopez L. Cosensitized Electron Transfer Photo-Oxygenation: The Photochemical Preparation of 1,2,4-Trioxolanes, 1,2-Dioxolanes and 1,2,4-Dioxazolidines. *J Photochem.* 1984; 25:167–181.
78. Mizuno K, Kamiyama N, Ichinose N, Otsuji Y. Photo-Oxygenation of 1,2-Diarylcyclopropanes via Electron Transfer. *Tetrahedron.* 1985; 41:2207–2214.
79. Shim SC, Song JS. Reactivity of 1, 1-Diphenyl-2-vinylcyclopropane to Singlet Oxygen. *Bull Korean Chem Soc.* 1984; 5:265–266.
80. Shim SC, Song JS. Dicyanoanthracene and Biphenyl Co-sensitized Photooxygenation of 1,1-Diphenyl-2-vinylcyclopropane. *Bull Korean Chem Soc.* 1986; 7:150–153.
81. Shim SC, Lee HJ. Salt Effects in Electron-Transfer Induced Photooxygenation of 1,1-Diphenyl-2-vinylcyclopropane; in the Presence of LiClO<sub>4</sub>, NaClO<sub>4</sub>, and (n-Bu)<sub>4</sub>NClO<sub>4</sub>. *Bull Korean Chem Soc.* 1988; 9:112–113.
82. Xu J-H, Song Y-L, Shang Y. Electron Transfer Photooxygenation of 8-Methoxypsoralen. *J Chem Soc, Chem Commun.* 1991:1621–1622.
83. Tamai T, Ichinose N, Tanaka T, Sasuga T, Hashida I, Mizuno K. Generation of Polyphenylene Radical Cations and Their Cosensitization Ability in the 9,10-Dicyanoanthracene-Sensitized Photochemical Chain Reactions of 1,2-Bis(4-methoxyphenyl)cyclopropane. *J Org Chem.* 1998; 63:3204–3212.
84. Tamai T, Mizuno K, Hashida I, Otsuji Y. Salt Effect on the 9,10-Dicyanoanthracene-Sensitized Photooxygenation of 1,2-Diarylcyclopropanes and the Photodecomposition of 3,5-Diaryl-1,2-dioxolanes. *J Org Chem.* 1992; 57:5338–5342.
85. Pandey G. Photoinduced Electron Transfer (PET) in Organic Synthesis. *Top Curr Chem.* 1993; 168:175–221.
86. Waske PA, Tzvetkov NT, Mattay J. Rearrangement and Cyclization Reactions by Photoinduced Electron Transfer: New Approaches for the Synthesis of Polycyclic Compounds. *Synlett.* 2007; 5:669–685.
87. Farid, S.; Hartman, SE.; Evans, TR. Electron-Transfer Reactions in Multicomponent Systems. In: Gordon, M.; Ware, WR., editors. *The Exciplex.* Academic Press; New York: 1975. p. 327-343.
88. Gassman PG, Bottorff KJ. Photoinduced Lactonization. A Useful but Mechanistically Complex Single Electron Transfer Process. *J Am Chem Soc.* 1987; 109:7547–7548.
89. Gassman PG, De Silva SA. Use of Sterically Hindered Sensitizers for Improved Photoinduced Electron-Transfer Reactions. *J Am Chem Soc.* 1991; 113:9870–9872.
90. Gassman PG, Bottorff KJ. Anti-Markovnikov Addition of Nucleophiles to a Non-Conjugated Olefin via Single Electron Transfer Photochemistry. *Tetrahedron Lett.* 1987; 28:5449–5452.
91. Mangion D, Arnold DR. The Photochemistry of 4-Halobenzonitriles and 4-Haloanisoles with 1,1-Diphenylethene in Methanol. Homolytic Cleavage versus Electron-Transfer Pathways. *Can J Chem.* 1999; 77:1655–1670.



92. Mangion D, Arnold DR. Photochemical Nucleophile–Olefin Combination, Aromatic Substitution Reaction. Its Synthetic Development and Mechanistic Exploration. *Acc Chem Res.* 2002; 35:297–304. [PubMed: 12020167]
93. Gassman PG, Bottorff KJ. Electron Transfer Induced Desilylation of Trimethylsilyl Enol Ethers. *J Org Chem.* 1988; 53:1097–1110.
94. Hintz S, Mattay J, van Eldik R, Fu W-F. Regio- and Stereoselective Cyclization Reactions of Unsaturated Silyl Enol Ethers by Photoinduced Electron Transfer – Mechanistic Aspects and Synthetic Approach. *Eur J Org Chem.* 1998:1583–1596.
95. Weng H, Scarlata C, Roth HD. Electron Transfer Photochemistry of Geraniol and (*E,E*)-Farnesol. A Novel “Tandem”, 1,5-Cyclization, Intramolecular Capture. *J Am Chem Soc.* 1996; 118:10947–10953.
96. Riemer M, Nicewicz DA. Synthesis of Cyclobutane Lignans *via* an Organic Single Electron Oxidant–Electron Relay System. *Chem Sci.* 2013; 4:2625–2629.
97. Armesto D, Caballero O, Ortiz MJ, Agarrabeitia AR, Martín-Fontecha M, Torres MR. Novel Photoreactions of 2-Aza-1,4-dienes in the Triplet Excited State and via Radical-Cation Intermediates. 2-Aza-di- $\pi$ -methane Rearrangements Yielding Cyclopropylimines and N-Vinylaziridines. *J Org Chem.* 2003; 68:6661–6671. [PubMed: 12919030]
98. Martínez-Alcázar MP, Cano FH, Ortiz MJ, Agarrabeitia AR. Unexpected Photochemical Reactivity of 3-(9-Fluorenylidene)-2,2-dimethylpropenal Oxime Acetate. *J Mol Struct.* 2003; 648:19–25.
99. Ikeda H, Minegishi T, Abe H, Konno A, Goodman JL, Miyashi T. Photoinduced Electron-Transfer Degenerate Cope Rearrangement of 2,5-Diaryl-1,5-hexadienes: A Cation-Radical Cyclization–Diradical Cleavage Mechanism. *J Am Chem Soc.* 1998; 120:87–95.
100. Arnold DR, Mines SA. Radical Ions in Photochemistry. 21. The Photosensitized (Electron Transfer) Tautomerization of Alkenes; the Phenyl Alkene System. *Can J Chem.* 1989; 67:689–698.
101. Lew CSQ, Brisson JR, Johnston LJ. Reactivity of Radical Cations: Generation, Characterization, and Reactivity of 1, 3-Diene Radical Cations. *J Org Chem.* 1997; 62:4047–4056.
102. Liu Z-L, Zhang M-X, Yang L, Liu Y-C, Chow YL, Johansson CI. Electron Transfer Photoisomerization of Norbornadiene to Quadricyclane Cosensitized by Dibenzoylemethanoboron Difluoride and Aromatic Hydrocarbons. *J Chem Soc, Perkin Trans.* 1994; 2:585–590.
103. Warzecha KD, Xing X, Demuth M, Goddard R, Kessler M, Krüger C. Cascade Cyclizations of Terpenoid Polyalkenes Triggered by Photoelectron Transfer – Biomimetics with Photons. *Helv Chim Acta.* 1995; 78:2065–2076.
104. Warzecha KD, Xing X, Demuth M. Cyclization of Terpenoid Polyalkenes via Photo-Induced Electron Transfer—Versatile Single-Step Syntheses of Mono- and Polycycles. *Pure Appl Chem.* 1997; 69:109–112.
105. Earlier experiments on this system were carried out in micellar media using Phen/DCB which likely operates by an oxidative quenching mechanism (see Ref. 67) rather than redox mediation. See: Hoffmann U, Gao Y, Pandey B, Klinge S, Warzecha K-D, Krüger C, Roth HD, Demuth M. Light-Induced Polyene Cyclizations via Radical Cations in Micellar Medium. *J Am Chem Soc.* 1993; 115:10358–10359.
106. Görner H, Warzecha KD, Demuth M. Cyclization of Terpenoid Dicarbonitrile Polyalkenes upon Photoinduced Electron Transfer to 1,4-Dicyano-2,3,5,6-tetramethylbenzene and Other Cyanoarenes. *J Phys Chem A.* 1997; 101:9964–9973.
107. Warzecha KD, Görner H, Demuth M. Photoinduced Electron Transfer from Isoprenoid Polyalkene Acetates to Dicyanoarenes. *J Chem Soc Faraday Trans.* 1998; 94:1701–1706.
108. Warzecha KD, Demuth M, Görner H. Photocyclization of Terpenoid Polyalkenes upon Electron Transfer to a Triphenylpyrylium Salt A Time-Resolved Study. *J Chem Soc Faraday Trans.* 1997; 93:1523–1530.
109. Goeller F, Heinemann C, Demuth M. Investigations of Cascade Cyclizations of Terpenoid Polyalkenes via Radical Cations. A Biomimetic-type Synthesis of ( $\pm$ )-3-Hydroxy-spongian-16-one. *Synthesis.* 2001; 8:1114–1116.

110. Xing X, Demuth M. Application of Photoinduced Biomimetic Cascade Cyclizations of Terpenoid Polyalkenes for the Synthesis of ( $\pm$ )-Stypoldione. *Eur J Org Chem.* 2001;537–544.
111. Heinemann C, Xing X, Warzecha KD, Ritterskamp P, Görner H, Demuth M. An Asymmetric Induction Principle and Biomimetics with Photons via Electron Transfer. *Pure Appl Chem.* 1998; 70:2167–2176.
112. Heinemann C, Demuth M. Biomimetic Cascade Cyclizations of Terpenoid Polyalkenes *via* Photoinduced Electron Transfer. Long-Distance Asymmetric Induction by a Chiral Auxiliary. *J Am Chem Soc.* 1997; 119:1129–1130.
113. Heinemann C, Demuth M. Short Biomimetic Synthesis of a Steroid by Photoinduced Electron Transfer and Remote Asymmetric Induction. *J Am Chem Soc.* 1999; 121:4894–4895.
114. Nonell S, Arbogast JW, Foote CS. Production of Fullerene (C<sub>60</sub>) Radical Cation by Photosensitized Electron Transfer. *J Phys Chem.* 1992; 96:4169–4170.
115. Dunsch L, Ziegs F, Siedschlag C, Mattay J. ESR Spectroscopy of the C<sub>60</sub> Cation Produced by Photoinduced Electron Transfer. *Chem Eur J.* 2000; 6:3547–3550. [PubMed: 11072820]
116. Siedschlag C, Luftmann H, Wolff C, Mattay J. Functionalization of [60]Fullerene by Photoinduced Electron Transfer (PET): Syntheses of 1-Substituted 1,2-Dihydro[60]fullerenes. *Tetrahedron.* 1997; 53:3587–3592.
117. Safonov IG, Courtney SH, Schuster DI. Laser Flash Photolysis Study of Methanol Addition to the C<sub>60</sub> Radical Cation. *Res Chem Intermed.* 1997; 23:541–548.
118. Siedschlag C, Luftmann H, Wolff C, Mattay J. [60]Fullerene Radical Cation: Reactions and Mechanism. *Tetrahedron.* 1999; 55:7805–7818.
119. Fagnoni M, Mella M, Albini A. Radical Addition to Alkenes via Electron Transfer Photosensitization. *J Am Chem Soc.* 1995; 117:7877–7881.
120. Campari G, Fagnoni M, Mella M, Albini A. Diastereoselective Photosensitized Radical Addition to Fumaric Acid Derivatives bearing Oxazolidine Chiral Auxiliaries. *Tetrahedron: Asymmetry.* 2000; 11:1891–1906.
121. Cumpstey I, Crich D. Photoinitiated Glycosylation at 350 nm. *J Carbohydr Chem.* 2011; 30:469–485.
122. Jonas M, Blechert S, Steckhan E. Photochemically Induced Electron Transfer (PET) Catalyzed Radical Cyclization: A Practical Method for Inducing Structural Changes in Peptides by Formation of Cyclic Amino Acid Derivatives. *J Org Chem.* 2001; 66:6896–6904. [PubMed: 11597207]
123. Gutenberger G, Steckhan E, Blechert S.  $\alpha$ -Silyl Ethers as Hydroxymethyl Anion Equivalents in Photoinduced Radical Electron Transfer Additions. *Angew Chem Int Ed.* 1998; 37:660–662.
124. Meggers E, Steckhan E, Blechert S. Radical C–C Bond Formation by Photoinduced Electron Transfer Addition of  $\alpha$ -Silyl Carbamates to Acceptor-Substituted Alkenes. *Angew Chem Int Ed.* 1995; 34:2137–2139.
125. Tyson EL, Niemeyer ZL, Yoon TP. Redox Mediators in Visible Light Photocatalysis: Photocatalytic Radical Thiol–Ene Additions. *J Org Chem.* 2014; 79:1427–1436. [PubMed: 24428433]
126. Xu J, Boyer C. Visible Light Photocatalytic Thiol–Ene Reaction: An Elegant Approach for Fast Polymer Postfunctionalization and Step-Growth Polymerization. *Macromolecules.* 2015; 48:520–529.
127. Ci X, Kellett MA, Whitten DG. Oxidative Photofragmentation of  $\alpha,\beta$ -Amino Alcohols via Single Electron Transfer: Cooperative Reactivity of Donor and Acceptor Ion Radicals in Photogenerated Contact Radical Ion Pairs. *J Am Chem Soc.* 1991; 113:3893–3904.
128. Ikeda H, Akiyama K, Takahashi Y, Nakamura T, Ishizaki S, Shiratori Y, Ohaku H, Goodman JL, Houmam A, Wayner DDM, et al. Spectroscopic and Calorimetric Studies on the Mechanism of Methylene-cyclopropane Rearrangements Triggered by Photoinduced Electron Transfer. *J Am Chem Soc.* 2003; 125:9147–9157. [PubMed: 15369372]
129. Adam W, Sendelbach J. Photosensitized Electron Transfer from Azoalkanes: Generation, Fragmentation, and Rearrangement of Radical Cations Structurally Related to Dicyclopentadiene. *J Org Chem.* 1993; 58:5310–5315.

130. Adam W, Sendelbach J. Denitrogenation of Bicyclic Azoalkanes through Photosensitized Electron Transfer: Generation and Intramolecular Trapping of Radical Cations. *J Org Chem.* 1993; 58:5316–5322.
131. Yamashita Y, Ikeda H, Mukai T. Organic Photochemistry. 80. Photoinduced Electron-Transfer Reactions of Cage Compounds. Novel Pericyclic Reactions Involving a Chain Process. *J Am Chem Soc.* 1987; 109:6682–6687.
132. Lund H, Michel MA, Simonet J. Homogeneous Electron Exchange in Catalytic Polarographic Reduction. *Acta Chem Scand.* 1974; 28B:900–904.
133. Andrieux CP, Blocman C, Dumas-Bouchiat JM, Saveant JM. Heterogeneous and Homogeneous Electron Transfers to Aromatic Halides. An Electrochemical Redox Catalysis Study in the Halobenzene and Halopyridine Series. *J Am Chem Soc.* 1979; 101:3431–3441.
134. Andrieux CP, Blocman C, Dumas-Bouchiat JM, M'halla F, Savéant JM. Homogeneous Redox Catalysis of Electrochemical Reactions: Part V. Cyclic Voltammetry. *J Electroanal Chem.* 1980; 113:19–40.
135. Swartz JE, Stenzel TT. Electrochemical Initiation of Sromatic  $S_{RN}1$  Reactions using Redox Catalysts. *J Am Chem Soc.* 1984; 106:2520–2524.
136. Alam N, Amatore C, Combellas C, Thiébaud A, Verpeaux JN. Theory and Experimental Illustration of Preparative Electrochemistry using Redox Catalysis of Electron Transfer Initiated Radical Chain Reactions. Application to the Cross-Coupling between Aryl Halides and Phenoxide ions. *J Org Chem.* 1990; 55:6347–6356.
137. Darwent JR, Kalyanasundaram K. Electron-Transfer Reactions of Quinones, Hydroquinones and Methyl Viologen, Photosensitized by Tris(2,2'-bipyridine)-ruthenium(II). *J Chem Soc Faraday Trans 2.* 1981; 77:373–382.
138. Herance JR, Ferrer B, Bourdelande JL, Marquet J, Garcia H. A Photocatalytic Acid- and Base-Free Meerwein–Ponndorf–Verley-Type Reduction Using a  $[Ru(bpy)_3]^{2+}$ /Viologen Couple. *Chem Eur J.* 2006; 12:3890–3895. [PubMed: 16521136]
139. Goren Z, Willner I. Photochemical and Chemical Reduction of Vicinal Dibromides via Phase Transfer of 4,4'-Bipyridinium Radical: The Role of Radical Disproportionation. *J Am Chem Soc.* 1983; 105:7764–7765.
140. Maidan R, Goren Z, Becker JY, Willner I. Application of multielectron charge relays in chemical and photochemical debromination processes. The role of induced disproportionation of N,N'-dioctyl-4,4'-bipyridinium radical cation in two-phase systems. *J Am Chem Soc.* 1984; 106:6217–6222.
141. Willner I, Goren Z, Mandler D, Maidan R, Degani Y. Transformation of single-electron transfer photoproducts into multielectron charge relays: the functions of water—oil two-phase systems and enzyme catalysis. *J Photochem.* 1985; 28:215–228.
142. Nakamura T, Takagi K, Sawaki Y. The One-Electron Transfer Induced Photocycloreversion of Stilbazolium Cyclodimers. *Bull Chem Soc Jpn.* 1998; 71:419–424.
143. Tahara K, Hisaeda Y. Eco-Friendly Molecular Transformations Catalyzed by a Vitamin B12 Derivative with a Visible-Light-Driven System. *Green Chem.* 2011; 13:558–561.
144. Abe M, Nojima M, Oku A. Photoinduced Electron Transfer Reactions of Cyclopropanone Acetal with Conjugated Enones in the Presence of a Redox-Type Photosensitizer. *Tetrahedron Lett.* 1996; 37:1833–1836.
145. Saito I, Ikehira H, Kasatani R, Watanabe M, Matsuura T. Photoinduced Reactions. 167. Selective Deoxygenation of Secondary Alcohols by Photosensitized Electron-Transfer Reaction. A General Procedure for Deoxygenation of Ribonucleosides. *J Am Chem Soc.* 1986; 108:3115–3117.
146. Pac C, Ihama M, Yasuda M, Miyauchi Y, Sakurai H. Tris(2,2'-bipyridine)ruthenium(2+)-Mediated Photoreduction of Olefins with 1-Benzyl-1,4-Dihydronicotinamide: a Mechanistic Probe for Electron-Transfer Reactions of NAD(P)H-Model Compounds. *J Am Chem Soc.* 1981; 103:6495–6497.
147. Ishitani O, Ihama M, Miyauchi Y, Pac C. Redox-Photosensitized Reactions. Part 12. Effects of Magnesium(II) Ion on the  $[Ru(bpy)_3]^{2+}$ -Photomediated Reduction of Olefins by 1-Benzyl-1,4-Dihydronicotinamide: Metal-Ion Catalysis of Electron Transfer Processes Involving an NADH Model. *J Chem Soc, Perkin Trans.* 1985; 1:1527–1531.

148. Mizuno K, Nakanishi K, Otsuji Y. Photosubstitution of Dicyanobenzenes by Group 14 Organometallic Compounds via Photoinduced Electron-Transfer. Additive and Medium Effects on Photoinduced Electron Transfer Reaction. *Chem Lett*. 1988; 17:1833–1836.
149. House HO, Huber LE, Umen MJ. Empirical Rules for Estimating the Reduction Potential of  $\alpha,\beta$ -Unsaturated Carbonyl Compounds. *J Am Chem Soc*. 1972; 94:8471–8475.
150. Ischay MA, Anzovino ME, Du J, Yoon TP. Efficient Visible Light Photocatalysis of [2+2] Enone Cycloadditions. *J Am Chem Soc*. 2008; 130:12886–12887. [PubMed: 18767798]
151. Du J, Yoon TP. Crossed Intermolecular [2+2] Cycloadditions of Acyclic Enones via Visible Light Photocatalysis. *J Am Chem Soc*. 2009; 131:14604–14605. [PubMed: 19473018]
152. Tyson EL, Farney EP, Yoon TP. Photocatalytic [2+2] Cycloadditions of Enones with Cleavable Redox Auxiliaries. *Org Lett*. 2012; 14:1110–1113. [PubMed: 22320352]
153. Du J, Skubi KL, Schultz DM, Yoon TP. A Dual-Catalysis Approach to Enantioselective [2+2] Photocycloadditions Using Visible Light. *Science*. 2014; 344:392–396. [PubMed: 24763585]
154. Hurtley AE, Cismesia MA, Ischay MA, Yoon TP. Visible Light Photocatalysis of Radical Anion Hetero-Diels–Alder Cycloadditions. *Tetrahedron*. 2011; 67:4442–4448. [PubMed: 21666769]
155. Lu Z, Shen M, Yoon TP. [3+2] Cycloadditions of Aryl Cyclopropyl Ketones by Visible Light Photocatalysis. *J Am Chem Soc*. 2011; 133:1162–1164. [PubMed: 21214249]
156. Amador AG, Sherbrook EM, Yoon TP. Enantioselective Photocatalytic [3+2] Cycloadditions of Aryl Cyclopropyl Ketones. *J Am Chem Soc*. 2016; doi: 10.1021/jacs.6b01728
157. Zhao G, Yang C, Guo L, Sun H, Lin R, Xia W. Reactivity Insight into Reductive Coupling and Aldol Cyclization of Chalcones by Visible Light Photocatalysis. *J Org Chem*. 2012; 77:6302–6306. [PubMed: 22731518]
158. Cibulka R, Vasold R, König B. Catalytic Photooxidation of 4-Methoxybenzyl Alcohol with a Flavin–Zinc(II)–Cyclen Complex. *Chem Eur J*. 2004; 10:6223–6231.
159. Loupy A, Tchoubar B, Astruc D. Salt Effects Resulting from Exchange Between Two Ion Pairs and Their Crucial Role in Reaction. *Chem Rev*. 1992; 92:1141–1165.
160. Goodson B, Schuster GB. Salt Effects in Photoinduced Electron Transfer Reactions. *Tetrahedron Lett*. 1986; 27:3123–3126.
161. Thompson PA, Simon JD. Electrolyte Effects on the Energetics and Dynamics of Intermolecular Electron Transfer Reactions. *J Am Chem Soc*. 1993; 115:5657–5664.
162. Mizuno K, Ichinose N, Otsuji Y. Cis-Trans Photoisomerization and Photooxygenation of 1,2-Diarylcyclopropanes. Salt Effects on the Photoinduced Electron Transfer Reactions. *Chem Lett*. 1985; 14:455–458.
163. Gollnick K, Wellnhofer G. Electron-Transfer-Induced Photo-Oxygenation Reactions and the Special Salt Effect: Determination of Efficiencies of Free Radical Ion Formation from Solvent-Separated Radical Ion Pairs in Oxygen-Saturated Acetonitrile Solutions. *J Photochem Photobiol A*. 1993; 74:137–145.
164. Akasaka T, Sato K, Kako M, Ando W. Formation of 1,2,3,6-Dioxadisilin in Photo-Induced Electron Transfer Oxygenation of 1,2-Disilene. *Tetrahedron Lett*. 1991; 32:6605–6608.
165. Mizuno K, Ichinose N, Tamai T, Otsuji Y. Electron-Transfer Mediated Photooxygenation of Biphenyl and its Derivatives in the Presence of  $\text{Mg}(\text{ClO}_4)_2$ . *Tetrahedron Lett*. 1985; 26:5823–5826.
166. Tamai T, Mizuno K, Hashida I, Otsuji Y. Photooxygenation of Biphenyl and its Derivatives via Photoinduced Electron Transfer: Effect of  $\text{Mg}(\text{ClO}_4)_2$  on Photooxygenation. *Photochem Photobiol*. 1991; 54:23–29.
167. Miyashi T, Konno A, Takahashi Y. Evidence for a Chair Cyclohexane-1,4-Radical Cation Intermediate in the Single Electron-Transfer-Induced Cope Rearrangement of 2,5-Diaryl-1,5-hexadienes. *J Am Chem Soc*. 1988; 110:3676–3677.
168. Mizuno K, Nakanishi I, Ichinose N, Otsuji Y. Structural Dependence on Photoaddition of Methanol to Arylalkenes. Solvent and Additive Effects on Photoinduced Electron Transfer Reaction. *Chem Lett*. 1989; 18:1095–1098.
169. Fukuzumi S, Kuroda S, Tanaka T. Catalytic Effects of  $\text{Mg}^{2+}$  Ion on Electron Transfer Reactions of Photo-Excited Flavin Analogues (3-Methyl-10-phenyl-5-deazaalloxazines and 3-

- Methyl-10-phenylisoalloxazine) with Methyl and Methoxy Substituted Benzenes. *Chem Lett.* 1984; 13:417–420.
170. Fukuzumi S, Kuroda S, Tanaka T. Photooxidation of *p*-Methylbenzyl Alcohol by Oxygen, Catalyzed by Flavin Analogues (3-Methyl-10-phenylisoalloxazine and 3-Methyl-10-phenyl-5-deazaalloxazine) in the Presence of  $Mg^{2+}$  Ion. *Chem Lett.* 1984; 13:1375–1378.
171. Fukuzumi S, Kuroda S, Tanaka T. Flavin Analog-Metal Ion Complexes Acting as Efficient Photocatalysts in the Oxidation of *p*-Methylbenzyl Alcohol by Oxygen under Irradiation with Visible Light. *J Am Chem Soc.* 1985; 107:3020–3027.
172. Zhu S, Rueping M. Merging Visible-Light Photoredox and Lewis Acid Catalysis for the Functionalization and Arylation of Glycine Derivatives and Peptides. *Chem Commun.* 2012; 48:11960–11962.
173. Liu W, Liu S, Xie H, Qing Z, Zeng J, Cheng P. TBHP Mediated Oxidation of *N*-2-Alkynylphenyl  $\alpha$ -Amino Carbonyl Compounds to Oxalic Amides using Visible Light Photoredox Catalysis and their Application in the Synthesis of 2-Aryl Indoles. *RSC Adv.* 2015; 5:17383–17388.
174. Yang Z, Li H, Zhang L, Zhang MT, Cheng JP, Luo S. Organic Photocatalytic Cyclization of Polyenes: A Visible-Light-Mediated Radical Cascade Approach. *Chem Eur J.* 2015; 21:14723–14727. [PubMed: 26332702]
175. Yoon, UC.; Su, Z.; Mariano, PS. 101. The Dynamics and Photochemical Consequences of Aminium Radical Reactions. In: Horspool, W.; Lenci, F., editors. *CRC Handbook of Organic Photochemistry and Photobiology.* 2. CRC Press; Boca Raton, FL: 2004. p. 101-1-101-18.
176. Kohls P, Jadhav D, Pandey G, Reiser O. Visible Light Photoredox Catalysis: Generation and Addition of *N*-Aryltetrahydroisoquinoline-Derived  $\alpha$ -Amino Radicals to Michael Acceptors. *Org Lett.* 2012; 14:672–675. [PubMed: 22260623]
177. Ruiz Espelt L, McPherson IS, Wiensch EM, Yoon TP. Enantioselective Conjugate Additions of  $\alpha$ -Amino Radicals via Cooperative Photoredox and Lewis Acid Catalysis. *J Am Chem Soc.* 2015; 137:2452–2455. [PubMed: 25668687]
178. Mayer JM. Proton-Coupled Electron Transfer: A Reaction Chemist's View. *Annu Rev Phys Chem.* 2004; 55:363–390. [PubMed: 15117257]
179. Weinberg DR, Gagliardi CJ, Hull JF, Murphy CF, Kent CA, Westlake BC, Paul A, Ess DH, McCafferty DG, Meyer TJ. Proton-Coupled Electron Transfer. *Chem Rev.* 2012; 112:4016–4093. [PubMed: 22702235]
180. Yayla HG, Knowles RR. Proton-Coupled Electron Transfer in Organic Synthesis: Novel Homolytic Bond Activations and Catalytic Asymmetric Reactions with Free Radicals. *Synlett.* 2014; 25:2819–2826.
181. Tarantino KT, Liu P, Knowles RR. Catalytic Ketyl-Olefin Cyclizations Enabled by Proton-Coupled Electron Transfer. *J Am Chem Soc.* 2013; 135:10022–10025. [PubMed: 23796403]
182. Rono LJ, Yayla JG, Wang DY, Armstrong MF, Knowles RR. Enantioselective Photoredox Catalysis Enabled by Proton-Coupled Electron Transfer: Development of an Asymmetric Aza-Pinacol Cyclization. *J Am Chem Soc.* 2013; 135:17735–17738. [PubMed: 24215561]
183. Du J, Ruiz Espelt L, Guzei IA, Yoon TP. Photocatalytic Reductive Cyclizations of Enones: Divergent Reactivity of Photogenerated Radical and Radical Anion Intermediates. *Chem Sci.* 2011; 2:2115–2119. [PubMed: 22121471]
184. Fukuzumi S, Mochizuki S, Tanaka T. Photocatalytic Reduction of Phenacyl Halides by 9,10-Dihydro-10-methylacridine. Control between the Reductive and Oxidative Quenching Pathways of Tris(bipyridine)ruthenium Complex Utilizing an Acid Catalysis. *J Phys Chem.* 1990; 94:722–726.
185. Fukuzumi S, Mochizuki S, Tanaka T. Acid-Catalyzed Electron-Transfer Processes in Reduction of  $\alpha$ -Haloketones by an NADH Model Compound and Ferrocene Derivatives. *J Am Chem Soc.* 1989; 111:1497–1499.
186. Fukuzumi S, Ishikawa K, Hironaka K, Tanaka T. Acid Catalysis in Thermal and Photoinduced Electron-Transfer Reactions. *J Chem Soc Perkin Trans.* 1987; 2:751–760.
187. Nicholls TP, Constable GE, Robertson JC, Gardiner MG, Bissember AC. Brønsted Acid Cocatalysis in Copper(I)-Photocatalyzed  $\alpha$ -Amino C–H Bond Functionalization. *ACS Catal.* 2016; 6:451–457.

188. Choi GJ, Knowles RR. Catalytic Alkene Carboaminations Enabled by Oxidative Proton-Coupled Electron Transfer. *J Am Chem Soc.* 2015; 137:9226–9229. [PubMed: 26166022]
189. Miller DC, Choi GJ, Orbe HS, Knowles RR. Catalytic Olefin Hydroamidation Enabled by Proton-Coupled Electron Transfer. *J Am Chem Soc.* 2015; 137:13492–13495. [PubMed: 26439818]
190. Ruiz Espelt L, Wiensch EM, Yoon TP. Brønsted Acid Cocatalysts in Photocatalysts in Photocatalytic Radical Addition of  $\alpha$ -Amino C–H Bonds across Michael Acceptors. *J Org Chem.* 2013; 78:4107–4114. [PubMed: 23537318]
191. Uraguchi D, Kinoshita N, Kizu T, Ooi T. Synergistic Catalysis of Ionic Brønsted Acid and Photosensitizer for a Redox Neutral Asymmetric  $\alpha$ -Coupling of *N*-Arylaminoethanes with Aldimines. *J Am Chem Soc.* 2015; 137:13768–13771. [PubMed: 26456298]
192. Cismesia MA, Ischay MA, Yoon TP. Reductive Cyclizations of Nitroarenes to Hydroxamic Acids by Visible Light Photoredox Catalysis. *Synthesis.* 2013; 45:2699–2705. [PubMed: 25143660]
193. Maity S, Zheng N. A Visible-Light-Mediated Oxidative C–N Bond Formation/Aromatization Cascade: Photocatalytic Preparation of *N*-Arylindoles. *Angew Chem Int Ed.* 2012; 51:9562–9566.
194. An XD, Yu S. Visible-Light-Promoted and One-Pot Synthesis of Phenanthridines and Quinolines from Aldehydes and *O*-Acyl Hydroxylamine. *Org Lett.* 2015; 17:2692–2695. [PubMed: 25964987]
195. Huang FQ, Dong X, Qi LW, Zhang B. Visible-Light Photocatalytic  $\alpha$ -Amino C(sp<sup>3</sup>)–H Activation through Radical Translocation: a Novel and Metal-Free Approach to  $\alpha$ -Alkoxybenzamides. *Tetrahedron Lett.* 2016; 57:1600–1604.
196. Lechner R, König B. Oxidation and Deprotection of Primary Benzylamines by Visible Light Flavin Photocatalysis. *Synthesis.* 2010; 10:1712–1718.
197. Nicewicz DA, MacMillan DWC. Merging Photoredox Catalysis with Organocatalysis: The Direct Asymmetric Alkylation of Aldehydes. *Science.* 2008; 322:77–80. [PubMed: 18772399]
198. Nagib DA, Scott ME, MacMillan DWC. Enantioselective  $\alpha$ -Trifluoromethylation of Aldehydes via Photoredox Organocatalysis. *J Am Chem Soc.* 2009; 131:10875–10877. [PubMed: 19722670]
199. Welin ER, Warkentin AA, Conrad JC, MacMillan DWC. Enantioselective  $\alpha$ -Alkylation of Aldehydes by Photoredox Organocatalysis: Rapid Access to Pharmacophore Fragments from  $\beta$ -Cyanoaldehydes. *Angew Chem Int Ed.* 2015; 54:9668–9672.
200. Shih HW, Vander Wal MN, Grange RL, MacMillan DWC. Enantioselective  $\alpha$ -Benzoylation of Aldehydes via Photoredox Organocatalysis. *J Am Chem Soc.* 2010; 132:13600–13603. [PubMed: 20831195]
201. Cecere G, König CM, Alleva JL, MacMillan DWC. Enantioselective Direct  $\alpha$ -Amination of Aldehydes via a Photoredox Mechanism: A Strategy for Asymmetric Amine Fragment Coupling. *J Am Chem Soc.* 2013; 135:11521–11524. [PubMed: 23869694]
202. Zhu Y, Zhang L, Luo S. Asymmetric  $\alpha$ -Photoalkylation of  $\beta$ -Ketocarboxyls by Primary Amine Catalysis: Facile Access to Acyclic All-Carbon Quaternary Stereocenters. *J Am Chem Soc.* 2014; 136:14642–14645. [PubMed: 25229998]
203. Koike T, Akita M. Photoinduced Oxyamination of Enamines and Aldehydes with TEMPO Catalyzed by [Ru(bpy)<sub>3</sub>]<sup>2+</sup>. *Chem Lett.* 2009; 38:166–167.
204. Yoon HS, Ho XH, Jang J, Lee HJ, Kim SJ, Jang HY. N719 Dye-Sensitized Organophotocatalysis: Enantioselective Tandem Michael Addition/Oxyamination of Aldehydes. *Org Lett.* 2012; 14:3272–3275. [PubMed: 22681592]
205. Gualandi A, Marchini M, Mengozzi L, Natali M, Lucarini M, Ceroni P, Cozzi PG. Organocatalytic Enantioselective Alkylation of Aldehydes with [Fe(bpy)<sub>3</sub>]Br<sub>2</sub> Catalyst and Visible Light. *ACS Catal.* 2015; 5:5927–5931.
206. Neumann M, Földner S, König B, Zeitler K. Metal-Free, Cooperative Asymmetric Organophotoredox Catalysis with Visible Light. *Angew Chem Int Ed.* 2011; 50:951–954.
207. Neumann M, Zeitler K. Application of Microflow Conditions to Visible Light Photoredox Catalysis. *Org Lett.* 2012; 14:2658–2661. [PubMed: 22587670]

208. Fidaly K, Ceballos C, Falguières A, Sylla-Iyarreta Veitia M, Guy A, Ferroud C. Visible Light Photoredox Organocatalysis: a Fully Transition Metal-Free Direct Asymmetric  $\alpha$ -Alkylation of Aldehydes. *Green Chem.* 2012; 14:1293–1297.
209. Pirnot MT, Rankic DA, Martin DBC, MacMillan DWC. Photoredox Activation for the Direct  $\beta$ -Arylation of Ketones and Aldehydes. *Science.* 2013; 339:1593–1596. [PubMed: 23539600]
210. Petronijevi FR, Nappi M, MacMillan DWC. Direct  $\beta$ -Functionalization of Cyclic Ketones with Aryl Ketones via the Merger of Photoredox and Organocatalysis. *J Am Chem Soc.* 2013; 135:18323–18326. [PubMed: 24237366]
211. Jeffrey JL, Petronijevi FR, MacMillan DWC. Selective Radical–Radical Cross-Couplings: Design of a Formal  $\beta$ -Mannich Reaction. *J Am Chem Soc.* 2015; 137:8404–8407. [PubMed: 26075347]
212. Terrett JA, Clift MD, MacMillan DWC. Direct  $\beta$ -Alkylation of Aldehydes via Photoredox Organocatalysis. *J Am Chem Soc.* 2014; 136:6858–6861. [PubMed: 24754456]
213. Santamaria J, Herlem D, Kyuong-Huu F. Oxydation Photochimique d'Amines Tertiaires et d'Alcaloïdes—VIII: Oxydation Photochimique d'Alcaloïdes Indolinoindolizidiniques, Vincadiformine, Tabersonine, N<sub>(a)</sub>-Acétyl dihydro-2,16 vincadiformine et N<sub>(a)</sub>-Acétyl dihydro-2,16 tabersonine. *Tetrahedron.* 1977; 33:2389–2392.
214. Pandey G, Reddy PY, Bhalerao UT. Regiocontrolled SET Promoted Photocyclisation of 2-Alkyl-1-piperidine and Pyrrolidine Propanols: Stereoselective Synthesis of cis- $\alpha,\alpha'$ -Dialkyl Piperidines and Pyrrolidines via Tetrahydro-1,3-oxazines. *Tetrahedron Lett.* 1991; 32:5147–5150.
215. Condie AG, González-Gómez JC, Stephenson CRJ. Visible-Light Photoredox Catalysis: Aza-Henry Reactions via C–H Functionalization. *J Am Chem Soc.* 2010; 132:1464–1465. [PubMed: 20070079]
216. Hu J, Wang J, Nguyen TH, Zheng N. The Chemistry of Amine Radical Cations Produced by Visible Light Photoredox Catalysis. *Beilstein J Org Chem.* 2013; 9:1977–2001. [PubMed: 24204409]
217. Rueping M, Vila C, Koenigs RM, Poscharyn K, Fabry DC. Dual Catalysis: Combining Photoredox and Lewis Base Catalysis for Direct Mannich Reactions. *Chem Commun.* 2011; 47:2360–2362.
218. Pan Y, Kee CW, Chen L, Tan CH. Dehydrogenative Coupling Reactions Catalysed by Rose Bengal Using Visible Light Irradiation. *Green Chem.* 2011; 13:2682–2685.
219. Huang L, Zhao J. Iodo-Bodipys as Visible-Light-Absorbing Dual-Functional Photoredox Catalysts for Preparation of Highly Functionalized Organic Compounds by Formation of C–C Bonds *via* Reductive and Oxidative Quenching Catalytic Mechanisms. *RSC Adv.* 2013; 3:23377–23388.
220. Hamilton DS, Nicewicz DA. Direct Catalytic Anti-Markovnikov Hydroetherification of Alkenols. *J Am Chem Soc.* 2012; 134:18577–18580. [PubMed: 23113557]
221. Wilger DJ, Gesmundo NJ, Nicewicz DA. Catalytic hydrotrifluoromethylation of styrenes and unactivated aliphatic alkenes *via* an organic photoredox system. *Chem Sci.* 2013; 4:3160–3165.
222. Nguyen TM, Nicewicz DA. Anti-Markovnikov Hydroamination of Alkenes Catalyzed by an Organic Photoredox System. *J Am Chem Soc.* 2013; 135:9588–9591. [PubMed: 23768239]
223. Perkowski AJ, Nicewicz DA. Direct Catalytic Anti-Markovnikov Addition of Carboxylic Acids to Alkenes. *J Am Chem Soc.* 2013; 135:10334–10337. [PubMed: 23808532]
224. Nguyen TM, Manohar N, Nicewicz DA. anti-Markovnikov Hydroamination of Alkenes Catalyzed by a Two-Component Organic Photoredox System: Direct Access to Phenethylamine Derivatives. *Angew Chem Int Ed.* 2014; 53:6198–6201.
225. Grandjean JMM, Nicewicz DA. Synthesis of Highly Substituted Tetrahydrofurans by Catalytic Polar-Radical-Crossover Cycloadditions of Alkenes and Alkenols. *Angew Chem Int Ed.* 2013; 52:3967–3971.
226. This transformation has also been accomplished using 1, 7-dicyanoperylene-3, 4, 9, 10-tetracarboxylic acid bisimide (PDI) with a thiophenol cocatalyst. See: Weiser M, Hermann S, Penner A, Wagenknecht H-A. Photocatalytic Nucleophilic Addition of Alcohols to Styrenes in Markovnikov and anti-Markovnikov Orientation. *Beilstein J Org Chem.* 2015; 11:568–575.

227. Wilger DJ, Grandjean JMM, Lammert TR, Nicewicz DA. The Direct anti-Markovnikov Addition of Mineral Acids to Styrenes. *Nature Chem.* 2014; 6:720–726. [PubMed: 25054943]
228. Morse PD, Nicewicz DA. Divergent Regioselectivity in Photoredox-Catalyzed Hydrofunctionalization Reactions of Unsaturated Amides and Thioamides. *Chem Sci.* 2015; 6:270–274. [PubMed: 25541590]
229. Zeller MA, Riener M, Nicewicz DA. Butyrolactone Synthesis via Polar Radical Crossover Cycloaddition Reactions: Diastereoselective Syntheses of Methylenolactocin and Protolichsterinic Acid. *Org Lett.* 2014; 16:4810–4813. [PubMed: 25190259]
230. Gesmundo NJ, Grandjean JMM, Nicewicz DA. Amide and Amine Nucleophiles in Polar Radical Crossover Cycloadditions: Synthesis of  $\gamma$ -Lactams and Pyrrolidines. *Org Lett.* 2015; 17:1316–1319. [PubMed: 25695366]
231. Cavanaugh CL, Nicewicz DA. Synthesis of  $\alpha$ -Benzyloxyamino- $\gamma$ -butyrolactones via a Polar Radical Crossover Cycloaddition Reaction. *Org Lett.* 2015; 17:6082–6085. [PubMed: 26646284]
232. For a contemporary review on visible light methods see: Xuan J, Zhang Z-G, Xiao W-J. Visible-Light-Induced Decarboxylative Functionalization of Carboxylic Acids and Their Derivatives. *Angew Chem Int Ed.* 2015; 54:15632–15641.
233. Cassani C, Bergonzini G, Wallentin CJ. Photocatalytic Decarboxylative Reduction of Carboxylic Acids and Its Application in Asymmetric Synthesis. *Org Lett.* 2014; 16:4228–4231. [PubMed: 25068198]
234. Griffin JD, Zeller MA, Nicewicz DA. Hydrodecarboxylation of Carboxylic and Malonic Acid Derivatives via Organic Photoredox Catalysis: Substrate Scope and Mechanistic Insight. *J Am Chem Soc.* 2015; 137:11340–11348. [PubMed: 26291730]
235. HAT catalyst turnover is not always apparent. For example, excess thiol was employed in: Yoshimi Y, Itou T, Hatanaka M. Decarboxylative Reduction of Free Aliphatic Carboxylic Acids by Photogenerated Cation Radical. *Chem Commun.* 2007:5244–5246.
236. Romero NA, Margrey KA, Tay NE, Nicewicz DA. Site-Selective Arene C-H Amination via Photoredox Catalysis. *Science.* 2015; 349:1326–1330. [PubMed: 26383949]
237. Qvortrup K, Rankic DA, MacMillan DWC. A General Strategy for Organocatalytic Activation of C–H Bonds via Photoredox Catalysis: Direct Arylation of Benzylic Ethers. *J Am Chem Soc.* 2014; 136:626–629. [PubMed: 24341523]
238. Hager D, MacMillan DWC. Activation of C–H Bonds via the Merger of Photoredox and Organocatalysis: A Coupling of Benzylic Ethers with Schiff Bases. *J Am Chem Soc.* 2014; 136:16986–16989. [PubMed: 25457231]
239. Kee CW, Chan KM, Wong MW, Tan CH. Selective Bromination of  $sp^3$  C–H Bonds by Organophotoredox Catalysis. *Asian J Org Chem.* 2014; 3:536–544.
240. Liu D, Zhou H, Gu X, Shen X, Li P. TEMPO-Mediated Oxidation of Primary Alcohols to Aldehydes under Visible Light and Air. *Chin J Chem.* 2014; 32:117–122.
241. Cuthbertson JD, MacMillan DWC. The Direct Arylation of Allylic  $sp^3$  C–H Bonds via Organic and Photoredox Catalysis. *Nature.* 2015; 519:74–77. [PubMed: 25739630]
242. Jin J, MacMillan DWC. Alcohols as Alkylating Agents in Heteroarene C–H Functionalization. *Nature.* 2015; 525:87–90. [PubMed: 26308895]
243. Jeffrey JL, Terrett JA, MacMillan DWC. O–H Hydrogen Bonding Promotes H-Atom Transfer from  $\alpha$  C–H Bonds for C-Alkylation of Alcohols. *Science.* 2015; 349:1532–1536. [PubMed: 26316601]
244. DiRocco DA, Rovis T. Catalytic Asymmetric  $\alpha$ -Acylation of Tertiary Amines Mediated by a Dual Catalysis Mode: N-Heterocyclic Carbene and Photoredox Catalysis. *J Am Chem Soc.* 2012; 134:8094–8097. [PubMed: 22548244]
245. Two other notable examples using this system are anion binding catalysis (Ref. 246) and nucleophilic Morita–Baylis–Hillman type catalysis (Ref. 247). However, these protocols were carried out in two separate steps, so the compatibility of the dual catalyst systems has not been explicitly validated.
246. Bergonzini G, Schindler CS, Wallentin CJ, Jacobsen EN, Stephenson CRJ. Photoredox Activation and Anion Binding Catalysis in the Dual Catalytic Enantioselective Synthesis of  $\beta$ -Amino Esters. *Chem Sci.* 2014; 5:112–116.



247. Feng ZJ, Xuan J, Xia XD, Ding W, Guo W, Chen JR, Zou YQ, Lu LQ, Xiao WJ. Direct  $sp^3$  C–H Acroleination of *N*-Aryl-tetrahydroisoquinolines by Merging Photoredox Catalysis with Nucleophilic Catalysis. *Org Biomol Chem*. 2014; 12:2037–2040. [PubMed: 24553793]
248. Konieczynska MD, Dai C, Stephenson CRJ. Synthesis of Symmetric Anhydrides using Visible Light-Mediated Photoredox Catalysis. *Org Biomol Chem*. 2012; 10:4509–4511. [PubMed: 22573373]
249. Honeker R, Garza-Sanchez RA, Hopkinson MN, Glorius F. Visible-Light-Promoted Trifluoromethylthiolation of Styrenes by Dual Photoredox/Halide Catalysis. *Chem Eur J*. 2016; 22:4395–4399. [PubMed: 26880666]
250. Feng Z, Zeng T, Xuan J, Liu Y, Lu L, Xiao WJ. C–H Allylation of *N*-Aryl-tetrahydroisoquinolines by Merging Photoredox Catalysis with Iodide Catalysis. *Sci China Chem*. 2016; 59:171–174.
251. Zoller J, Fabry DC, Ronge MA, Rueping M. Synthesis of Indoles Using Visible Light: Photoredox Catalysis for Palladium-Catalyzed C–H Activation. *Angew Chem Int Ed*. 2014; 53:13264–13268.
252. Fabry DC, Zoller J, Raja S, Rueping M. Combining Rhodium and Photoredox Catalysis for C–H Functionalizations of Arenes: Oxidative Heck Reactions with Visible Light. *Angew Chem Int Ed*. 2014; 53:10228–10231.
253. Fabry DC, Ronge MA, Zoller J, Rueping M. C–H Functionalization of Phenols Using Combined Ruthenium and Photoredox Catalysis: In Situ Generation of the Oxidant. *Angew Chem Int Ed*. 2015; 54:2801–2805.
254. Terrett JA, Cuthbertson JD, Shurtleff VW, MacMillan DWC. Switching on Elusive Organometallic Mechanisms with Photoredox Catalysis. *Nature*. 2015; 524:330–334. [PubMed: 26266976]
255. Le C, MacMillan DWC. Fragment Couplings via  $CO_2$  Extrusion–Recombination: Expansion of a Classic Bond-Forming Strategy via Metal-lphotoredox. *J Am Chem Soc*. 2015; 137:11938–11941. [PubMed: 26333771]
256. Tasker SZ, Jamison TF. Highly Regioselective Indoline Synthesis under Nickel/Photoredox Dual Catalysis. *J Am Chem Soc*. 2015; 137:9531–9534. [PubMed: 26196355]
257. Yoo WJ, Tsukamoto T, Kobayashi S. Visible-Light-Mediated Chan–Lam Coupling Reactions of Aryl Boronic Acids and Aniline Derivatives. *Angew Chem Int Ed*. 2015; 54:6587–6590.
258. Choi S, Chatterjee T, Choi WJ, You Y, Cho EJ. Synthesis of Carbazoles by a Merged Visible Light Photoredox and Palladium-Catalyzed Process. *ACS Catal*. 2015; 5:4796–4802.
259. Lang SB, O’Nele KM, Tunge JA. Decarboxylative Allylation of Amino Alkanoic Acids and Esters via Dual Catalysis. *J Am Chem Soc*. 2014; 136:13606–13609. [PubMed: 25228064]
260. Maestri G, Malacria M, Derat E. Radical Pd(III)/Pd(I) Reductive Elimination in Palladium Sequences. *Chem Commun*. 2013; 49:10424–10426.
261. Lang SB, O’Nele KM, Douglas JT, Tunge JA. Dual Catalytic Decarboxylative Allylations of  $\alpha$ -Amino Acids and Their Divergent Mechanisms. *Chem Eur J*. 2015; 21:18589–18593. [PubMed: 26526115]
262. Xuan J, Zeng TT, Feng ZJ, Deng QH, Chen JR, Lu LQ, Xiao WJ, Alper H. Redox-Neutral  $\alpha$ -Allylation of Amines by Combining Palladium Catalysis and Visible-Light Photoredox Catalysis. *Angew Chem Int Ed*. 2015; 54:1625–1628.
263. Freeman DB, Furst L, Condie AG, Stephenson CRJ. Functionally Diverse Nucleophilic Trapping of Iminium Intermediates Generated Utilizing Visible Light. *Org Lett*. 2012; 14:94–97. [PubMed: 22148974]
264. Rueping M, Koenigs RM, Poscharyn K, Fabry DC, Leonori D, Vila C. Dual Catalysis: Combination of Photocatalytic Aerobic Oxidation and Metal Catalyzed Alkynylation Reactions —C–C Bond Formation Using Visible Light. *Chem Eur J*. 2012; 18:5170–5174. [PubMed: 22431393]
265. Perepichka I, Kundu S, Hearne Z, Li CJ. Efficient Merging of Copper and Photoredox Catalysis for the Asymmetric Cross-Dehydrogenative-Coupling of Alkynes and Tetrahydroisoquinolines. *Org Biomol Chem*. 2015; 13:447–451. [PubMed: 25372475]

266. Guo S, Tao R, Zhao J. Photoredox Catalytic Organic Reactions Promoted with Broadband Visible Light-Absorbing Bodipy-iodo-aza-Bodipy Triad Photocatalyst. *RSC Adv.* 2014; 4:36131–36139.
267. Kalyani D, McMurtrey KB, Neufeldt SR, Sanford MS. Room-Temperature C–H Arylation: Merger of Pd-Catalyzed C–H Functionalization and Visible-Light Photocatalysis. *J Am Chem Soc.* 2011; 133:18566–18569. [PubMed: 22047138]
268. Neufeldt SR, Sanford MS. Combining Transition Metal Catalysis with Radical Chemistry: Dramatic Acceleration of Palladium-Catalyzed C–H Arylation with Diaryliodonium Salts. *Adv Synth Catal.* 2012; 354:3517–3522. [PubMed: 23950736]
269. Cano-Yelo H, Deronzier A. Photocatalysis of the Pschorr Reaction by Tris-(2,2'-bipyridyl)ruthenium(II) in the Phenanthrene Series. *J Chem Soc, Perkin Trans.* 1984; 2:1093–1098.
270. Sahoo B, Hopkinson MN, Glorius F. Combining Gold and Photoredox Catalysis: Visible Light-Mediated Oxy- and Aminoarylation of Alkenes. *J Am Chem Soc.* 2013; 135:5505–5508. [PubMed: 23565980]
271. Hopkinson MN, Sahoo B, Glorius F. Dual Photoredox and Gold Catalysis: Intermolecular Multicomponent Oxyarylation of Alkenes. *Adv Synth Catal.* 2014; 356:2794–2800.
272. Shu XZ, Zhang M, He Y, Frei H, Toste FD. Dual Visible Light Photoredox and Gold-Catalyzed Arylative Ring Expansion. *J Am Chem Soc.* 2014; 136:5844–5847. [PubMed: 24730447]
273. Recent computational work suggests this is also the operative mechanism in Glorius' system. See: Zhang Q, Zhang ZQ, Fu Y, Yu HZ. Mechanism of the Visible Light-Mediated Gold-Catalyzed Oxyarylation Reaction of Alkenes. *ACS Catal.* 2016; 6:798–808.
274. Kim S, Rojas-Martin J, Toste FD. Visible Light-Mediated Gold-Catalysed Carbon(sp<sup>2</sup>)–Carbon(sp) Cross-Coupling. *Chem Sci.* 2016; 7:85–88.
275. Tlahuext-Aca A, Hopkinson MN, Sahoo B, Glorius F. Dual Gold/Photoredox-Catalyzed C(sp)–H Arylation of Terminal Alkynes with Diazonium Salts. *Chem Sci.* 2016; 7:89–93.
276. Um J, Yun H, Shin S. Cross-Coupling of Meyer–Schuster Intermediates under Dual Gold-Photoredox Catalysis. *Org Lett.* 2016; 18:484–487. [PubMed: 26761155]
277. Tlahuext-Aca A, Hopkinson MN, Garza-Sanchez RA, Glorius F. Alkyne Difunctionalization by Dual Gold/Photoredox Catalysis. *Chem Eur J.* 2016; doi: 10.1002/chem.201600710
278. He Y, Wu H, Toste FD. A Dual Catalytic Strategy for Carbon–Phosphorus Cross-Coupling *via* Gold and Photoredox Catalysis. *Chem Sci.* 2015; 6:1194–1198. [PubMed: 25685313]
279. Tellis JC, Primer DN, Molander GA. Single-Electron Transmetalation in Organoboron Cross-Coupling by Photoredox/Nickel Dual Catalysis. *Science.* 2014; 345:433–436. [PubMed: 24903560]
280. Gutierrez O, Tellis JC, Primer DN, Molander GA, Kozlowski MC. Nickel-Catalyzed Cross-Coupling of Photoredox-Generated Radicals: Uncovering a General Manifold for Stereoconvergence in Nickel-Catalyzed Cross-Couplings. *J Am Chem Soc.* 2015; 137:4896–4899. [PubMed: 25836634]
281. Ryu D, Primer DN, Tellis JC, Molander GA. Single-Electron Transmetalation: Synthesis of 1,1-Diaryl-2,2,2-trifluoroethanes by Photoredox/Nickel Dual Catalytic Cross-Coupling. *Chem Eur J.* 2016; 22:120–123. [PubMed: 26550805]
282. Primer DN, Karakaya I, Tellis JC, Molander GA. Single-Electron Transmetalation: An Enabling Technology for Secondary Alkylboron Cross-Coupling. *J Am Chem Soc.* 2015; 137:2195–2198. [PubMed: 25650892]
283. Karakaya I, Primer DN, Molander GA. Photoredox Cross-Coupling: Ir/Ni Dual Catalysis for the Synthesis of Benzylic Ethers. *Org Lett.* 2015; 17:3294–3297. [PubMed: 26079182]
284. Amani J, Sodagar E, Molander GA. Visible Light Photoredox Cross-Coupling of Acyl Chlorides with Potassium Alkoxyethyltrifluoroborates: Synthesis of  $\alpha$ -Alkoxyketones. *Org Lett.* 2016; 18:732–735. [PubMed: 26828576]
285. El Khatib M, Serafim RAM, Molander GA.  $\alpha$ -Arylation/Heteroarylation of Chiral  $\alpha$ -Aminomethyltrifluoroborates by Synergistic Iridium Photoredox/Nickel Cross-Coupling Catalysis. *Angew Chem Int Ed.* 2016; 55:254–258.

286. Yamashita Y, Tellis JC, Molander GA. Protecting Group-Free, Selective Cross-Coupling of Alkyltrifluoroborates with Borylated Aryl Bromides via Photoredox/Nickel Dual Catalysis. *Proc Nat Acad Sci USA*. 2015; 112:12026–12029. [PubMed: 26371299]
287. Zuo Z, Ahneman DT, Chut L, Terrett JA, Doyle AG, MacMillan DWC. Merging Photoredox with Nickel Catalysis: Coupling of  $\alpha$ -Carboxyl  $sp^3$ -Carbons with Aryl Halides. *Science*. 2014; 345:437–440. [PubMed: 24903563]
288. Noble, Adam; McCarver, SJ.; MacMillan, DWC. Merging Photoredox and Nickel Catalysis: Decarboxylative Cross-Coupling of Carboxylic Acids with Vinyl Halides. *J Am Chem Soc*. 2015; 137:624–627. [PubMed: 25521443]
289. Gu L, Jin C, Liu J, Zhang H, Yuan M, Li G. Acylation of Indoles *via* Photoredox Catalysis: a Route to 3-Acylindoles. *Green Chem*. 2016; 18:1201–1205.
290. Chu L, Lipshultz JM, MacMillan DWC. Merging Photoredox and Nickel Catalysis: The Direct Synthesis of Ketones by the Decarboxylative Arylation of  $\alpha$ -Oxo Acids. *Angew Chem Int Ed*. 2015; 54:7929–7933.
291. Zhou C, Li P, Zhu X, Wang L. Merging Photoredox with Palladium Catalysis: Decarboxylative ortho-Acylation of Acetanilides with  $\alpha$ -Oxocarboxylic Acids under Mild Reaction Conditions. *Org Lett*. 2015; 17:6198–6201. [PubMed: 26646667]
292. Luo J, Zhang J. Donor–Acceptor Fluorophores for Visible-Light-Promoted Organic Synthesis: Photoredox/Ni Dual Catalytic C( $sp^3$ )–C( $sp^2$ ) Cross-Coupling. *ACS Catal*. 2016; 6:873–877.
293. Zuo Z, Cong H, Li W, Choi J, Fu GC, MacMillan DWC. Enantioselective Decarboxylative Arylation of  $\alpha$ -Amino Acids via the Merger of Photoredox and Nickel Catalysis. *J Am Chem Soc*. 2016; 138:1832–1835. [PubMed: 26849354]
294. Oderinde MS, Varela-Alvarez A, Aquila B, Robbins DW, Johannes JW. Effects of Molecular Oxygen, Solvent, and Light on Iridium-Photoredox/Nickel Dual-Catalyzed Cross-Coupling Reactions. *J Org Chem*. 2015; 80:7642–7651. [PubMed: 26140623]
295. Jouffroy M, Primer DN, Molander GA. Base-Free Photoredox/Nickel Dual-Catalytic Cross-Coupling of Ammonium Alkylsilicates. *J Am Chem Soc*. 2016; 138:475–478. [PubMed: 26704168]
296. Patel NR, Kelly CB, Jouffroy M, Molander GA. Engaging Alkenyl Halides with Alkylsilicates via Photoredox Dual Catalysis. *Org Lett*. 2016; 18:764–767. [PubMed: 26828317]
297. Corcé V, Chamoreau LM, Derat E, Goddard JP, Ollivier C, Fensterbank L. Silicates as Latent Alkyl Radical Precursors: Visible-Light Photocatalytic Oxidation of Hypervalent Bis-Catecholato Silicon Compounds. *Angew Chem Int Ed*. 2015; 54:11414–11418.
298. Lévêque C, Chenneberg L, Corcé V, Goddard JP, Ollivier C, Fensterbank L. Primary alkyl bis-catecholato silicates in dual photoredox/nickel catalysis: aryl- and heteroaryl-alkyl cross coupling reactions. *Org Chem Front*. 2016; 3:462–465.
299. Oderinde MS, Frenette M, Robbins DW, Aquila B, Johannes JW. Photoredox Mediated Nickel Catalyzed Cross-Coupling of Thiols with Aryl and Heteroaryl Iodides via Thiyl Radicals. *J Am Chem Soc*. 2016; 138:1760–1763. [PubMed: 26840123]
300. Jouffroy M, Kelly CB, Molander GA. Thioetherification via Photoredox/Nickel Dual Catalysis. *Org Lett*. 2016; 18:876–879. [PubMed: 26852821]
301. Xuan J, Zeng TT, Chen JR, Lu LQ, Xiao WJ. Room Temperature C–P Bond Formation Enabled by Merging Nickel Catalysis and Visible-Light-Induced Photoredox Catalysis. *Chem Eur J*. 2015; 21:4962–4965. [PubMed: 25688851]
302. Ye Y, Sanford M. Merging Visible-Light Photocatalysis and Transition-Metal Catalysis in the Copper-Catalyzed Trifluoromethylation of Boronic Acids with  $CF_3I$ . *J Am Chem Soc*. 2012; 134:9034–9037. [PubMed: 22624669]
303. Saito I, Takayama M, Matsuura T. A Novel Photooxidation of Hydrocarbons Sensitized by 2,7-Diazapyrenium Dication in the Presence of Iron Catalyst. *Tetrahedron Lett*. 1989; 30:2237–2240.
304. Walling C. Fenton's Reagent Revisited. *Acc Chem Res*. 1975; 8:125–131.
305. Zhang G, Liu C, Yi H, Meng Q, Bian C, Chen H, Jian JX, Wu LZ, Lei A. External Oxidant-Free Oxidative Cross-Coupling: A Photoredox Cobalt-Catalyzed Aromatic C–H Thiolation for Constructing C–S Bonds. *J Am Chem Soc*. 2015; 137:9273–9280. [PubMed: 26158688]

306. Gao XW, Meng QY, Li JX, Zhong JJ, Lei T, Li XB, Tung CH, Wu LZ. Visible Light Catalysis Assisted Site-Specific Functionalization of Amino Acid Derivatives by C–H Bond Activation without Oxidant: Cross-Coupling Hydrogen Evolution Reaction. *ACS Catal.* 2015; 5:2391–2396.
307. Zhong JJ, Wu CJ, Meng QY, Gao XW, Lei T, Tung CH, Wu LZ. A Cascade Cross-Coupling and *in Situ* Hydrogenation Reaction by Visible Light Catalysis. *Adv Synth Catal.* 2014; 356:2846–2852.
308. The possibility of concerted PCET was not discussed.
309. Cheng Y, Yang J, Qu Y, Li P. Aerobic Visible-Light Photoredox Radical C–H Functionalization: Catalytic Synthesis of 2-Substituted Benzothiazoles. *Org Lett.* 2012; 14:98–101. [PubMed: 22146071]
310. Xiang M, Meng QY, Li JX, Zheng YW, Ye C, Li ZJ, Chen B, Tung CH, Wu LZ. Activation of C–H Bonds through Oxidant-Free Photoredox Catalysis: Cross-Coupling Hydrogen-Evolution Transformation of Isochromans and  $\beta$ -Keto Esters. *Chem Eur J.* 2015; 21:18080–18084. [PubMed: 26515479]
311. Mandler D, Willner I. Solar Light Induced Formation of Chiral 2-Butanol in an Enzyme-Catalyzed Chemical System. *J Am Chem Soc.* 1984; 106:5352–5353.
312. Mandler D, Willner I. Photoinduced Enzyme-Catalysed Synthesis of Amino Acids by Visible Light. *J Chem Soc, Chem Commun.* 1986:851–853.
313. Mandler D, Willner I. Photosensitized NAD(P)H Regeneration Systems; Application in the Reduction of Butan-2-one, Pyruvic, and Acetoacetic Acids and in the Reductive Amination of Pyruvic and Oxoglutaric Acid to Amino Acid. *J Chem Soc, Perkin Trans.* 1986; 2:805–811.
314. Kim JH, Lee SH, Lee JS, Lee M, Park CB. Zn-Containing Porphyrin as a Biomimetic Light-Harvesting Molecule for Biocatalyzed Artificial Photosynthesis. *Chem Commun.* 2011; 47:10227–10229.
315. Ryu J, Nam DH, Lee SH, Park CB. Biocatalytic Photosynthesis with Water as an Electron Donor. *Chem Eur J.* 2014; 20:12020–12025. [PubMed: 25088448]
316. Maidan R, Willner I. Photochemical and Chemical Enzyme Catalyzed Debromination of meso-1,2-Dibromostilbene in Multiphase Systems. *J Am Chem Soc.* 1986; 108:1080–1082.
317. Ruppert R, Steckhan E. Efficient Photoelectrochemical in-situ Regeneration of NAD(P)<sup>+</sup> Coupled to Enzymatic Oxidation of Alcohols. *J Chem Soc, Perkin Trans.* 1989; 2:811–814.
318. Churakova E, Kluge M, Ullrich R, Arends I, Hofrichter M, Hollmann F. Specific Photobiocatalytic Oxyfunctionalization Reactions. *Angew Chem Int Ed.* 2011; 50:10716–10719.
319. Zachos I, Gaßmeyer SK, Bauer D, Sieber V, Hollmann F, Kourist R. Photobiocatalytic Decarboxylation for Olefin Synthesis. *Chem Commun.* 2015; 51:1918–1921.
320. Taglieber A, Schulz F, Hollmann F, Rusek M, Reetz MT. Light-Driven Biocatalytic Oxidation and Reduction Reactions: Scope and Limitations. *ChemBioChem.* 2008; 9:565–572. [PubMed: 18288667]
321. Jones GH, Edwards DW, Parr D. A Room Temperature Photochemical Dehydrogenation Catalyst. *J Chem Soc, Chem Commun.* 1976:969–970.
322. West JG, Huang D, Sorensen EJ. Acceptorless Dehydrogenation of Small Molecules through Cooperative Base Metal Catalysis. *Nat Commun.* 2015; 6:10093. [PubMed: 26656087]
323. Ogilby PR, Foote CS. Chemistry of Singlet Oxygen. 42. Effect of Solvent, Solvent Isotopic Substitution, and Temperature on the Lifetime of Singlet Molecular Oxygen (<sup>1</sup>g). *J Am Chem Soc.* 1983; 105:3423–3430.
324. Adam W, Griesbeck A, Staab E. A Convenient “One-Pot” Synthesis of Epoxy Alcohols via Photooxygenation of Olefins in the Presence of Titanium(IV) Catalyst. *Tetrahedron Lett.* 1986; 27:2839–2842.
325. Campestrini S, Tonellato U. Photoinitiated Olefin Epoxidation with Molecular Oxygen, Sensitized by Free Base Porphyrins and Promoted by Hexacarbonylmolybdenum in Homogeneous Solution. *Eur J Org Chem.* 2002:3827–3832.
326. Krief A, Colaux-Castillo C. Catalytic Asymmetric Dihydroxylation of  $\alpha$ -Methylstyrene by Air. *Tetrahedron Lett.* 1999; 40:4189–4192.
327. Hevesi L, Krief A. Photo-Oxygenation of Selenides—A New Pathway to Selenoxides. *Angew Chem Int Ed.* 1976; 15:381.

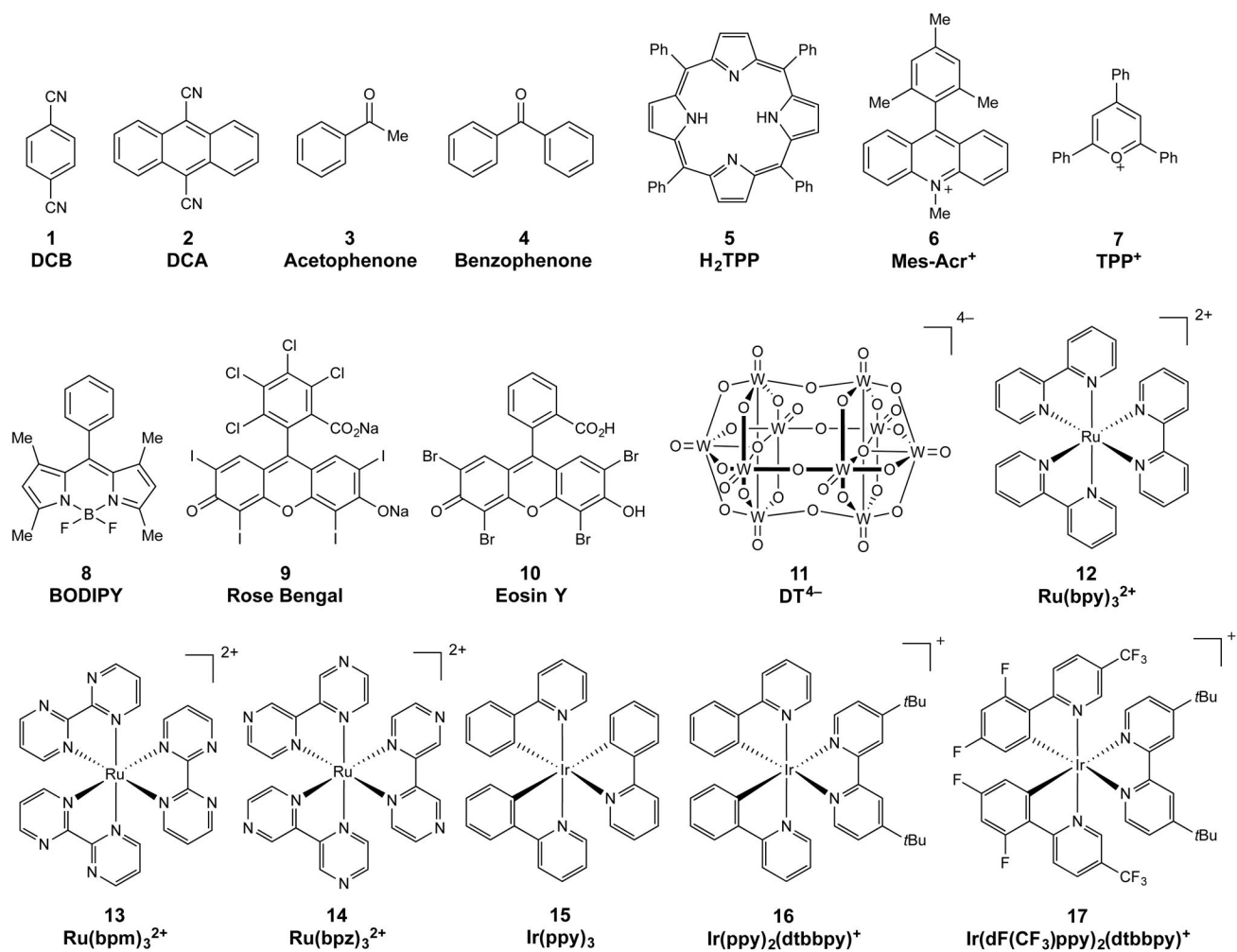
328. Abatjoglou AG, Bryant DR. Organic Selenoxides as Oxidants in Osmium Tetroxide Catalyzed Oxidation of Olefins to Glycols. *Tetrahedron Lett.* 1981; 22:2051–2054.
329. Kolb HC, VanNieuwenhze MS, Sharpless KB. Catalytic Asymmetric Dihydroxylation. *Chem Rev.* 1994; 94:2483–2547.
330. Yoo WJ, Tsukamoto T, Kobayashi S. Visible Light-Mediated Ullmann-Type C–N Coupling Reactions of Carbazole Derivatives and Aryl Iodides. *Org Lett.* 2015; 17:3640–3642. [PubMed: 26151428]
331. Creutz SE, Lotito KJ, Fu GC, Peters JC. Photoinduced Ullmann C–N Coupling: Demonstrating the Viability of a Radical Pathway. *Science.* 2012; 338:647–651. [PubMed: 23118186]
332. Bissember AC, Lundgren RJ, Creutz SE, Peters JC, Fu GC. Transition-Metal-Catalyzed Alkylations of Amines with Alkyl Halides: Photoinduced, Copper-Catalyzed Couplings of Carbazoles. *Angew Chem Int Ed.* 2013; 52:5129–5133.
333. Ratani TS, Bachman S, Fu GC, Peters JC. Photoinduced, Copper-Catalyzed Carbon–Carbon Bond Formation with Alkyl Electrophiles: Cyanation of Unactivated Secondary Alkyl Chlorides at Room Temperature. *J Am Chem Soc.* 2015; 137:13902–13907. [PubMed: 26491957]
334. Sakai A, Tani H, Aoyama T, Shiori T. Enantioselective Photosensitized Oxygenation. Its Application to N<sub>l</sub>-Methoxycarbonyltryptamine and Determination of Absolute Configuration of the Product. *Synlett.* 1998; 9:257–258.
335. Donslund BS, Johansen TK, Poulsen PS, Halskov KS, Jørgensen KA. The Diarylprolinol Silyl Ethers: Ten Years After. *Angew Chem Int Ed.* 2015; 54:13860–13847.
336. Córdova A, Sundén H, Engqvist M, Ibrahim I, Casasm J. The Direct Amino Acid-Catalyzed Asymmetric Incorporation of Molecular Oxygen to Organic Compounds. *J Am Chem Soc.* 2004; 126:8914–8915. [PubMed: 15264820]
337. Ibrahim I, Zhao GL, Sundén H, Córdova A. A Route to 1,2-Diols by Enantioselective Organocatalytic  $\alpha$ -Oxidation with Molecular Oxygen. *Tetrahedron Lett.* 2006; 47:4659–4663.
338. Sundén H, Engqvist M, Casas J, Ibrahim I, Córdova A. Direct Amino Acid Catalyzed Asymmetric  $\alpha$  Oxidation of Ketones with Molecular Oxygen. *Angew Chem Int Ed.* 2004; 43:6532–6535.
339. Walaszek DJ, Rybicka-Jasinska K, Smolen S, Karczewski M, Gryko D. Mechanistic Insights into Enantioselective C–H Photooxygenation of Aldehydes *via* Enamine Catalysis. *Adv Synth Catal.* 2015; 357:2061–2070.
340. Lian M, Li Z, Cai Y, Meng Q, Gao Z. Enantioselective Photooxygenation of  $\beta$ -Keto Esters by Chiral Phase-Transfer Catalysis using Molecular Oxygen. *Chem Asian J.* 2012; 7:2019–2023. [PubMed: 22740435]
341. Silverman SK, Foote CS. Singlet Oxygen and Electron-Transfer Mechanisms in the Dicyanoanthracene-Sensitized Photooxidation of 2,3-Diphenyl-1,4-dioxene. *J Am Chem Soc.* 1991; 113:7672–7675.
342. Manring LE, Kramer MK, Foote CS. Interception of O<sub>2</sub><sup>-</sup> by Benzoquinone in Cyanoaromatic-Sensitized Photooxygenations. *Tetrahedron Lett.* 1984; 25:2523–2526.
343. Brachet E, Ghosh T, Ghosh I, König B. Visible Light C–H Amidation of Heteroarenes with Benzoyl Azides. *Chem Sci.* 2015; 6:987–992.
344. Das A, Banerjee T, Hanson K. Protonation of Silylenol Ether *via* Excited State Proton Transfer Catalysis. *Chem Commun.* 2016; 52:1350–1353.

## Biographies

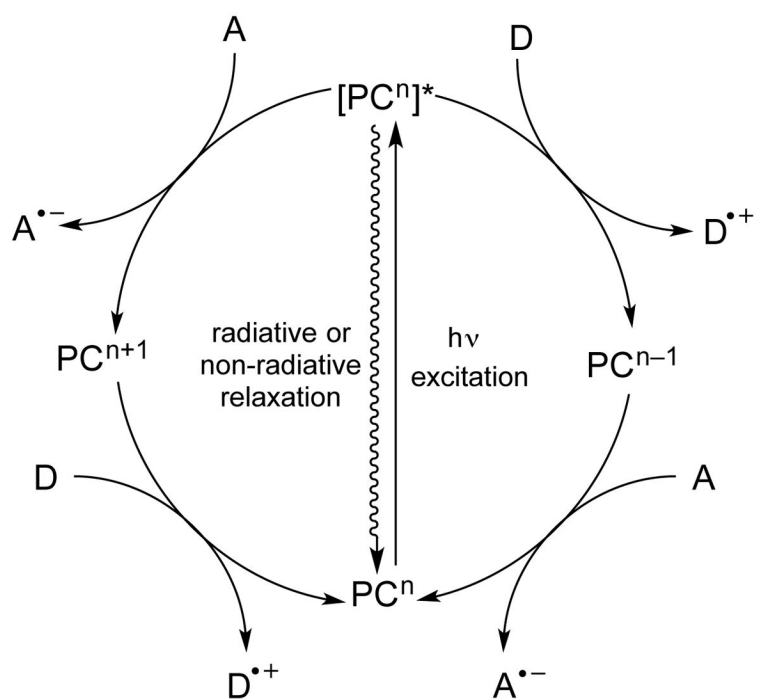
Kaz Skubi attended Carleton College, where he carried out research in the labs of David Alberg and Gretchen Hofmeister on enantioselective desymmetrization reactions using organocatalysis. After earning his bachelor's degree in 2011, he began graduate studies at the University of Wisconsin–Madison in the group of Tehshik Yoon. His current research focuses on new strategies to control the absolute stereochemistry of photocatalytic processes.

Travis Blum received his bachelor's degree in Biochemistry from Hobart and Williams Smith Colleges in 2010 studying the total synthesis of bioactive depsipeptide natural products. In 2016, he completed graduate studies in both electron transfer and energy transfer photocatalysis at the University of Wisconsin–Madison under Prof. Tehshik Yoon. He is currently a postdoctoral fellow in the laboratory of Prof. David Liu at Harvard University.

Tehshik Yoon has been on the faculty at the University of Wisconsin–Madison since 2005. He received his M.S. at Caltech working with Erick Carreira and his Ph.D. from the same institution with David MacMillan. After a postdoc at Harvard studying with Eric Jacobsen, he established an independent research program at the University of Wisconsin focusing on synthetic aspects of photochemistry and radical chemistry. His teaching and scholarship have recently been recognized through a Bessel Award from the Humboldt Foundation (2015) and UW–Madison's Kiekhofers Distinguished Teaching Award (2013).

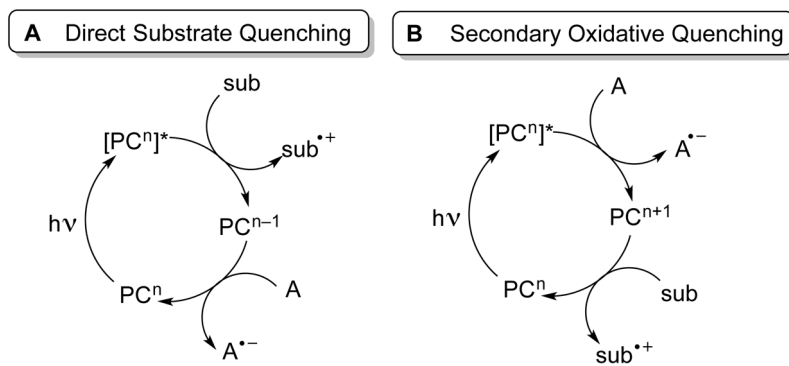


**Figure 1.**  
Chemical Structures of Common Photocatalysts

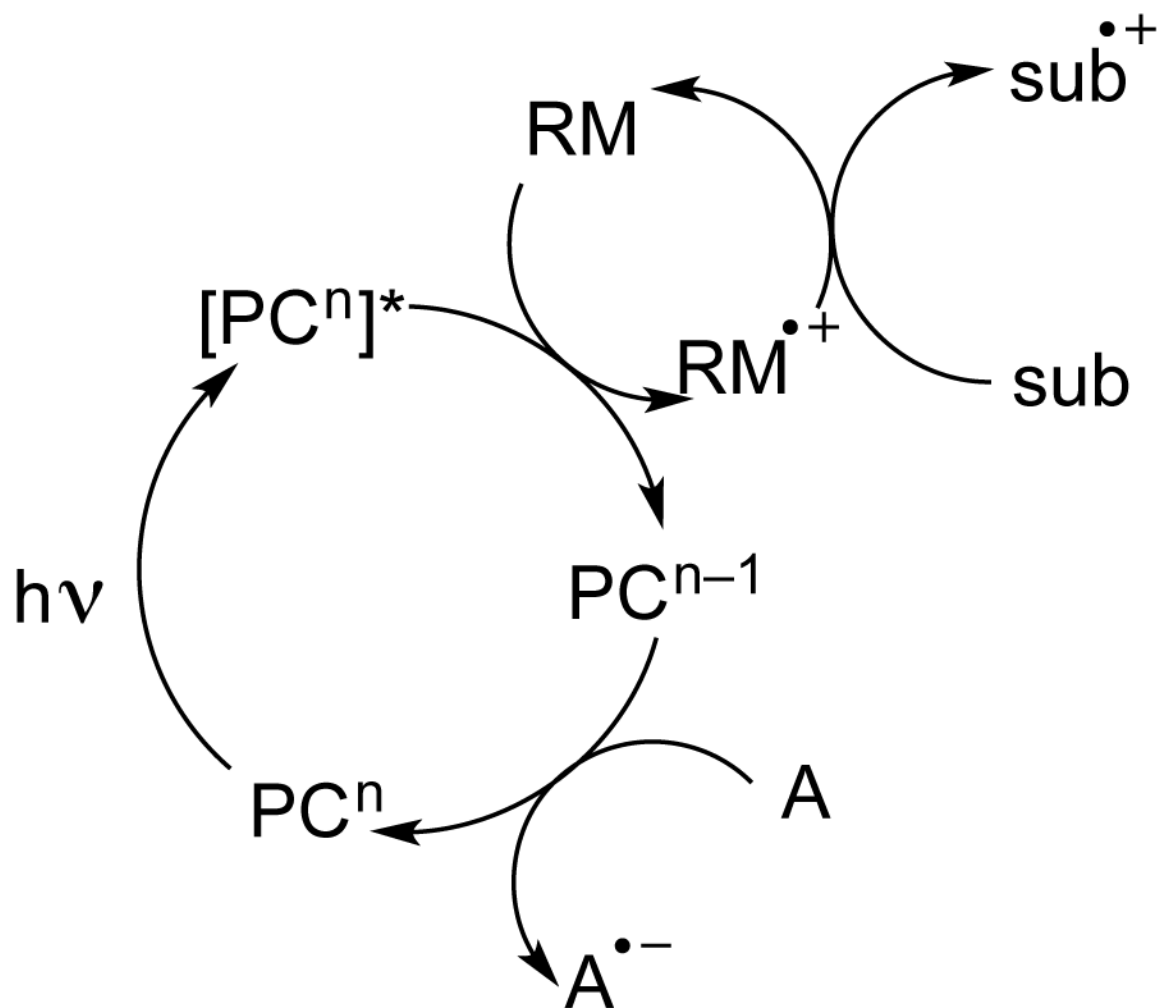


**Figure 2.**  
Photoinduced Electron Transfer (PET)

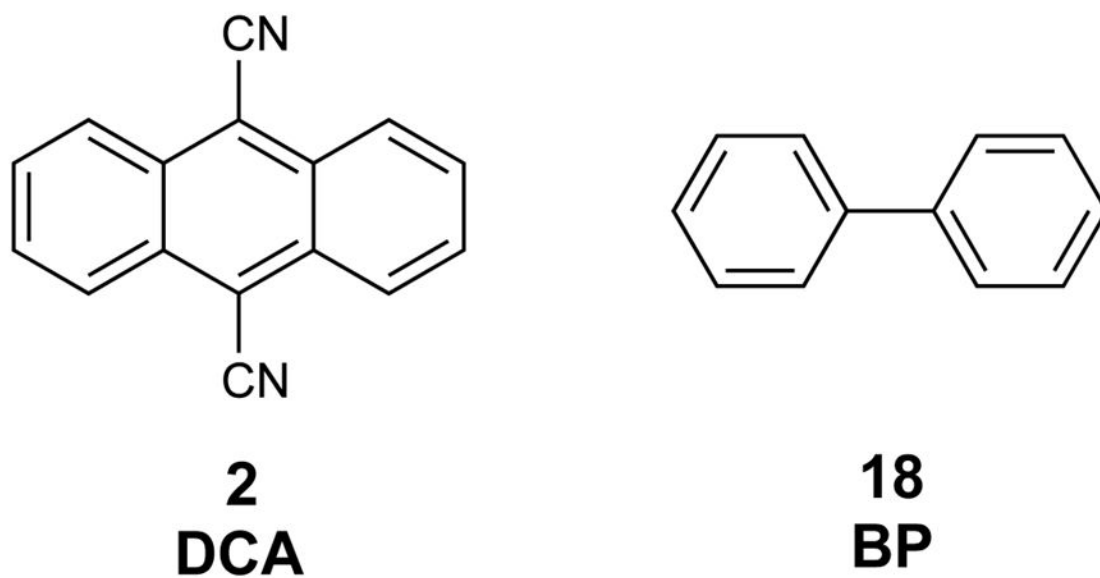




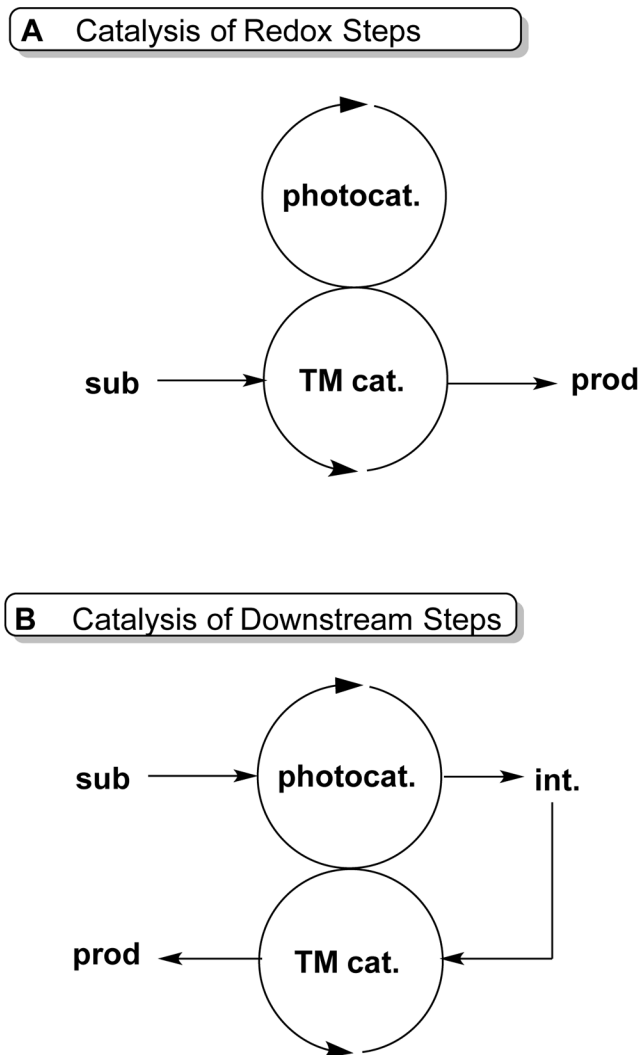
**Figure 3.**  
Direct and Secondary Quenching for an Oxidative Reaction



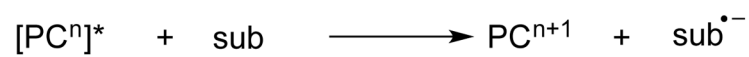
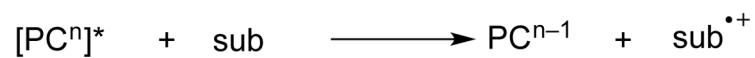
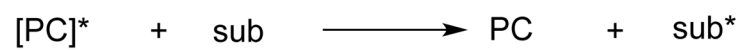
**Figure 4.**  
Redox Mediation of an Oxidative Transformation



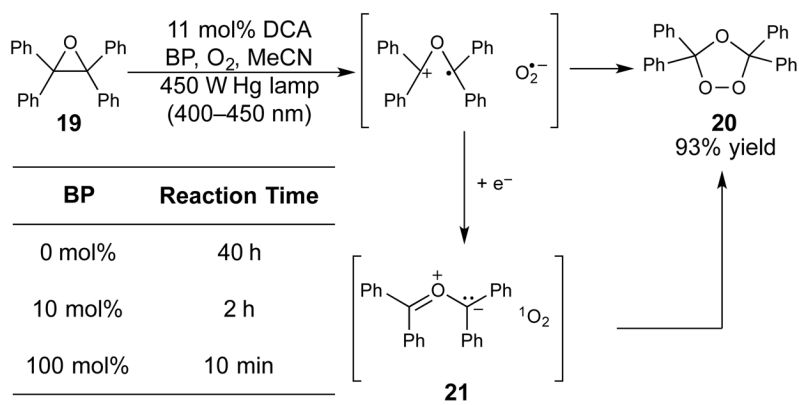
**Figure 5.**  
Common Photocatalyst/Redox Mediator Pair 9,10-Dicyanoanthracene (DCA) and Biphenyl (BP)



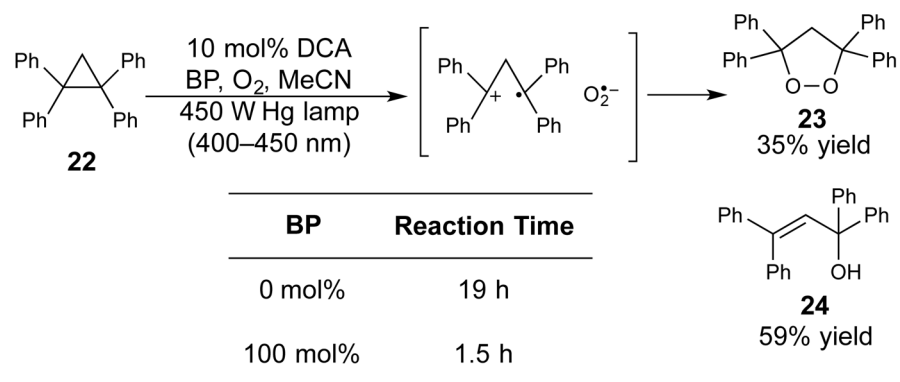
**Figure 6.**  
Common Modes of Tandem Transition Metal/Photocatalysis

**A** Electron Transfer**B** Atom Transfer**C** Energy Transfer

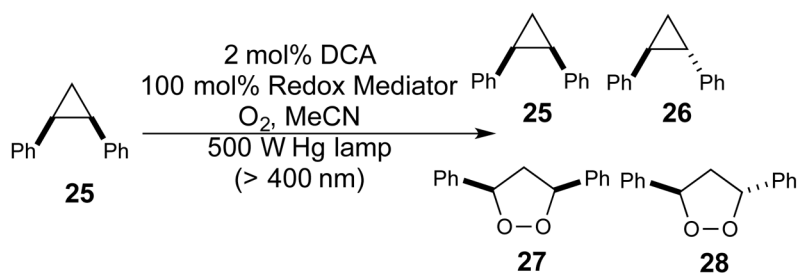
**Scheme 1.**  
Mechanisms of Homogeneous Photocatalysis



**Scheme 2.**  
Redox Mediated Epoxide Photooxygenation



**Scheme 3.**  
Redox Mediated Cyclopropane Photooxygenation



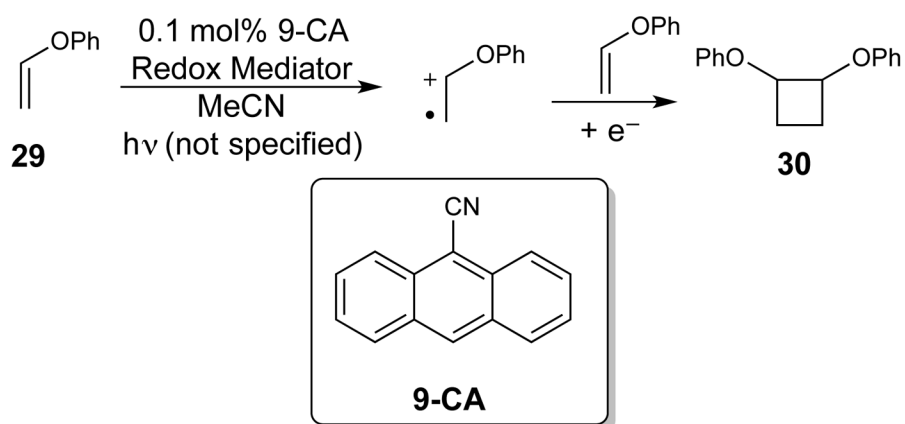
Redox Mediator	$k_q$ (M <sup>-1</sup> s <sup>-1</sup> )	$E_{ox}$ (V) <sup>a</sup>	$\Phi_{sep}$
None	$1.1 \times 10^{10}$	1.38 <sup>b</sup>	0.12
Biphenyl	$3.6 \times 10^9$	1.45	0.72
<i>o</i> -Terphenyl	$7.0 \times 10^9$	1.42	0.64
<i>m</i> -Terphenyl	$5.5 \times 10^9$	1.40	0.32
Napthalene	$1.4 \times 10^{10}$	1.22	0.58
Phenanthrene	$1.4 \times 10^{10}$	1.17	0.62

<sup>a</sup> Oxidation potentials vs. Ag/AgClO<sub>4</sub> in MeCN

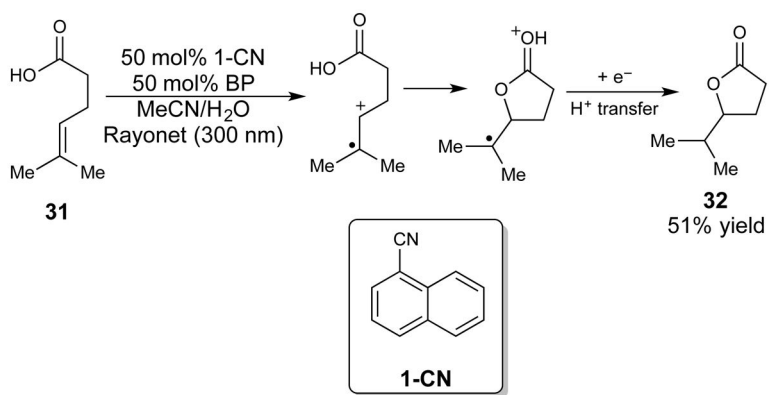
<sup>b</sup> Oxidation potential of cyclopropane **25**

**Scheme 4.**  
Effect of Redox Mediator on Ion Pair Separation for Cyclopropane Isomerization and Photooxygenation

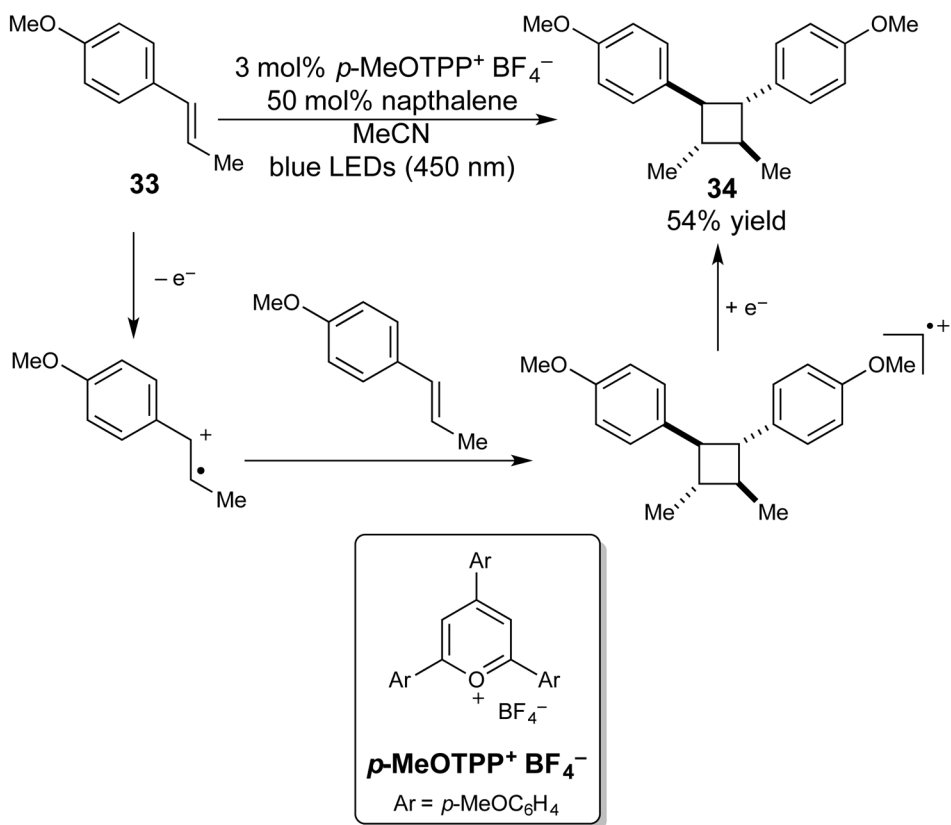




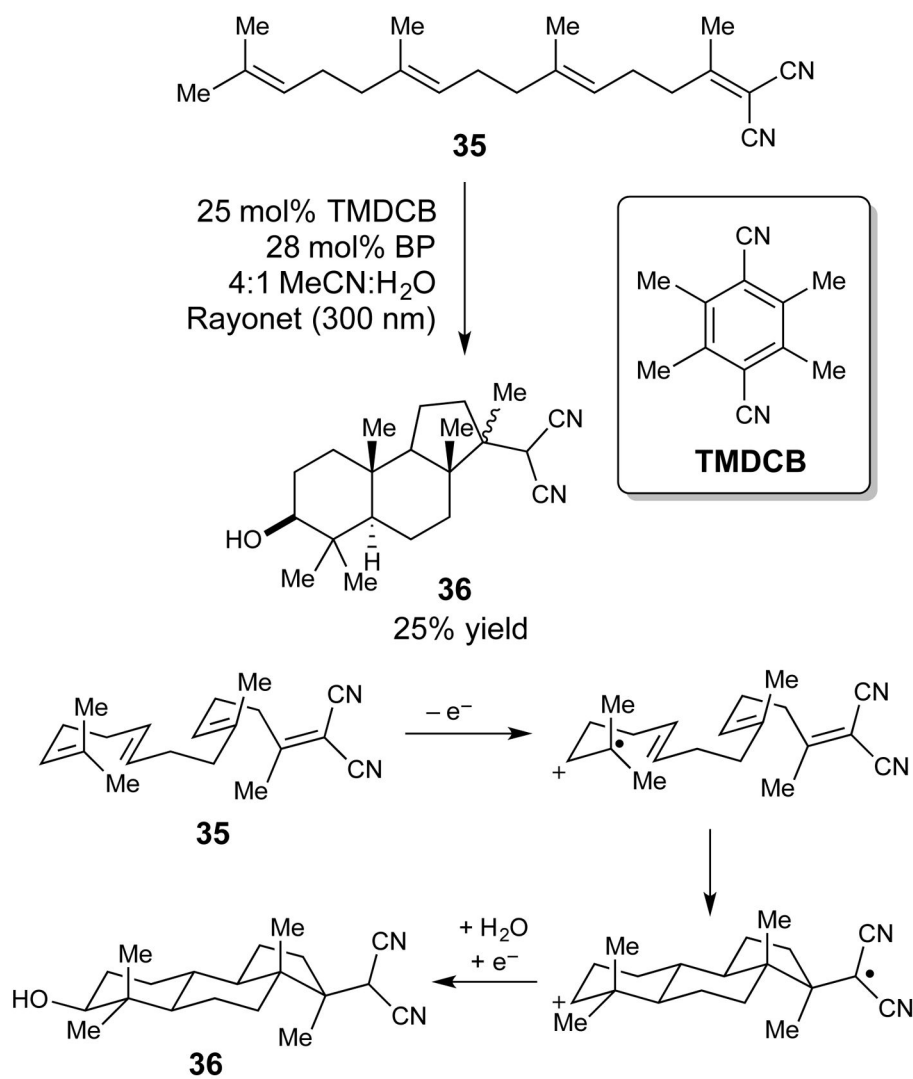
**Scheme 5.**  
Dimerization of Phenyl Vinyl Ether by Redox Mediated PET



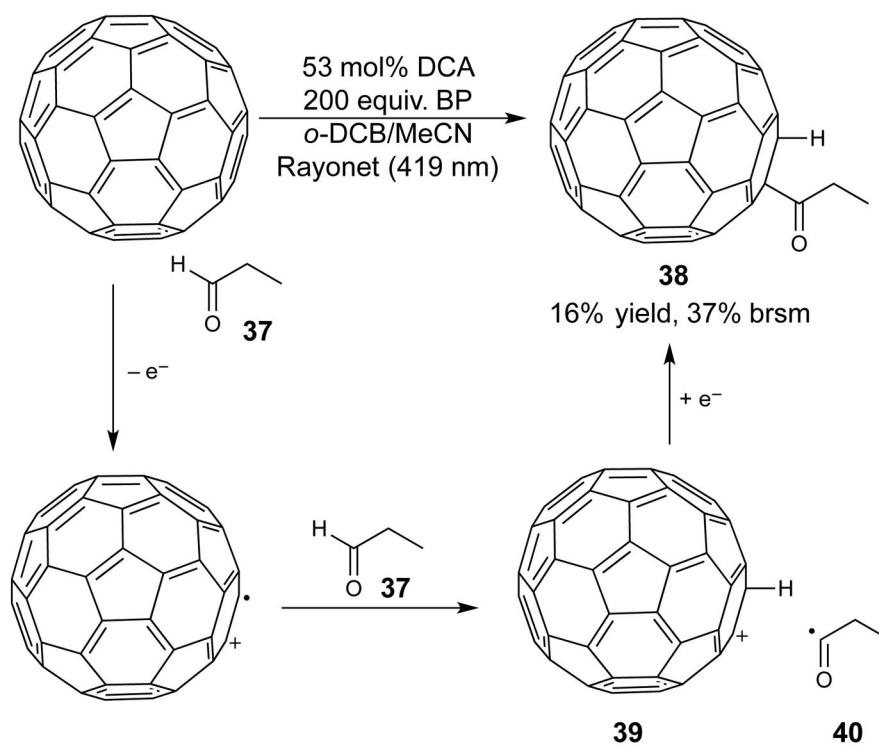
**Scheme 6.**  
Alkene Photooxygenation and Trapping



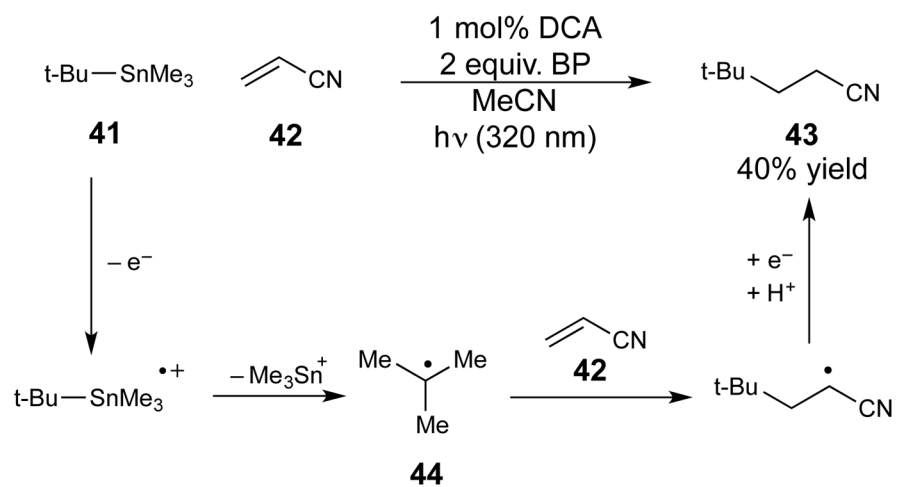
**Scheme 7.**  
 [2+2] Cycloaddition of Styrenes by PET



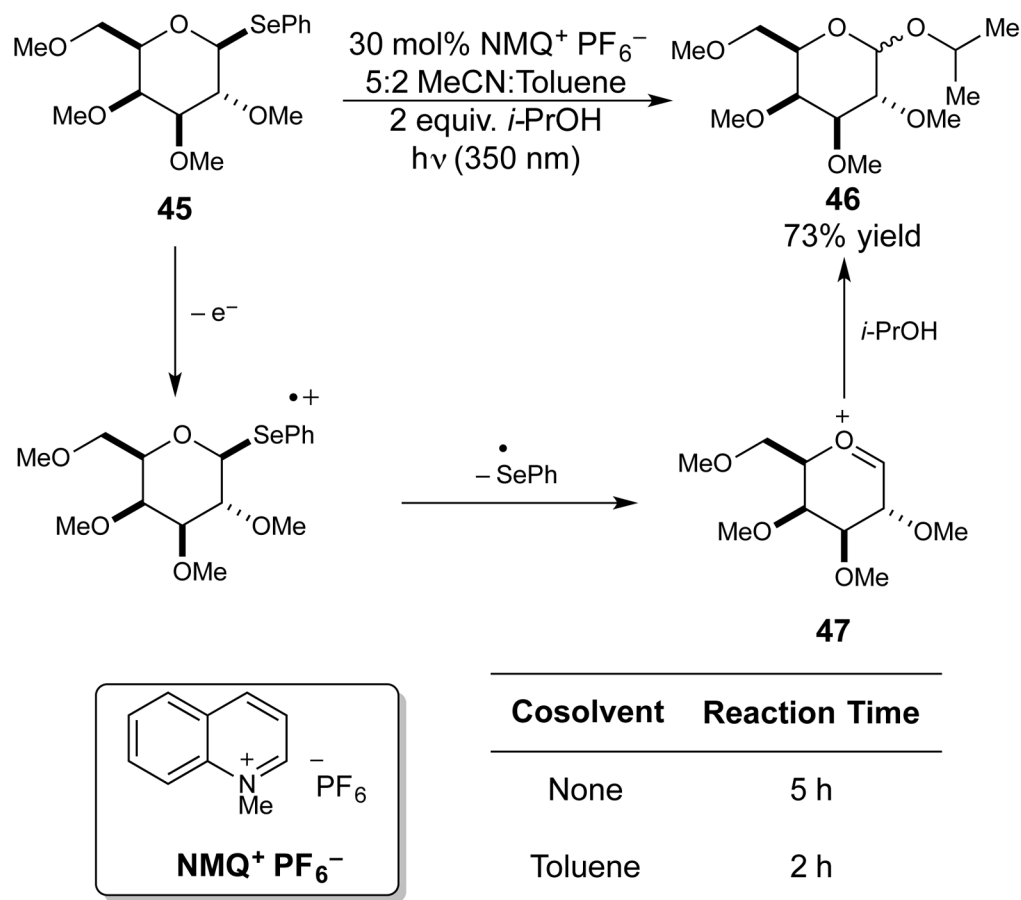
**Scheme 8.**  
 Photooxidative Radical Cation Cascade Employing Redox Mediation



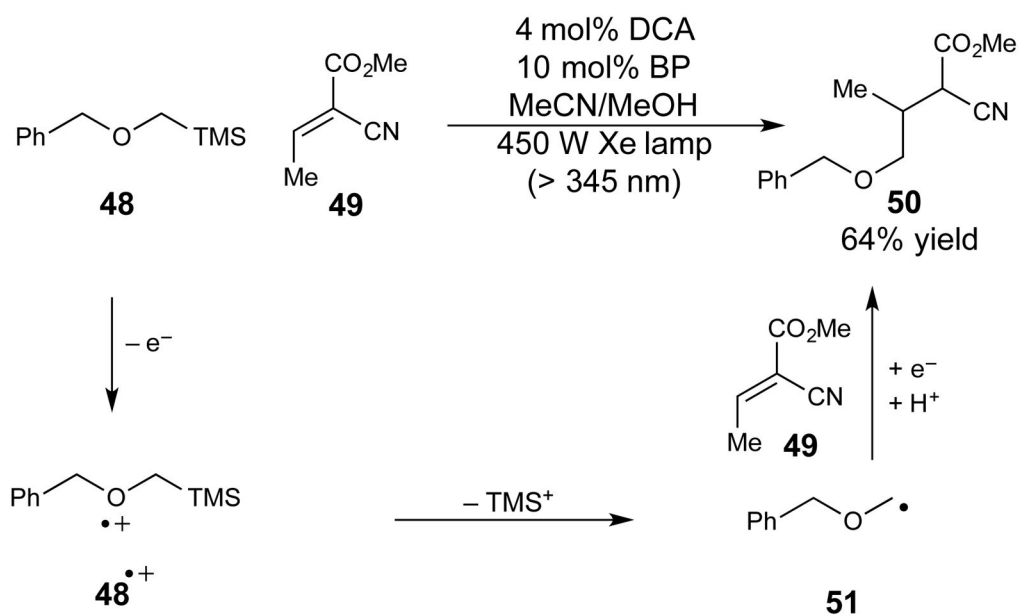
**Scheme 9.**  
Acylation of  $C_{60}$  using PET and Redox Mediation



**Scheme 10.**  
Oxidative Destannylation and Radical Addition

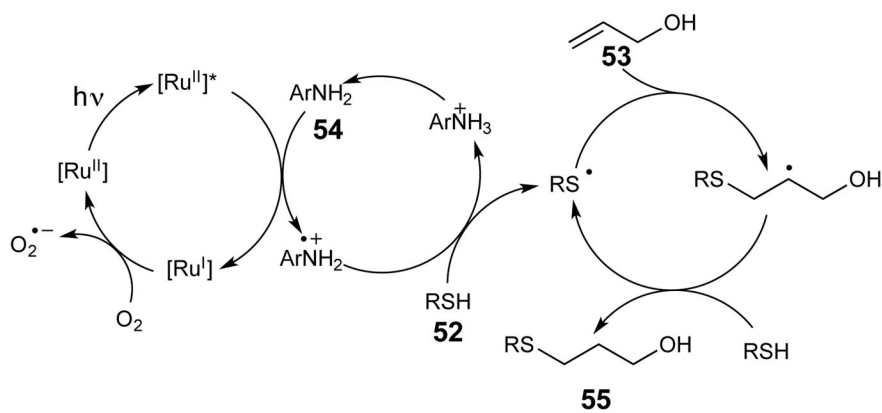
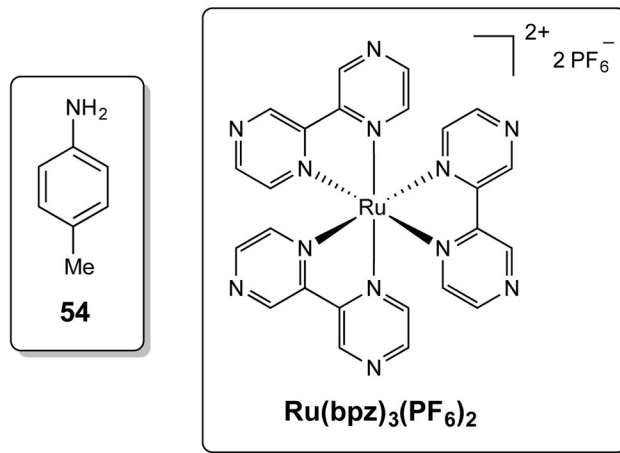
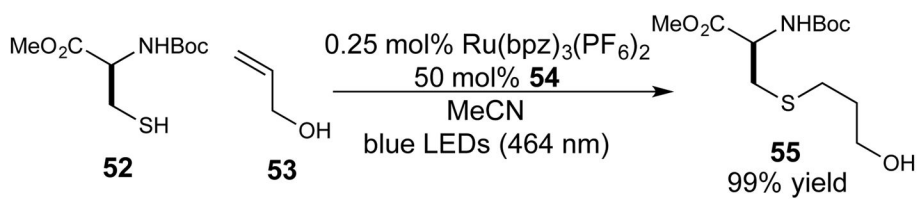


**Scheme 11.**  
Oxidative Deselenation and Nucleophilic Trapping

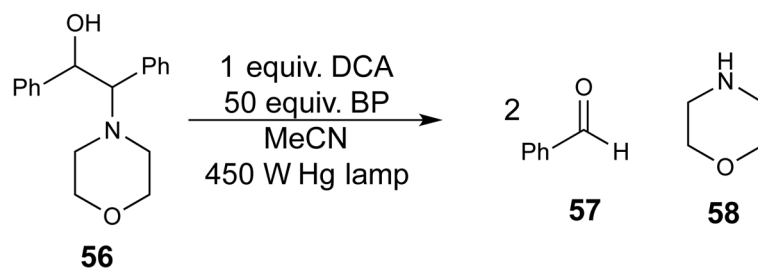


**Scheme 12.**  
Photooxidative Desilylation and Radical Addition



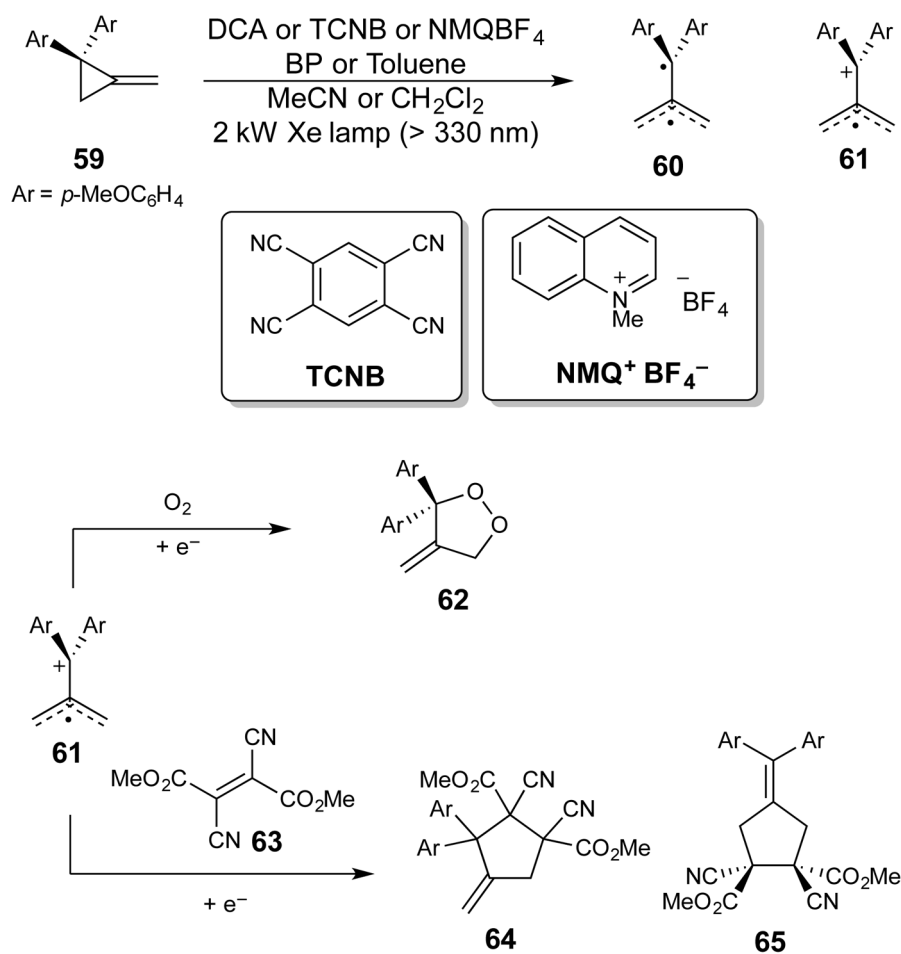


**Scheme 13.**  
Radical Thiol–Ene Reaction with Anilines as Redox Mediators

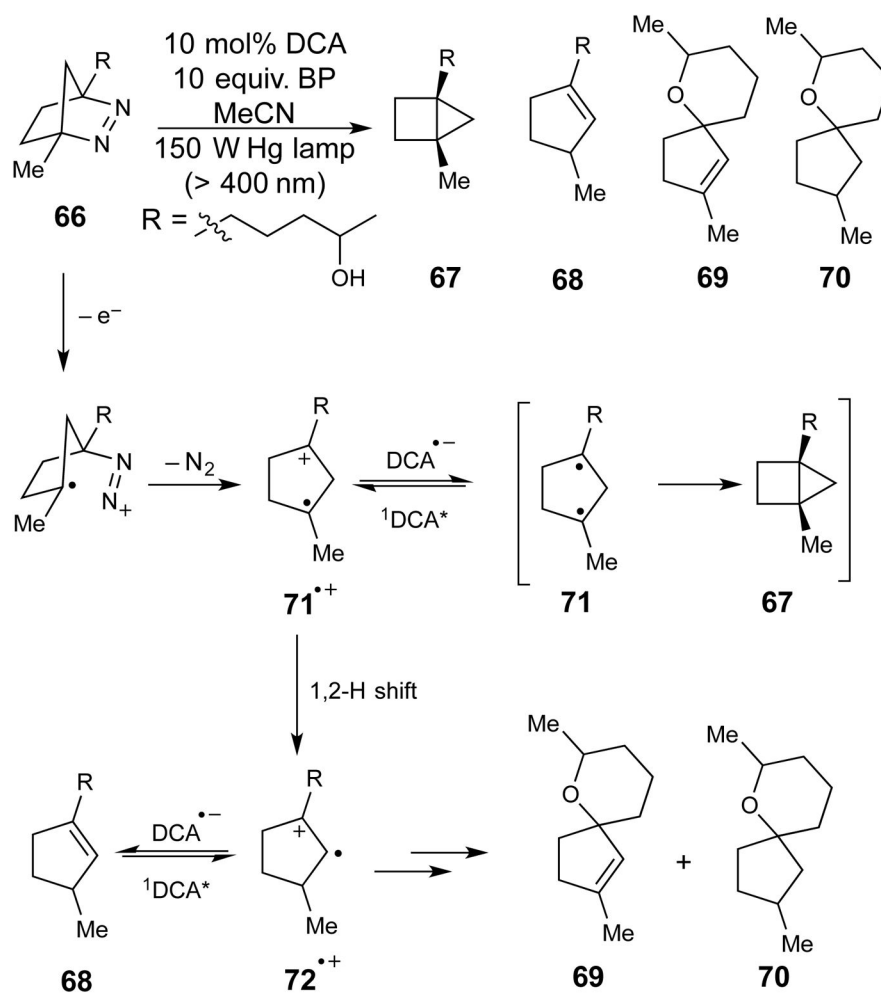


Photocatalyst	$\Phi_{ox}$
DCA	0.0017
DCA/BP	1.10

**Scheme 14.**  
Oxidative Fragmentation of  $\alpha,\beta$  Amino Alcohols

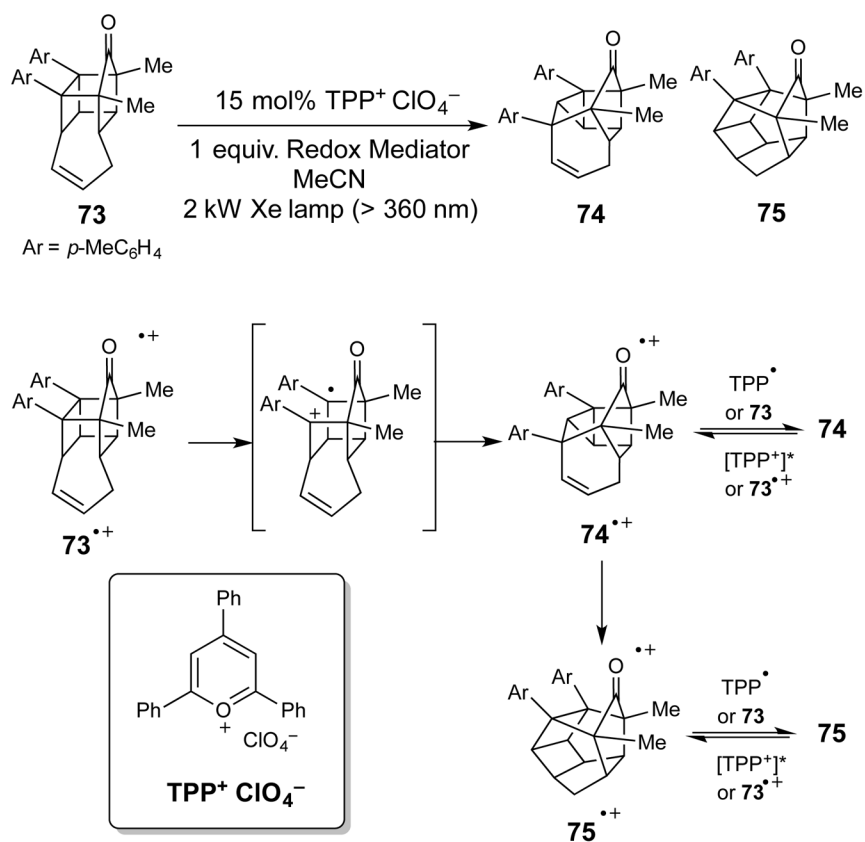


**Scheme 15.**  
Methylene Cyclopropane Rearrangement and Cycloadditions



Photocatalyst	Conv.	67	68	69	70
DCA	30%	52%	48%	--	--
DCA/BP	40%	25%	62%	7%	6%

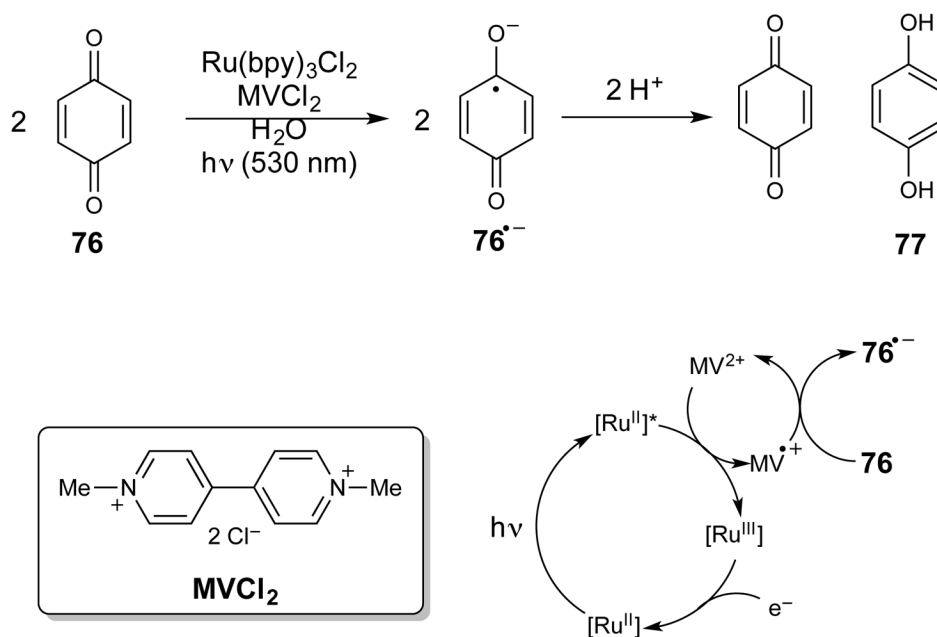
**Scheme 16.**  
 Effect of Redox Mediator on Chemoselectivity of a Photooxidative Azoalkane Rearrangement



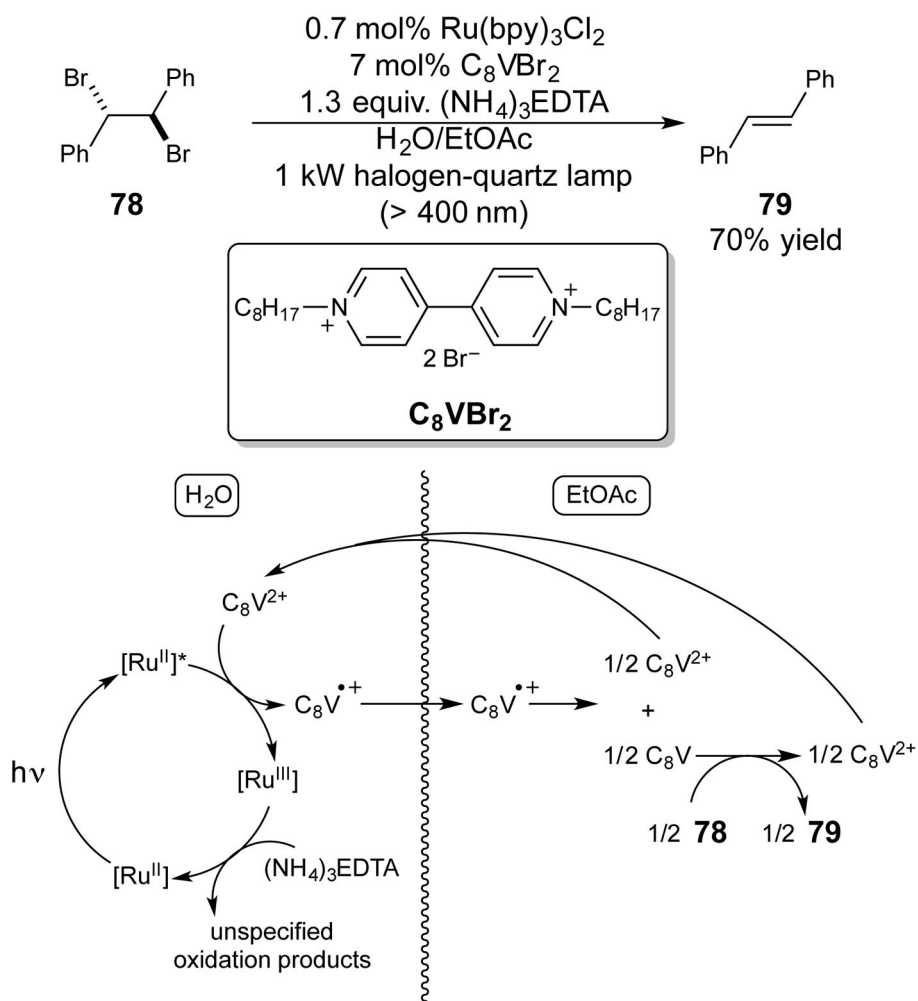
Redox Mediator	E <sub>ox</sub> (V) <sup>a</sup>	Time	73	74	75
None	—	60 min	93%	--	7%
Pyrene	1.15	5 min	100%	--	trace
Phenanthrene	1.58	5 min	41%	59%	--
Biphenyl	1.90	5 min	46%	46%	--

<sup>a</sup> Oxidation potentials vs. SCE in MeCN

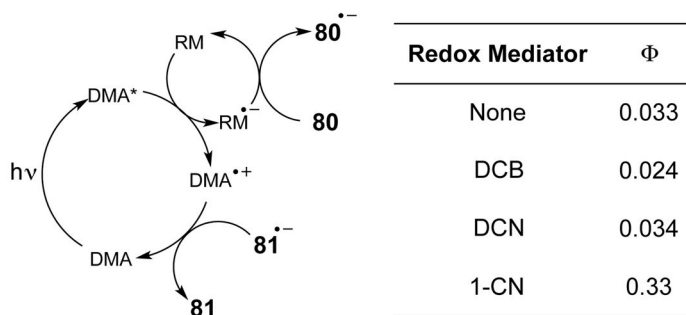
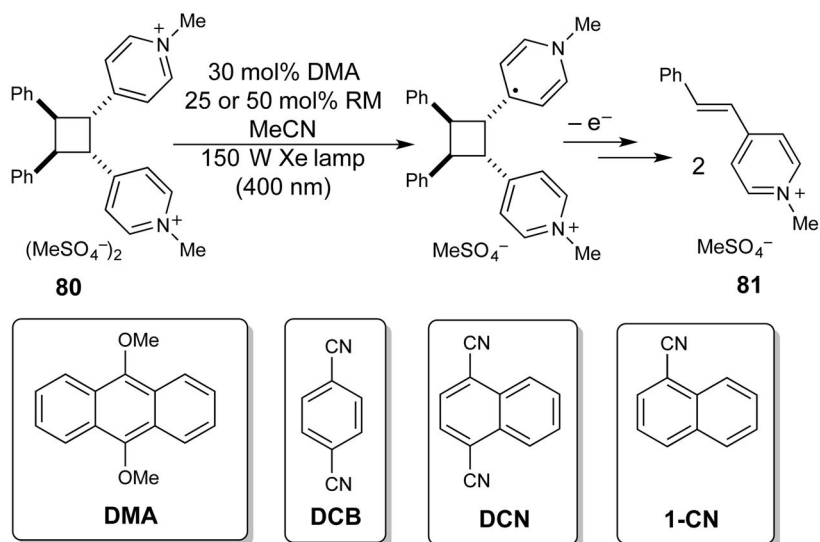
**Scheme 17.**  
Oxidative Cage Ketone Rearrangement and Influence of Redox Mediators



**Scheme 18.**  
Redox Mediation Applied to Benzoquinone Reduction

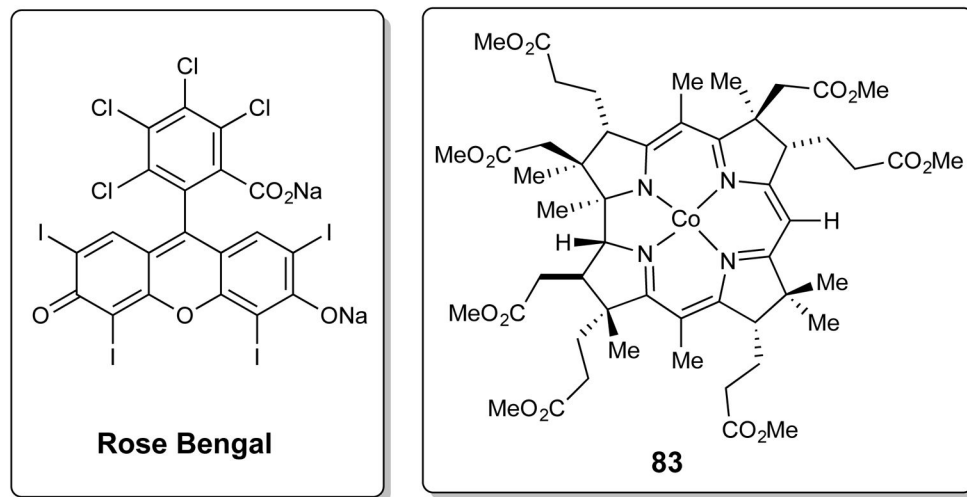
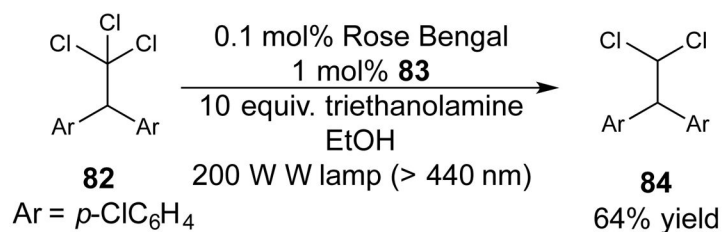


**Scheme 19.**  
 Reductive Mediation Combined with Phase Transfer Catalysis

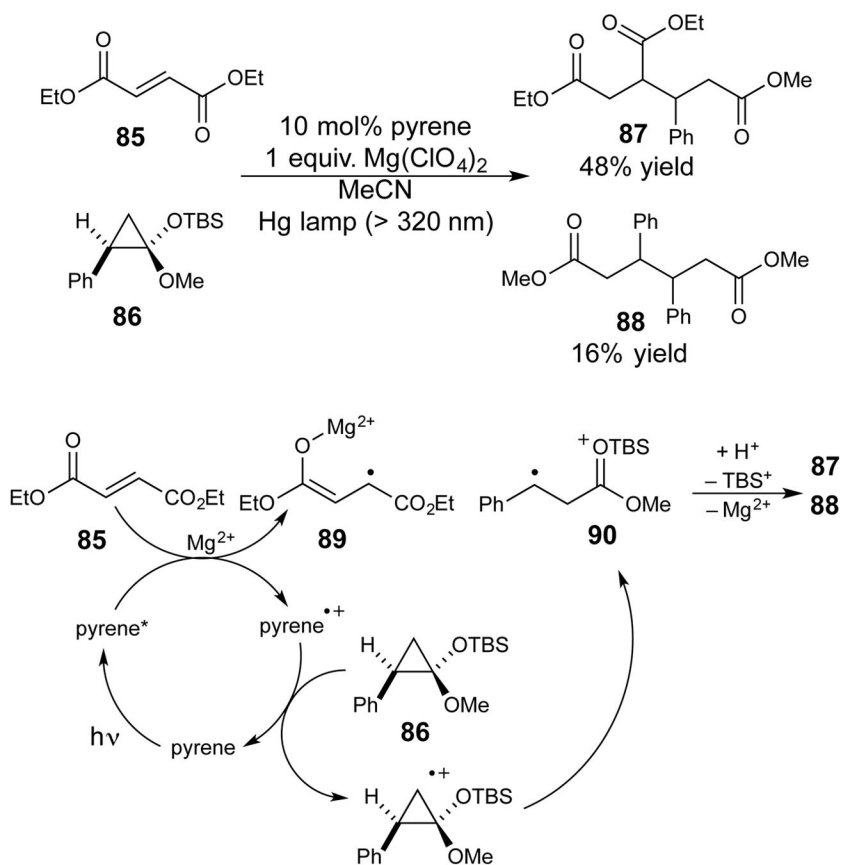


**Scheme 20.**  
Effect of Redox Mediators on Photoreductive Cycloreversion

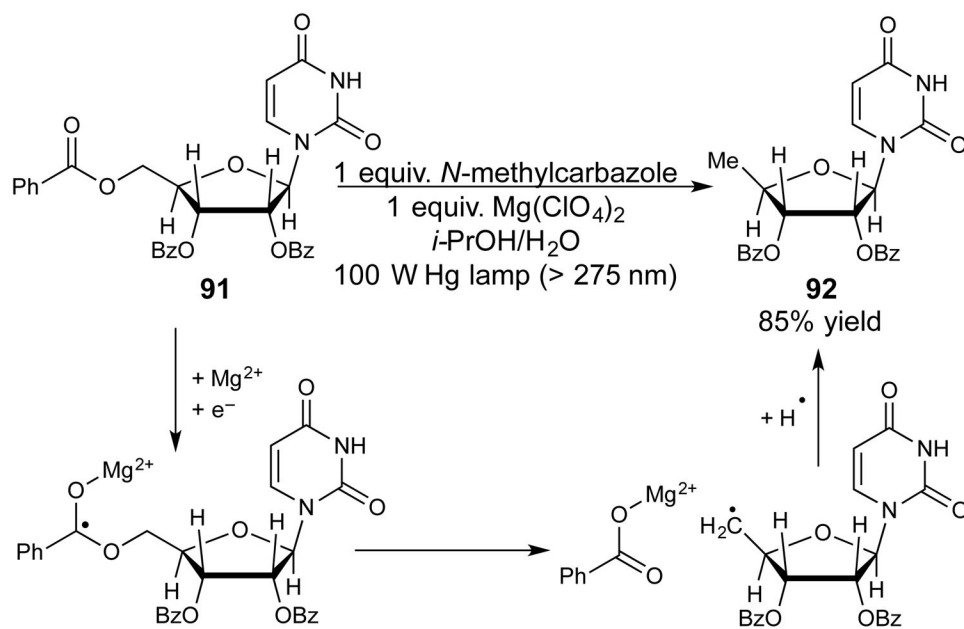




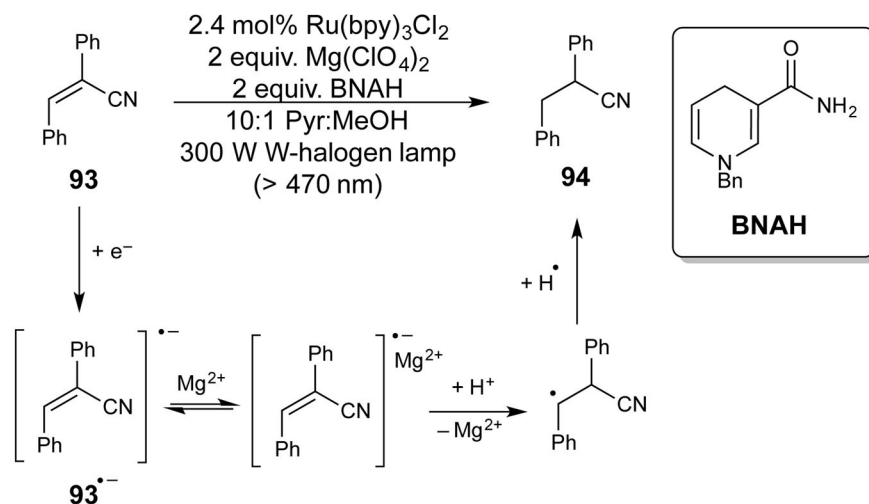
**Scheme 21.**  
Reductive Dehalogenation Using a  $\text{Co}^{\text{II}}$  Redox Mediator



**Scheme 22.**  
Photoreduction of Fumarate Promoted by Lewis Acid Coordination



**Scheme 23.**  
Reductive Deoxygenation by Lewis Acid-Promoted PET

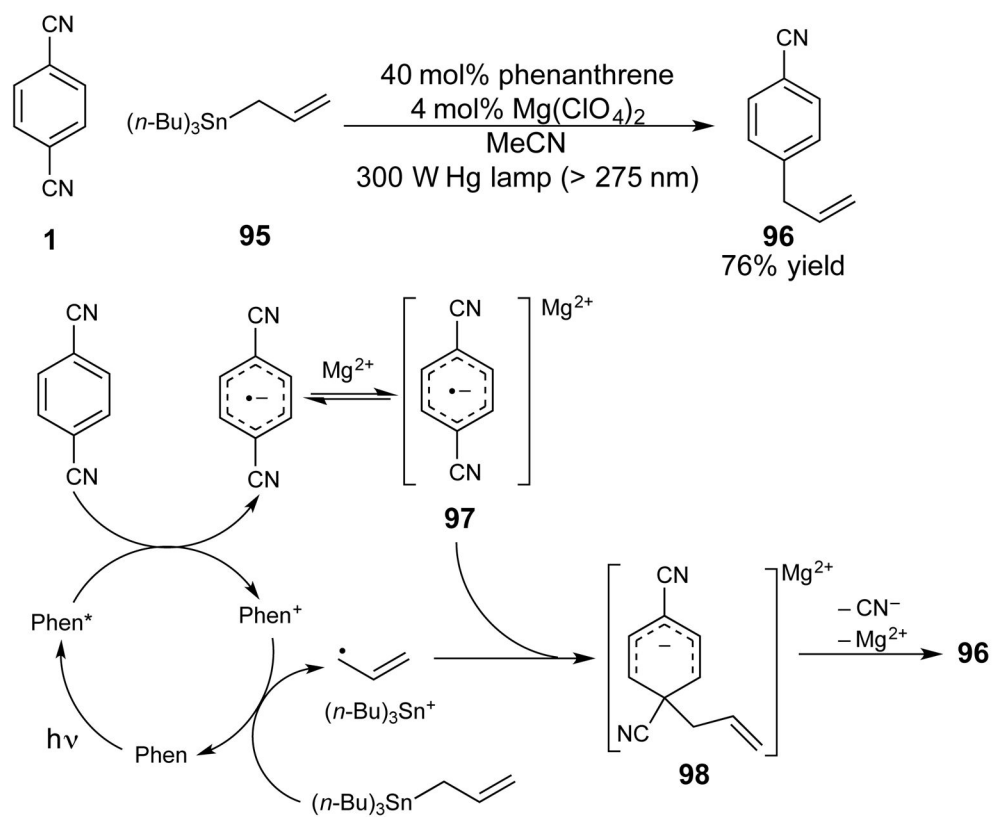


Substrate	$E_{\text{red}}(\text{V})^{\text{a,b}}$	$\Phi_{\text{Mg}}/\Phi$	Yield <sup>b</sup>
	-1.95 (-1.82)	3.6	30% (47%)
	-1.80 (-1.63)	1.3	100% (100%)
	-1.72 (-1.49)	1.6	70% (80%)

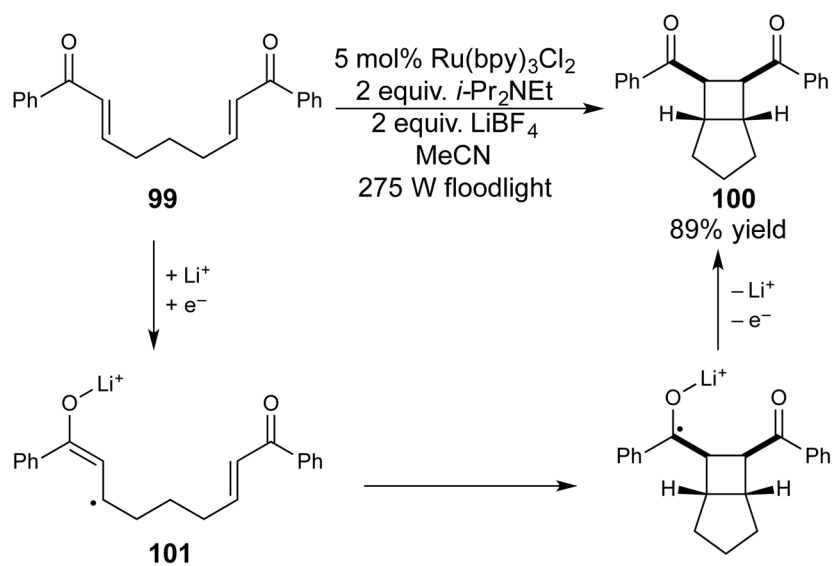
<sup>a</sup> Reduction potential vs. Ag/AgNO<sub>3</sub> in MeCN.

<sup>b</sup> The listed values are in the absence of Mg<sup>2+</sup>. The parenthetical values are when Mg<sup>2+</sup> is added.

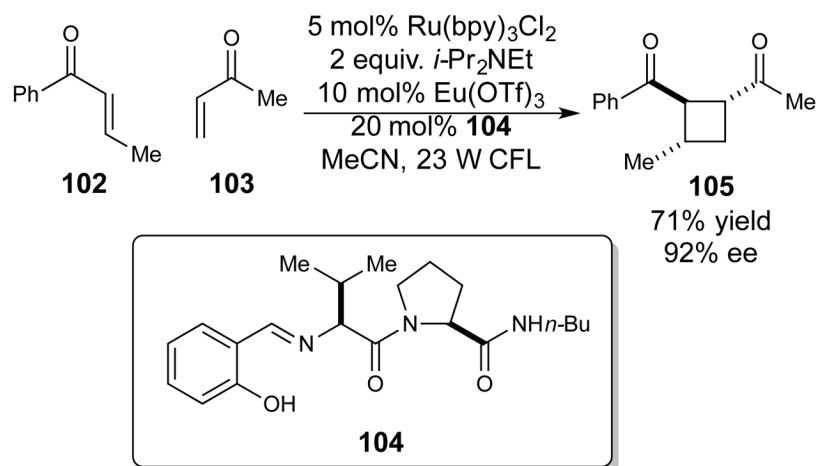
**Scheme 24.**  
Effect of Mg<sup>2+</sup> on Photocatalytic Alkene Reduction



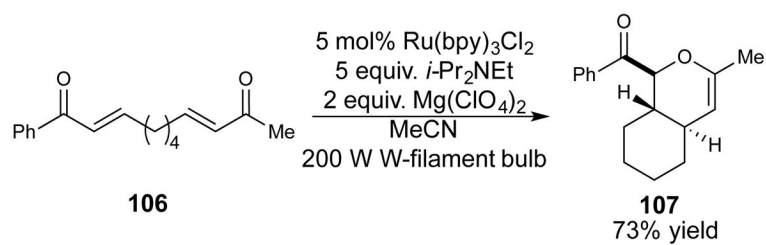
**Scheme 25.**  
Photoreductive Substitution with  $\text{Mg}(\text{ClO}_4)_2$  Co-Catalyst



**Scheme 26.**  
Photoreductive [2+2] Cycloaddition with  $\text{LiBF}_4$

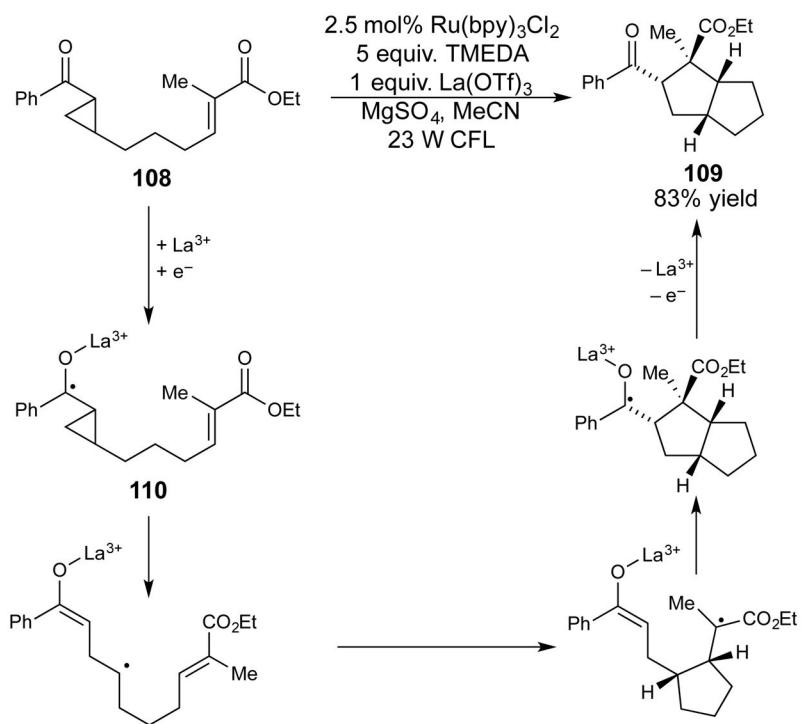


**Scheme 27.**  
Enantioselective [2+2] Cycloaddition Using a Chiral Lewis Acid Co-catalyst

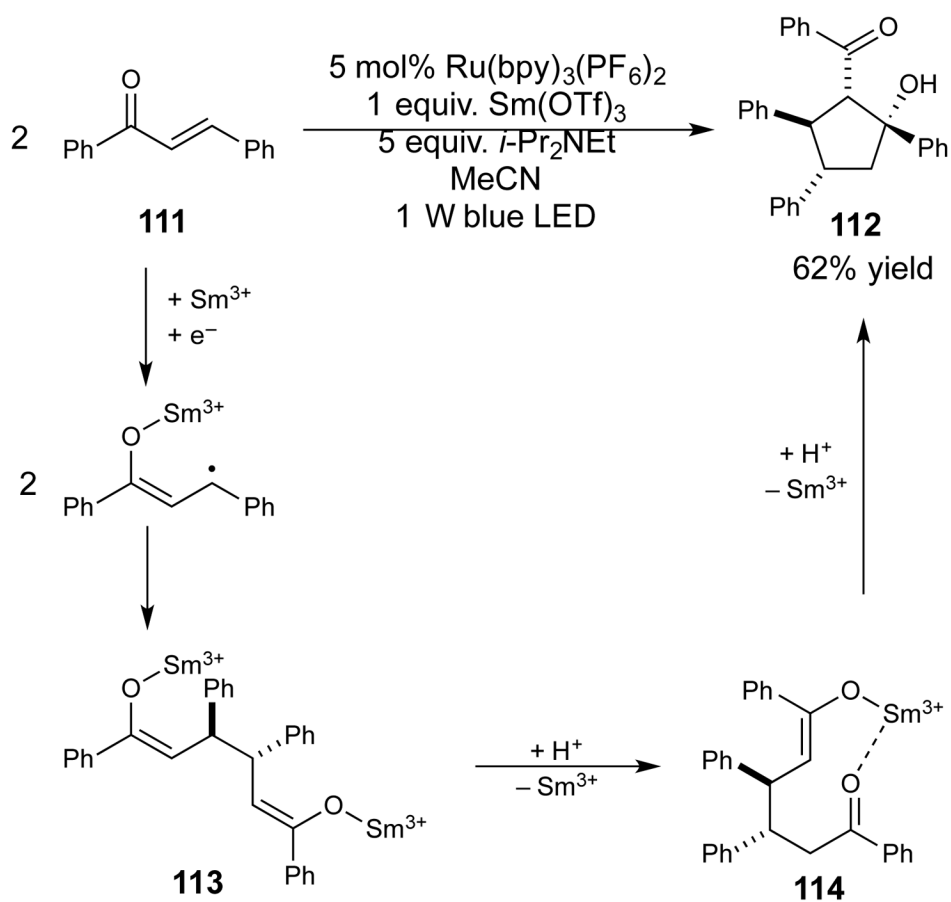
**Scheme 28.**

$\text{Ru}(\text{bpy})_3\text{Cl}_2/\text{Mg}(\text{ClO}_4)_2$  Catalyzed [4+2] Bis(Enone) Cycloaddition

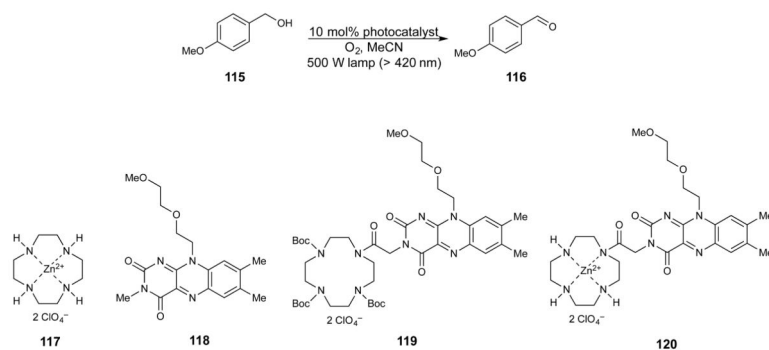




**Scheme 29.**  
Photoreductive [3+2] Cycloadditions by Lanthanide Co-catalysis

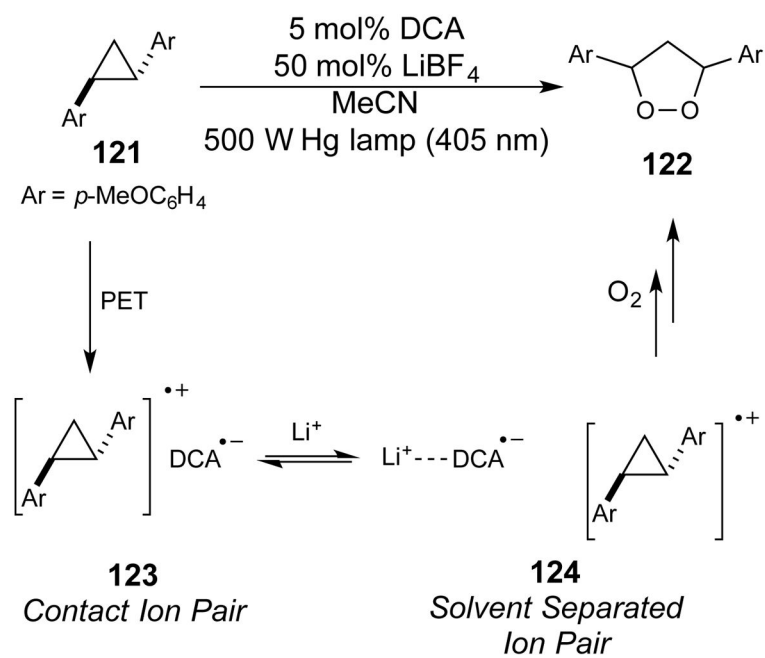


**Scheme 30.**  
 Reductive Chalcone Dimerization Catalyzed by  $\text{Sm}^{3+}$  and  $\text{Ru}(\text{bpy})_3(\text{PF}_6)_2$

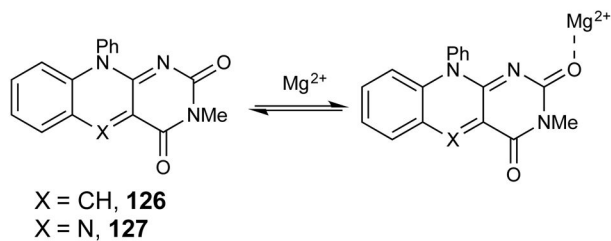
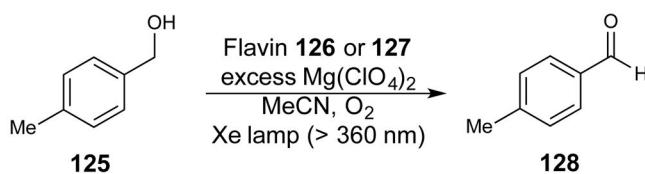


Photocatalyst(s)	$\Phi$	Conv. at 1 h
None	--	0%
117 + 118	$1.8 \times 10^{-3}$	2%
119	$9.1 \times 10^{-4}$	1%
120	$3.8 \times 10^{-2}$	51%

**Scheme 31.**  
Lewis Acid-Templated Photocatalytic Alcohol Oxidation



**Scheme 32.**  
Lewis Acid Accelerated Cyclopropane Photooxidation by BET Suppression

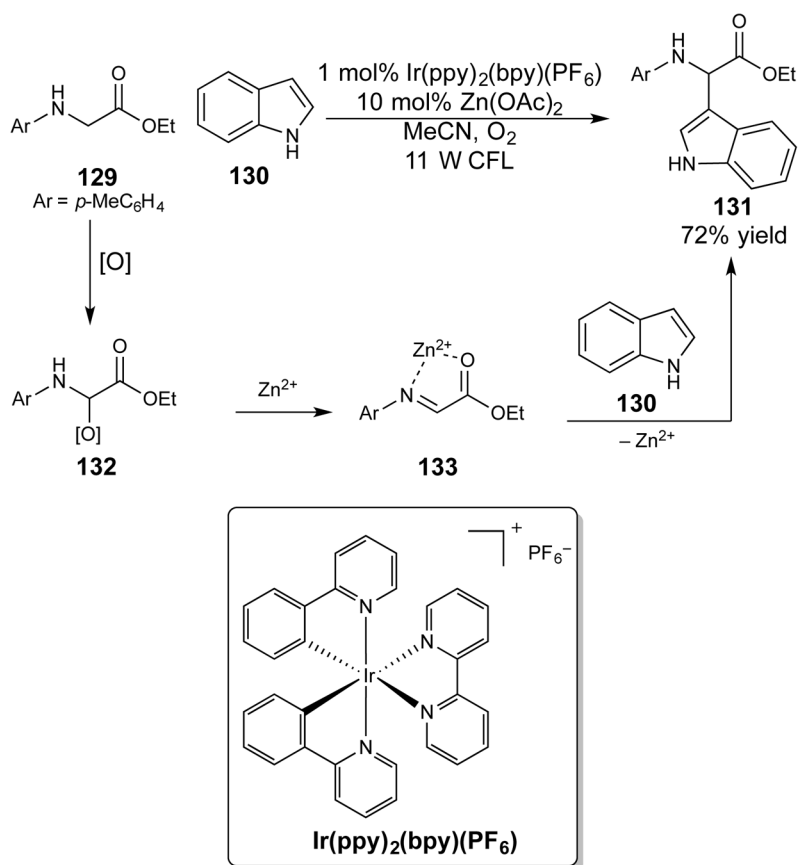


Flavin	$K_{\text{assoc.}}$	$E(\text{fl}^*/\text{fl}^{(-)})(\text{V})^{\text{a,b}}$
<b>126</b>	$1.1 \times 10^3$	1.85 (2.16)
<b>127</b>	$1.7 \times 10^2$	2.06 (2.35)

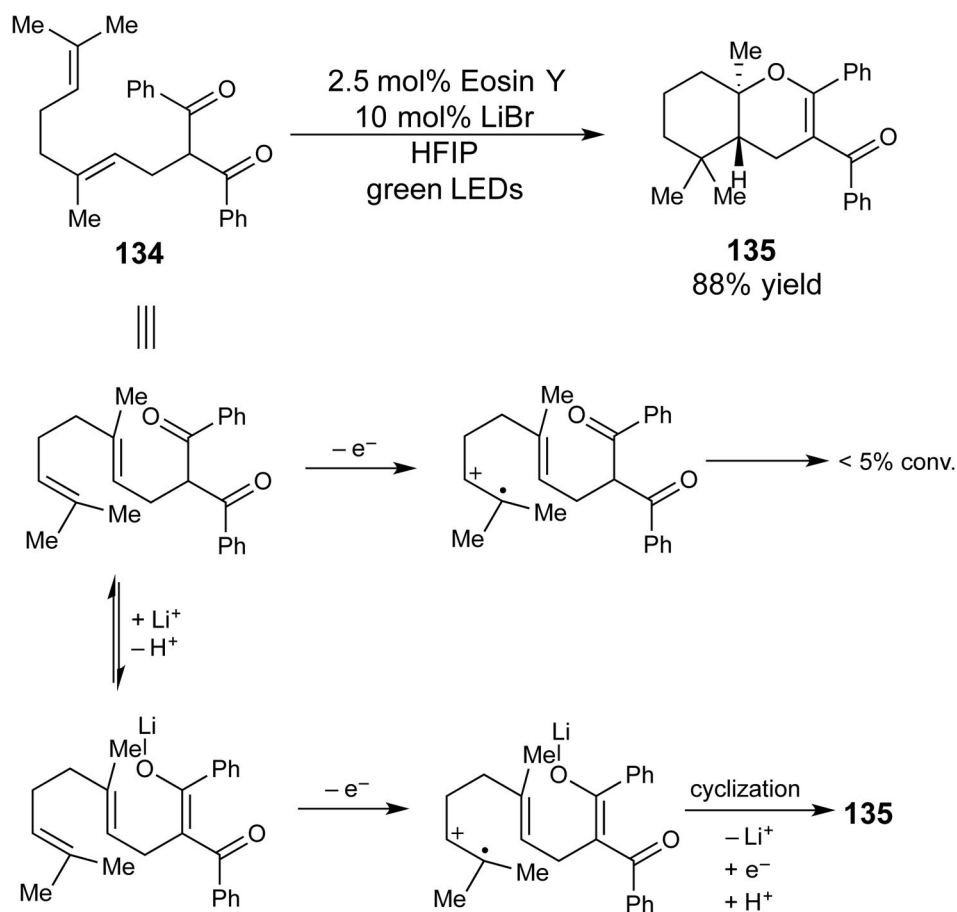
<sup>a</sup> Determined indirectly based on the oxidation potentials of various arenes vs. SCE in MeCN. See ref. 169 for details.

<sup>b</sup> The listed values are in the absence of  $\text{Mg}^{2+}$ . The parenthetical values are when  $\text{Mg}^{2+}$  is added.

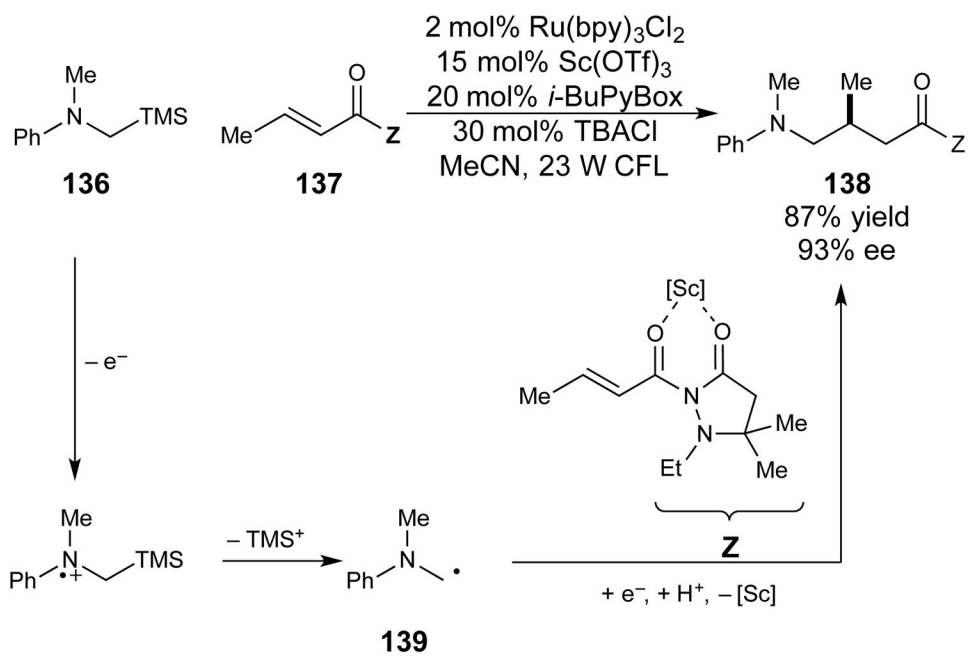
**Scheme 33.**  
Effect of  $\text{Mg}^{2+}$  Binding of Flavin Photoredox Properties



**Scheme 34.**  
Lewis Acid Accelerated Addition after PET

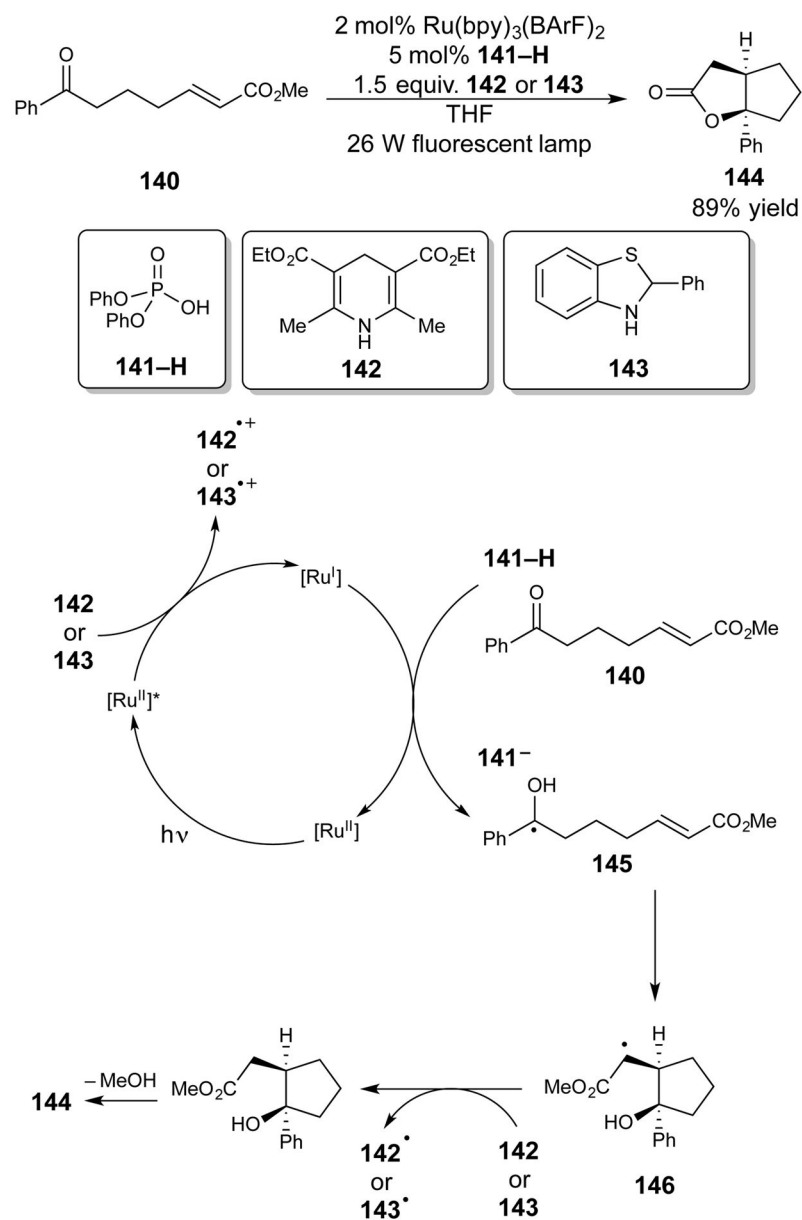


**Scheme 35.**  
Radical Cation Cascade Promoted by Lewis Acid Activation

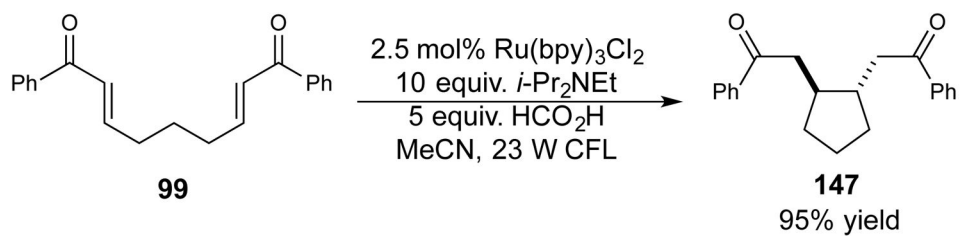


**Scheme 36.**  
 Enantioselective Lewis Acid-Catalyzed Addition of Radical Generated by PET

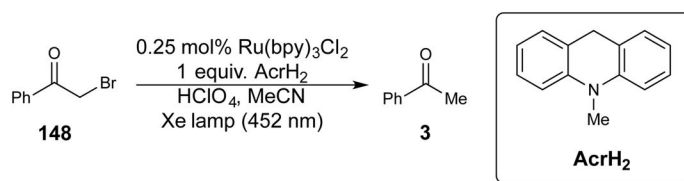




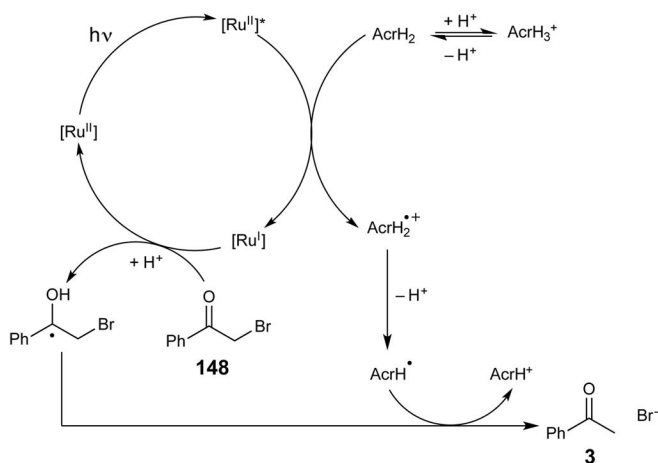
**Scheme 37.**  
PCET Reductive Cyclization of Ketones



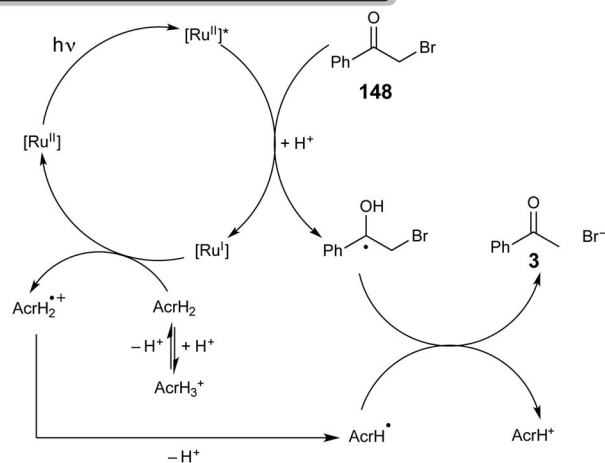
**Scheme 38.**  
Reductive Cyclization of Bis(Enones)



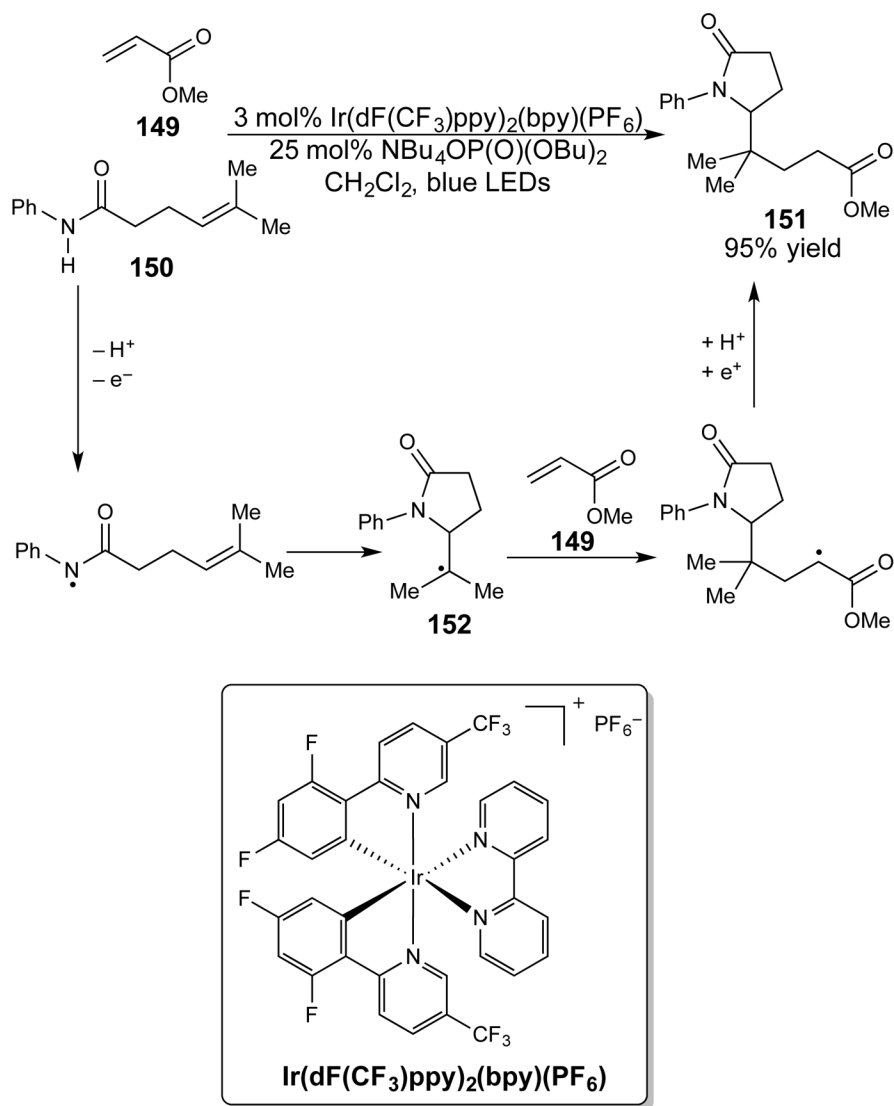
proposed mechanism in the absence of acid



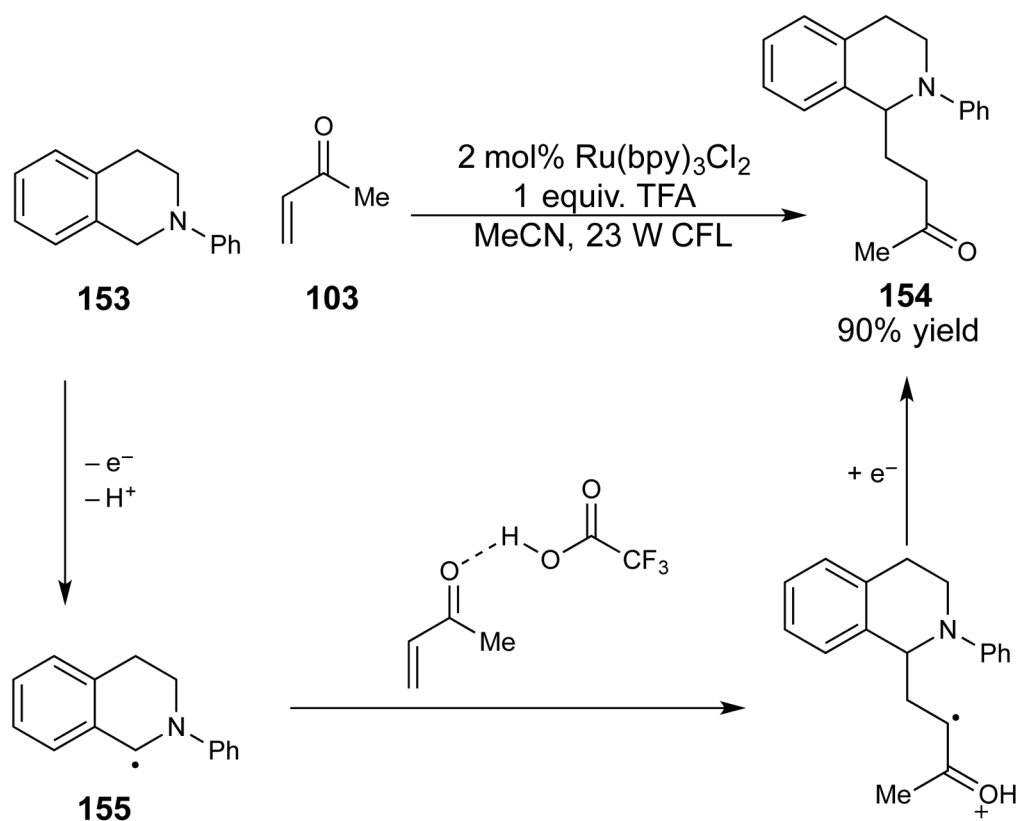
proposed mechanism in the presence of acid



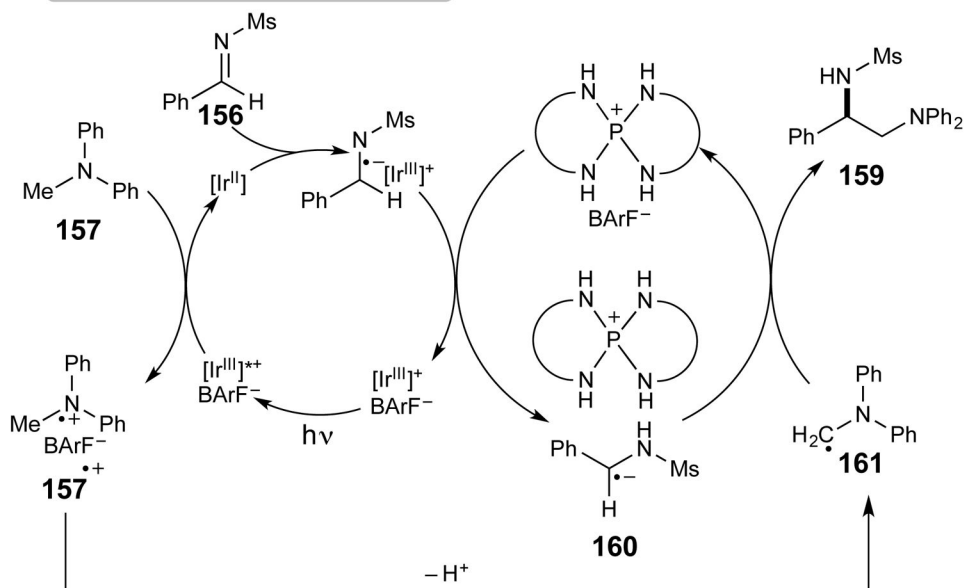
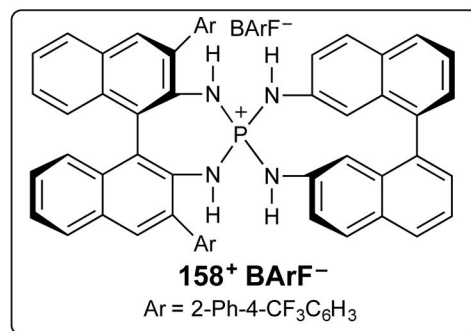
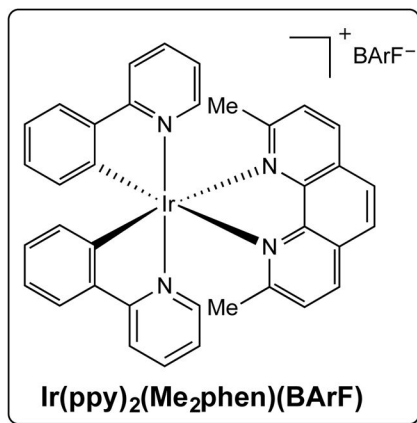
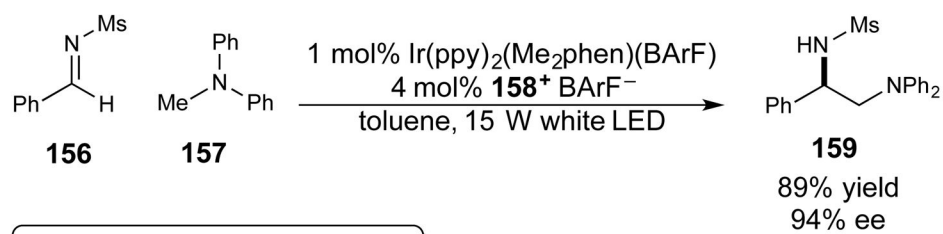
**Scheme 39.**  
Effect of Brønsted Acid on Rates of Electron Transfer to  $\alpha$ -Bromoketones



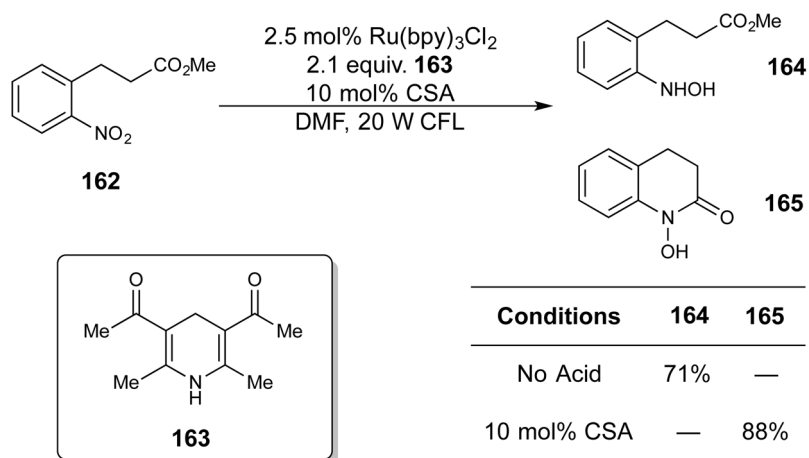
**Scheme 40.**  
PCET and Amide Cyclization



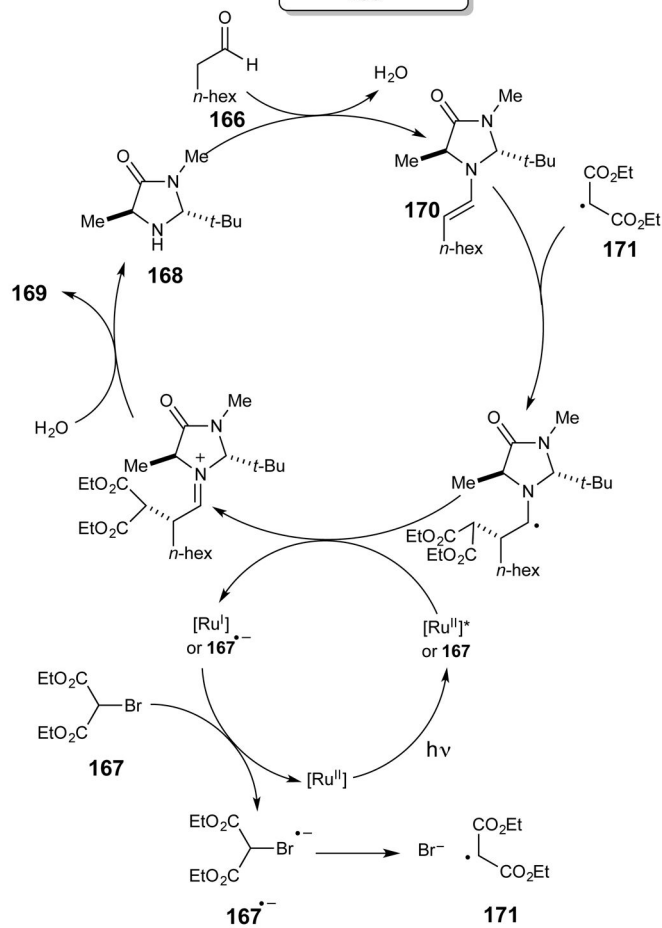
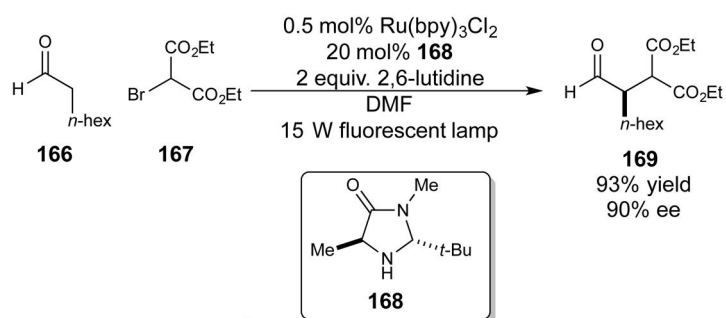
**Scheme 41.**  
Brønsted Acid Catalyzed Addition of PET-Generated  $\alpha$ -Amino Radicals to Enones



**Scheme 42.**  
Enantioselective Radical Coupling Reaction using Chiral Ion Pairing

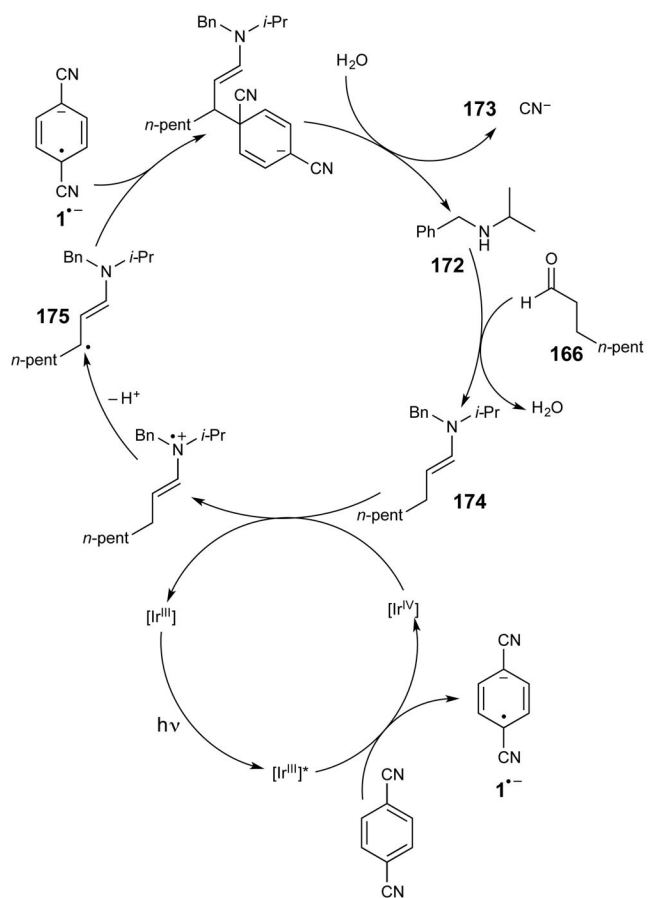
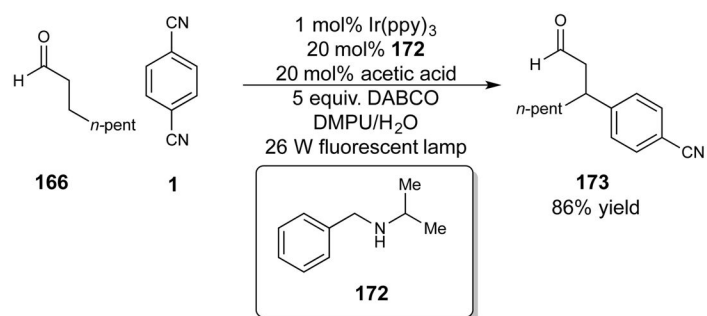


**Scheme 43.**  
 Nitroarene Reduction and Post-PET Cyclization

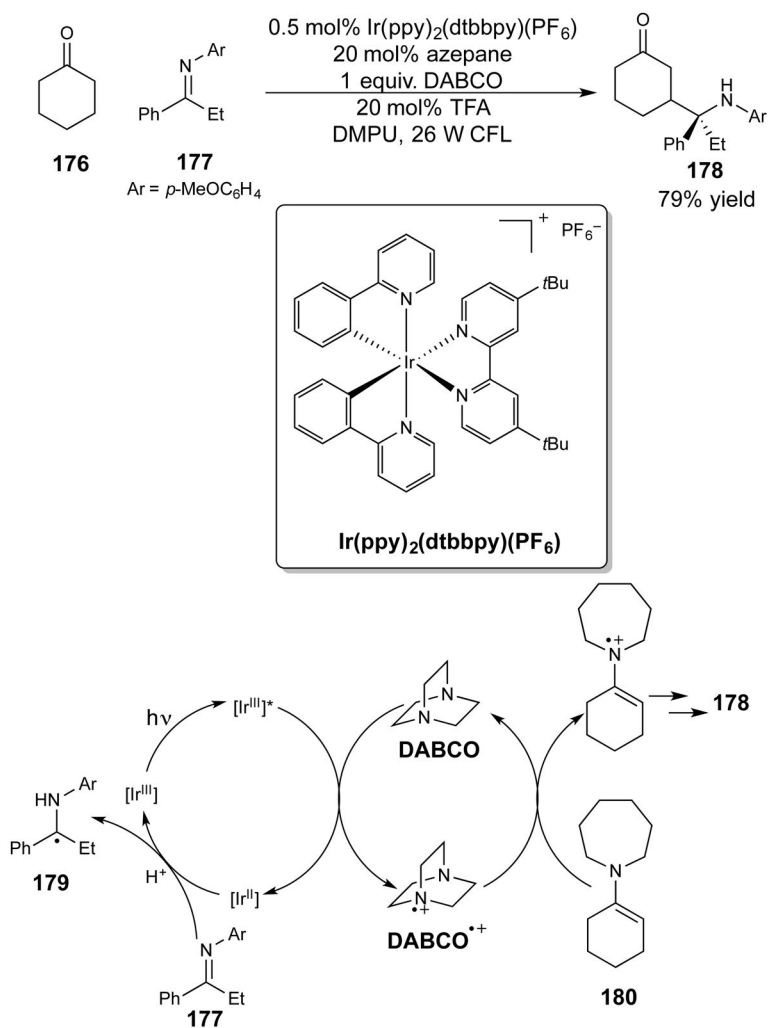


**Scheme 44.**  
 Aldehyde  $\alpha$ -Alkylation by Tandem Photo/Organocatalysis

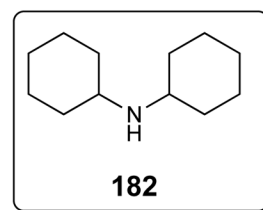
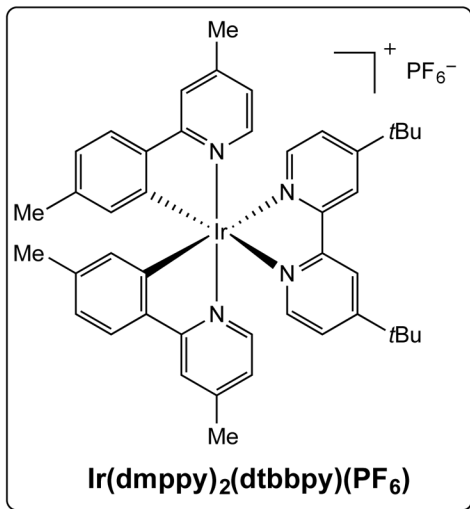
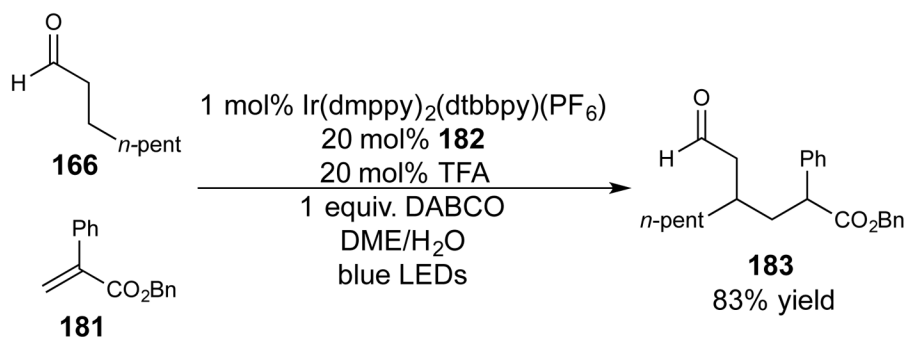




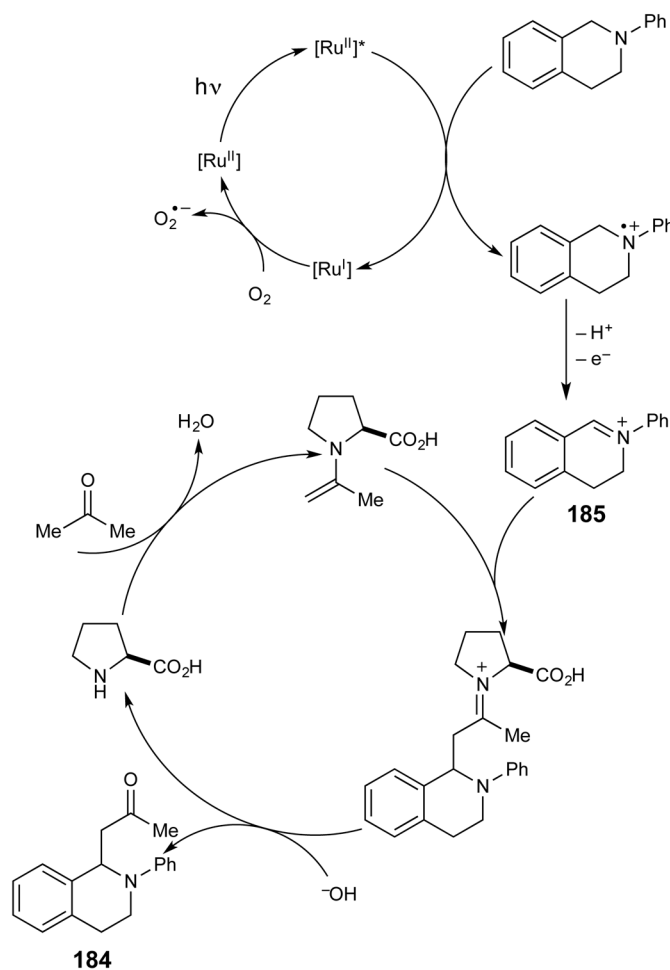
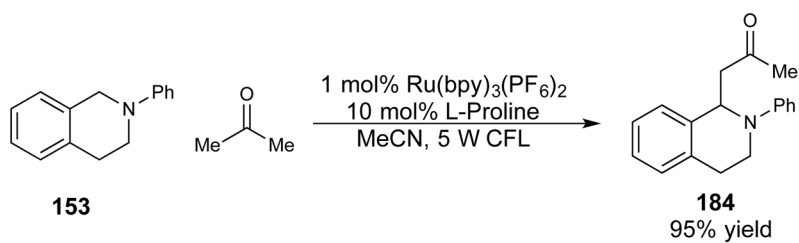
**Scheme 45.**  
Aldehyde  $\beta$ -Arylation by Tandem Photo/Organocatalysis



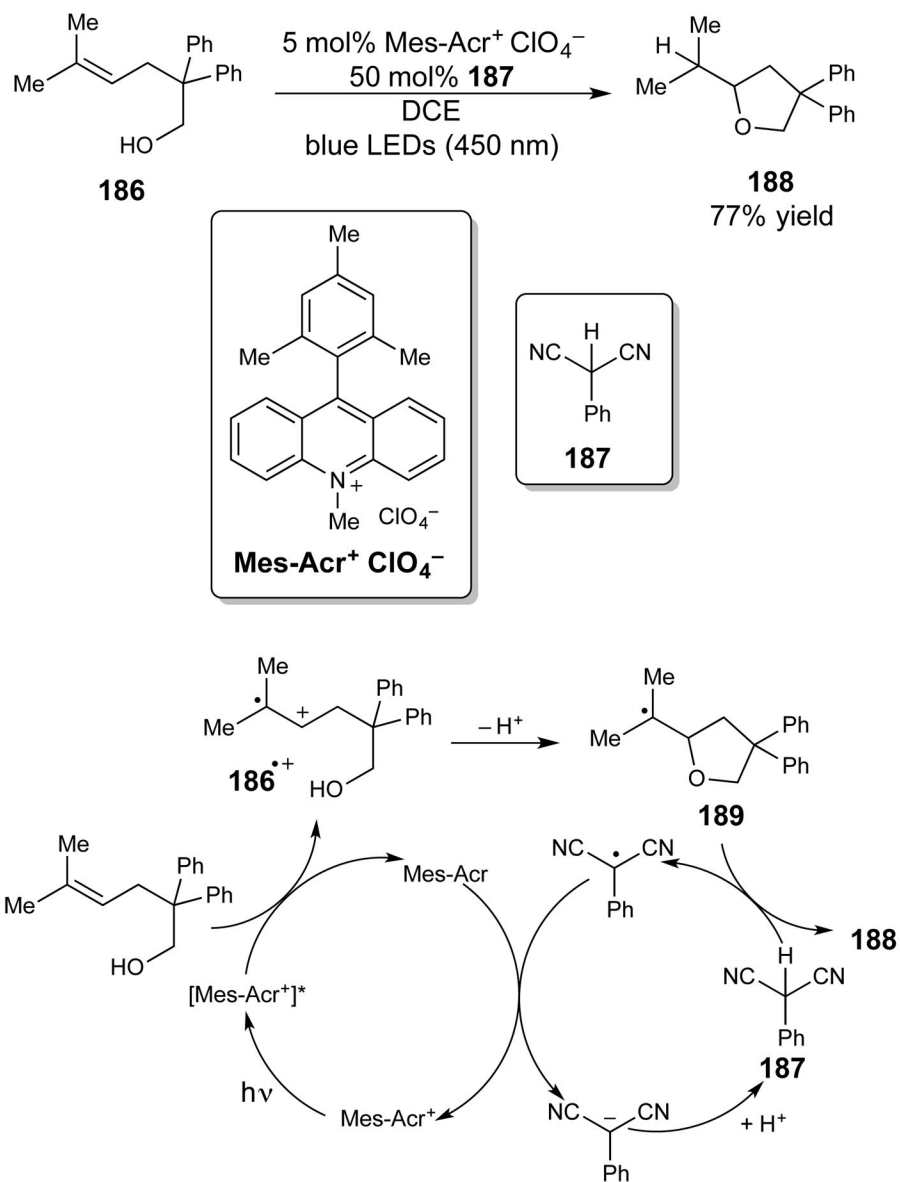
**Scheme 46.**  
Formal  $\beta$ -Mannich Reaction using Several Types of Co-Catalysis



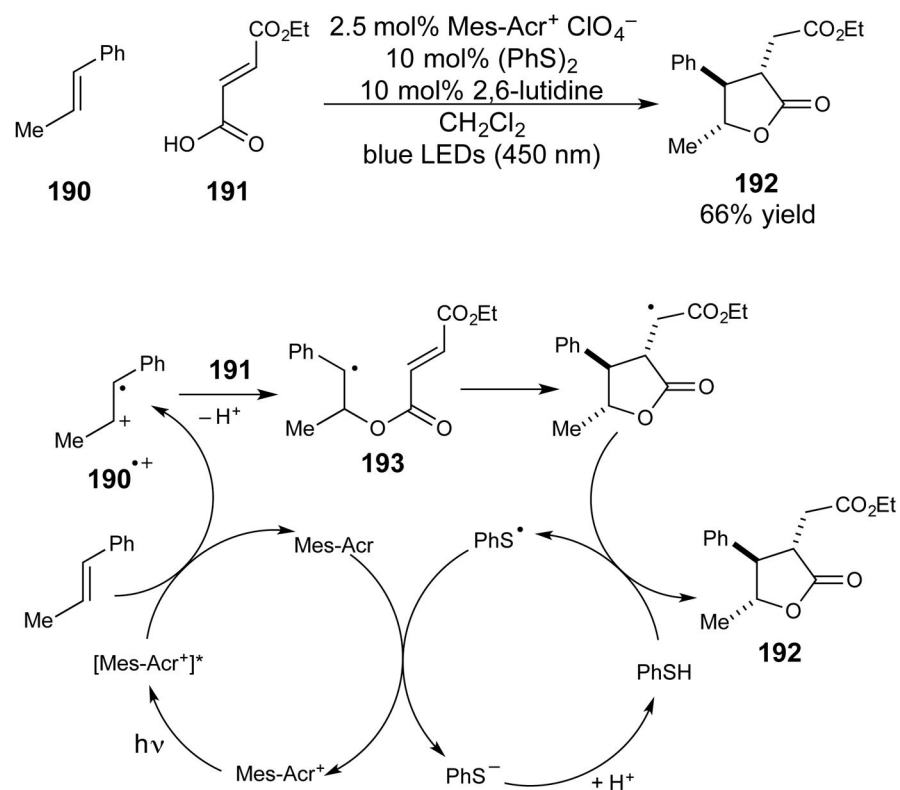
**Scheme 47.**  
 Aldehyde  $\beta$ -Alkylation

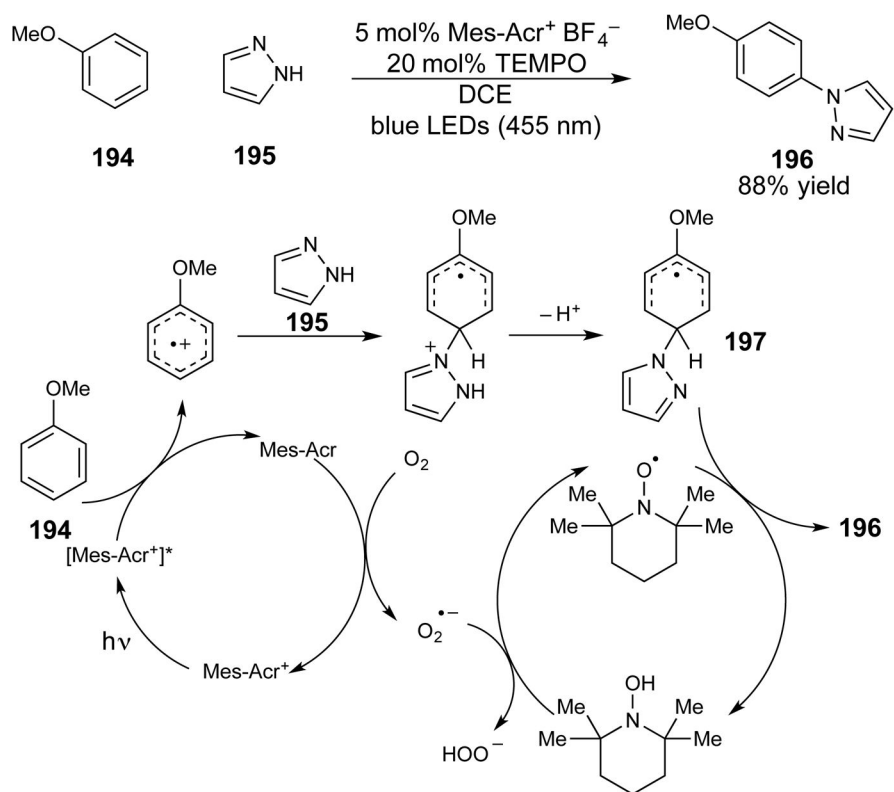


**Scheme 48.**  
Oxidation of THIQ and Interception by an Organocatalytic Nucleophile

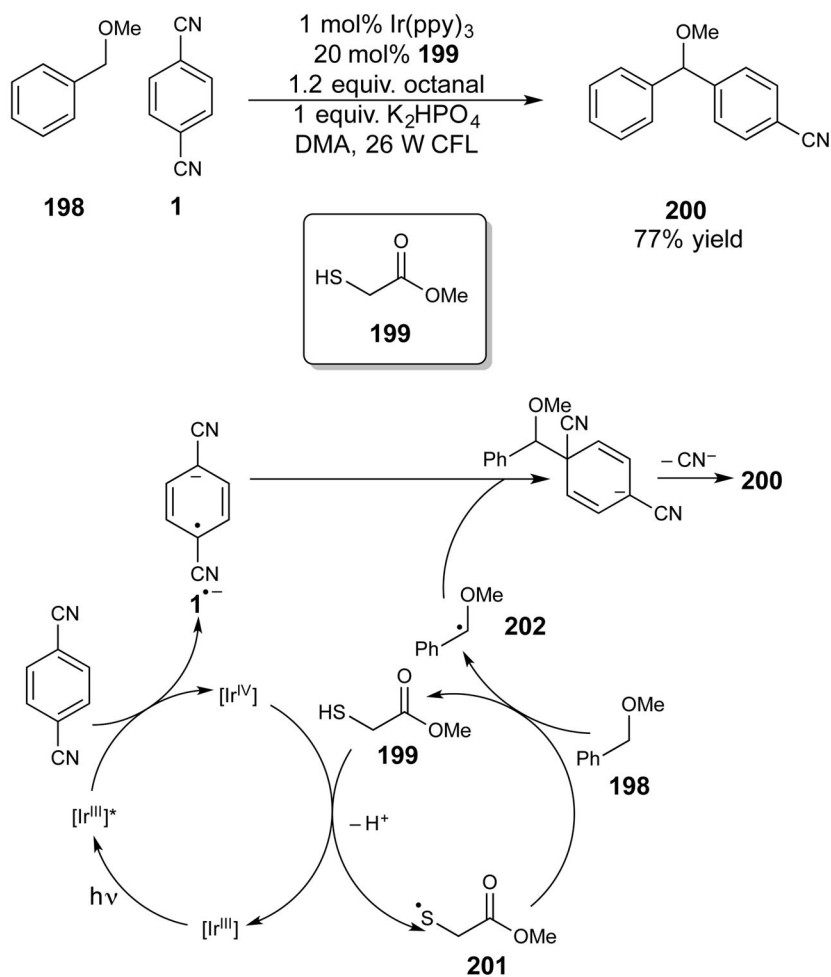


**Scheme 49.**  
Photooxidative Cyclization Merged with HAT Catalysis



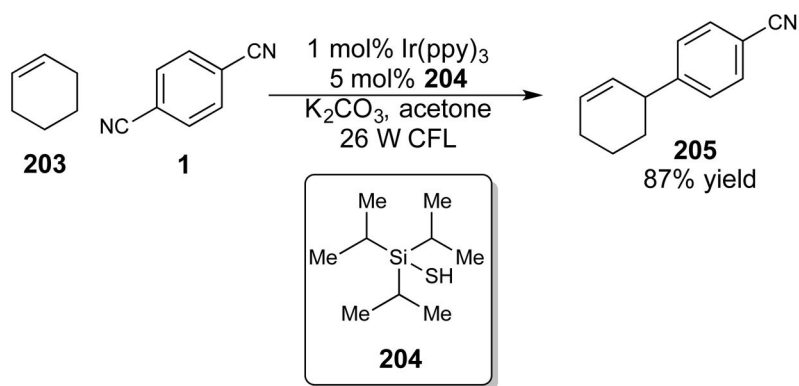
**Scheme 51.**

Aromatic C–H Amination using Photocatalysis and TEMPO as an HAT Catalyst

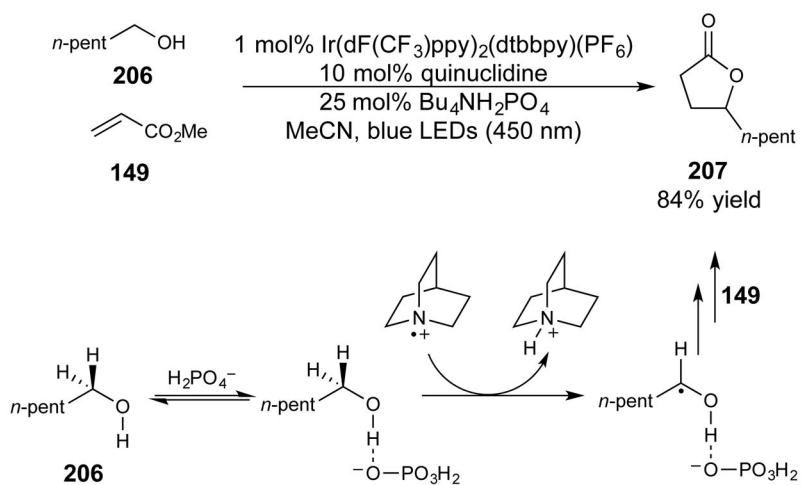


**Scheme 52.**  
Benzylic C–H Arylation by Photo/HAT Co-catalysis

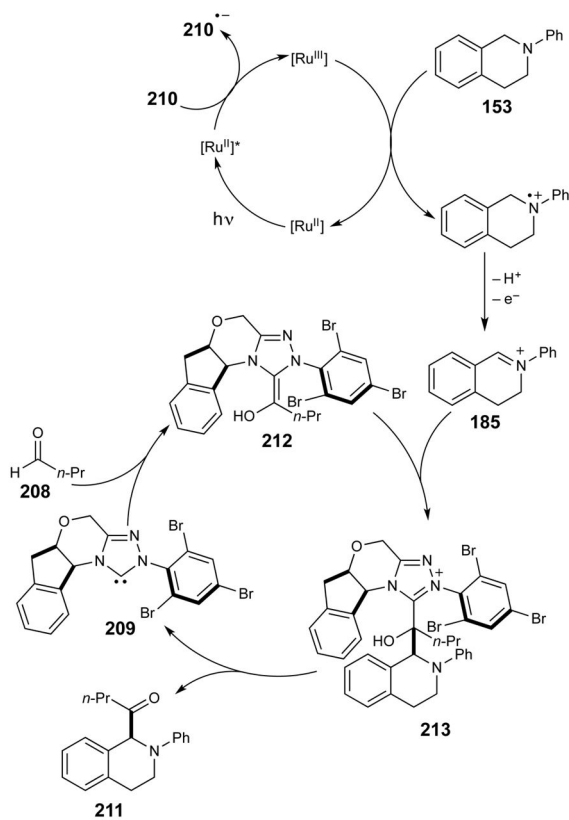
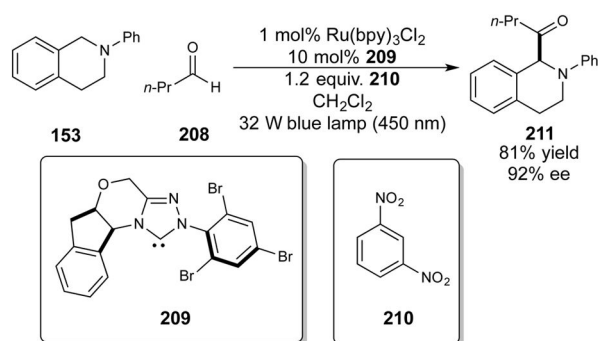




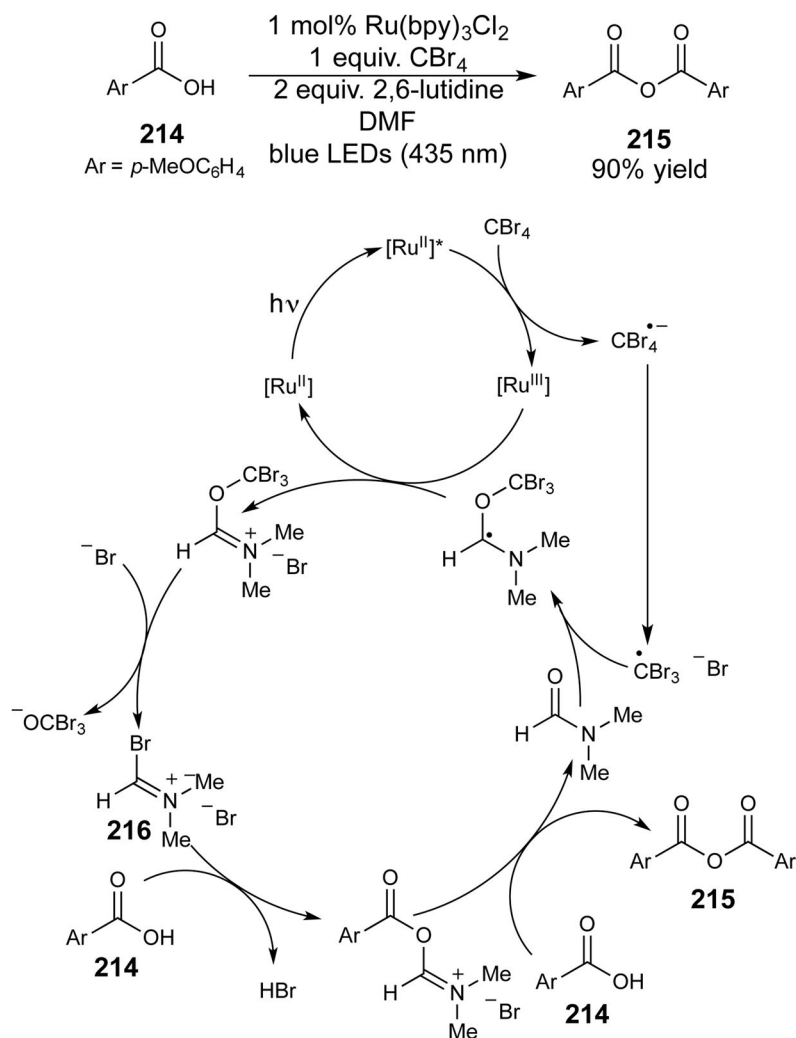
**Scheme 53.**  
C-H Arylation of Simple Alkenes



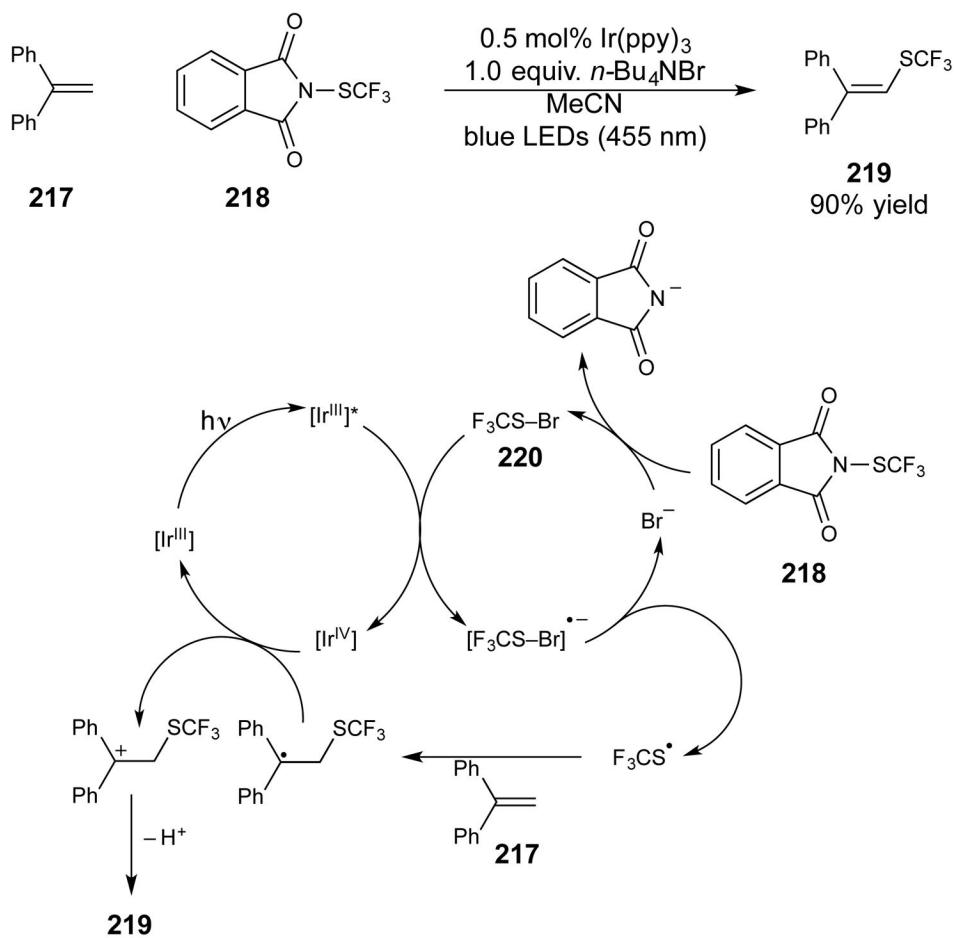
**Scheme 54.**  
Alkene-Alcohol Coupling Catalyzed by Site-Selective HAT.



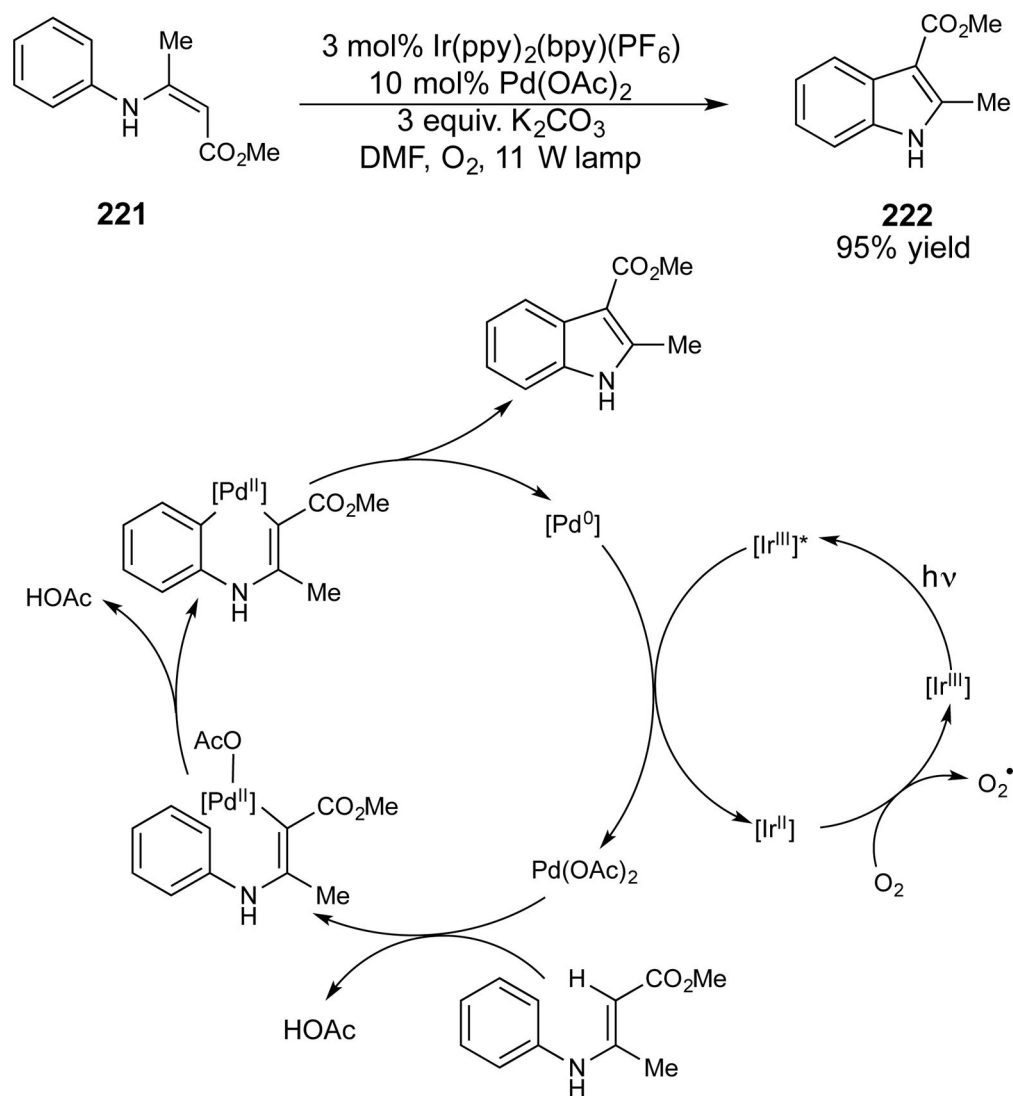
**Scheme 55.**  
Umpolung Reactivity using Dual Photo/NHC Catalysis



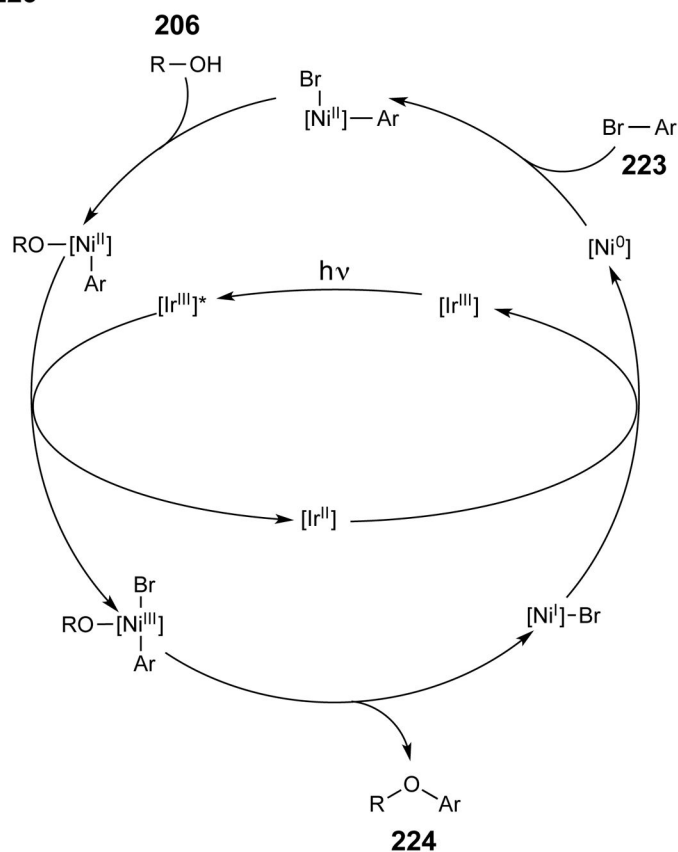
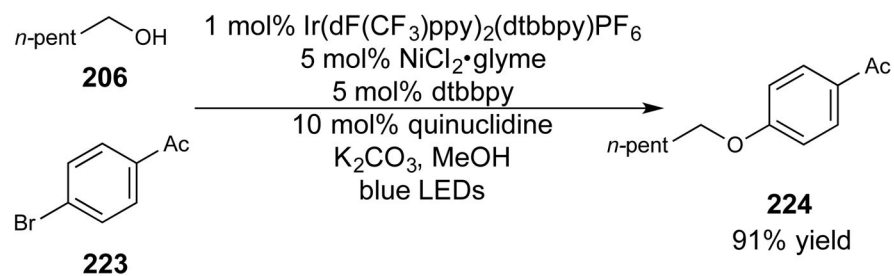
**Scheme 56.**  
Photocatalytic Carboxylic Acid Dehydration with Acyl Transfer Co-catalysis



**Scheme 57.**  
Dual Halide/Photoredox Catalysis



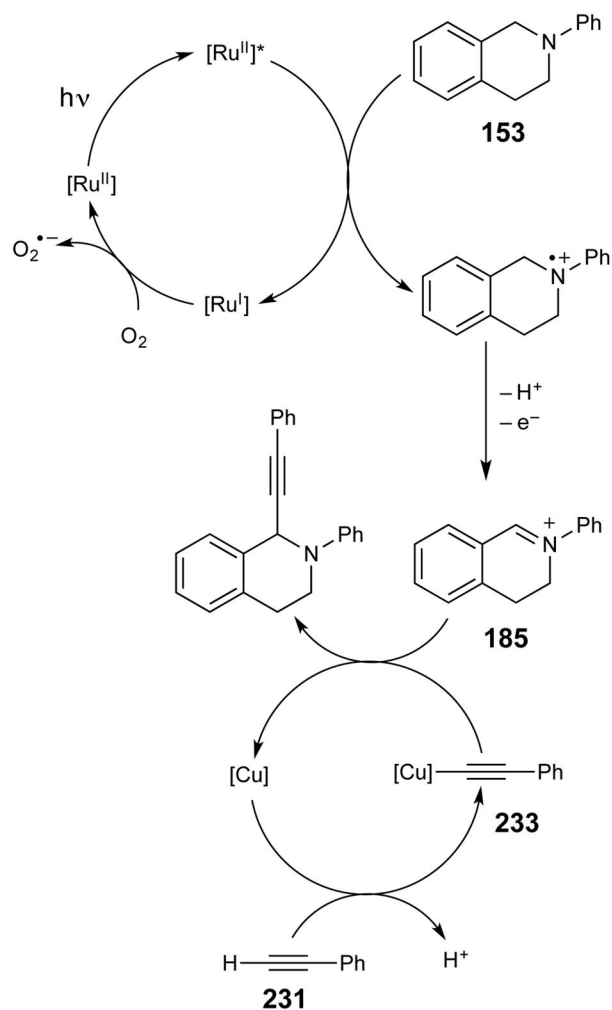
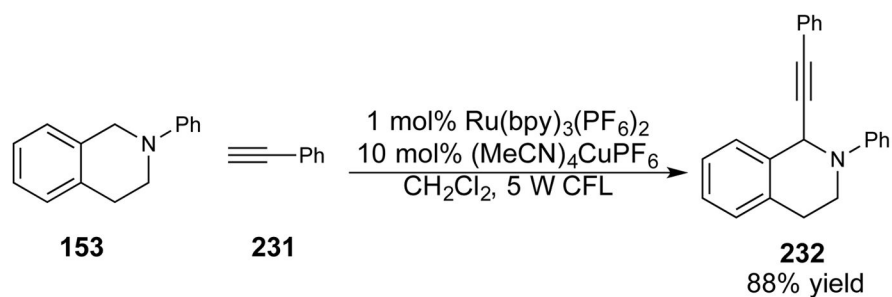
**Scheme 58.**  
Oxidative Heck Reaction Employing Photocatalytic Palladium Turnover



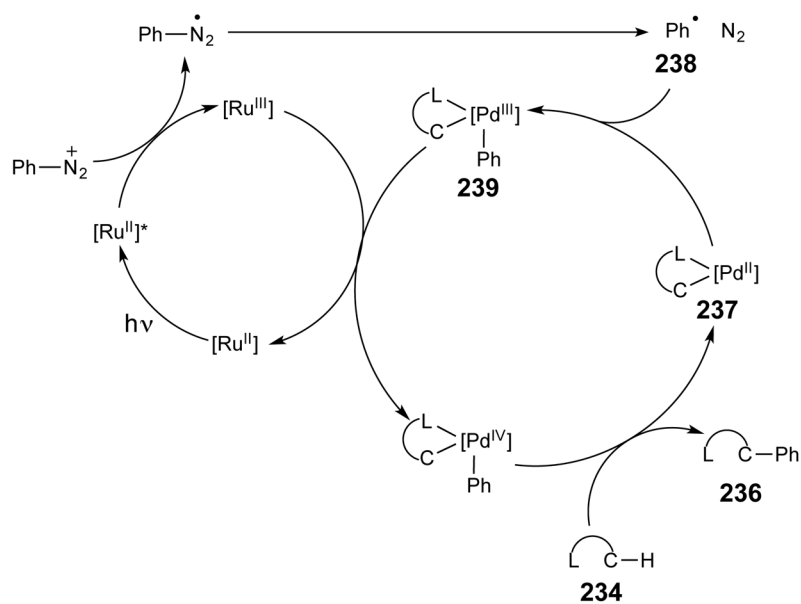
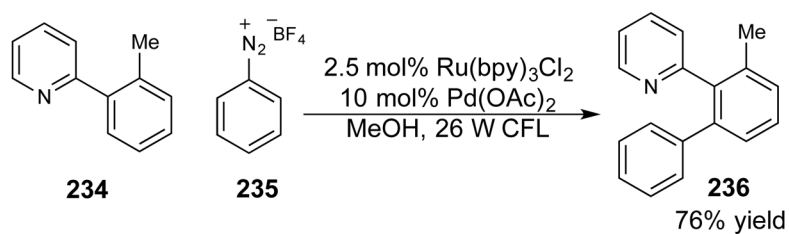
**Scheme 59.**  
Nickel Catalyzed Cross Coupling Enabled by Photocatalysis



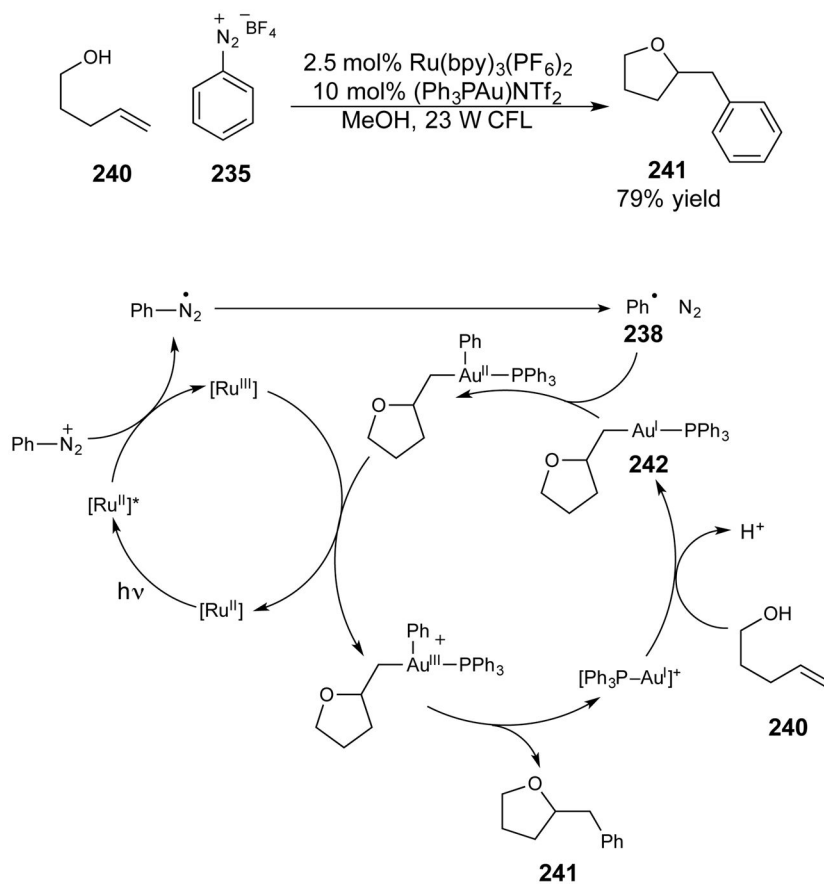




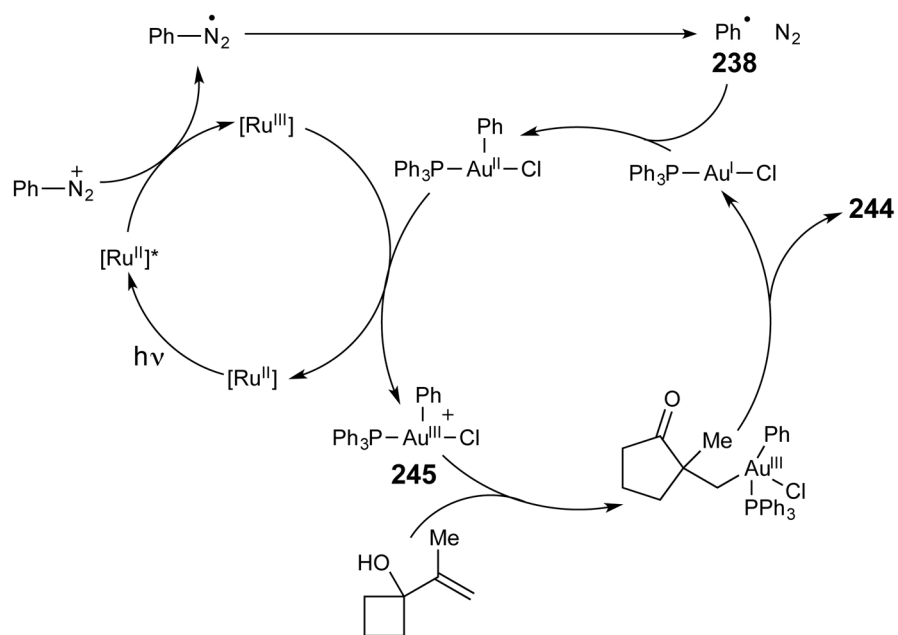
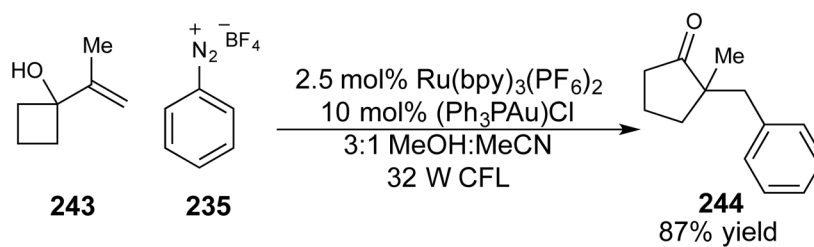
**Scheme 61.**  
Oxidation of THIQ and Trapping with Metal Acetylides



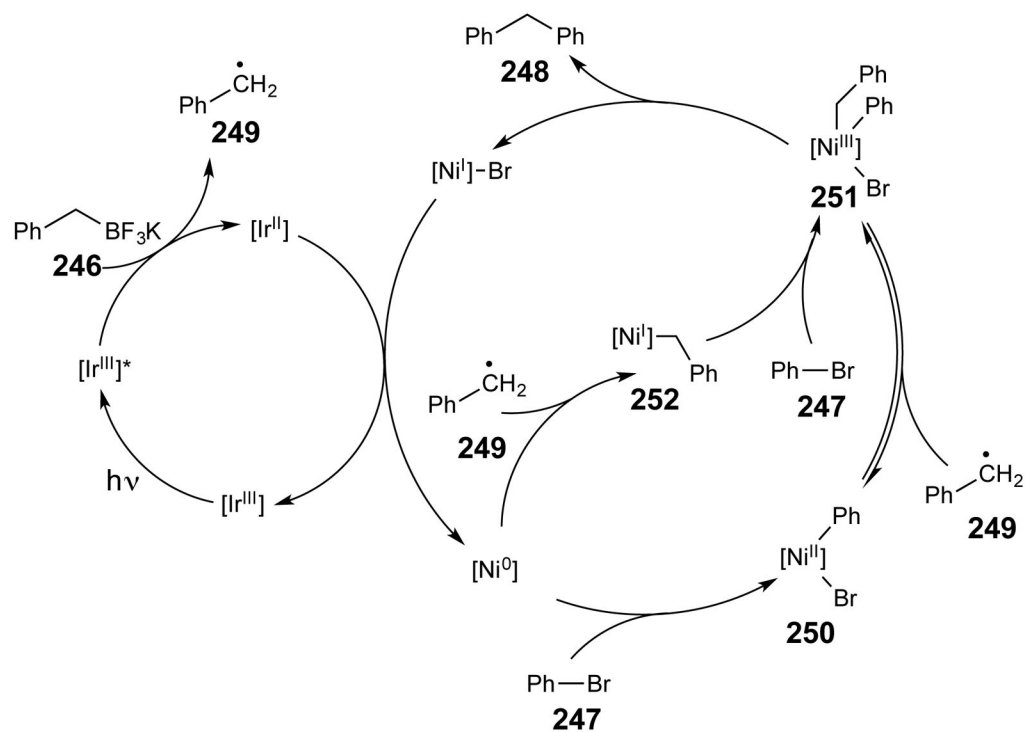
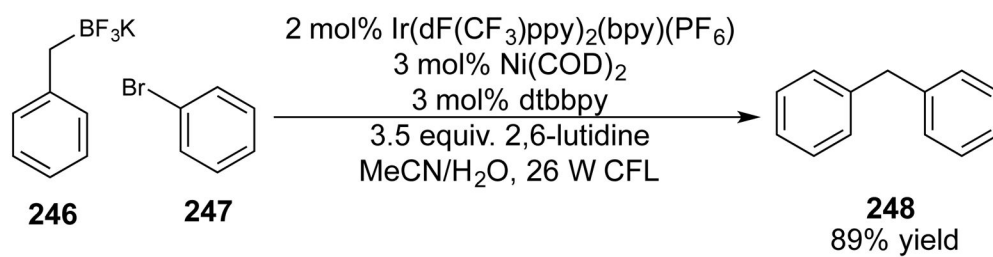
**Scheme 62.**  
Photocatalytic Diazonium Reduction and Palladium Catalysis with Resulting Aryl Radical



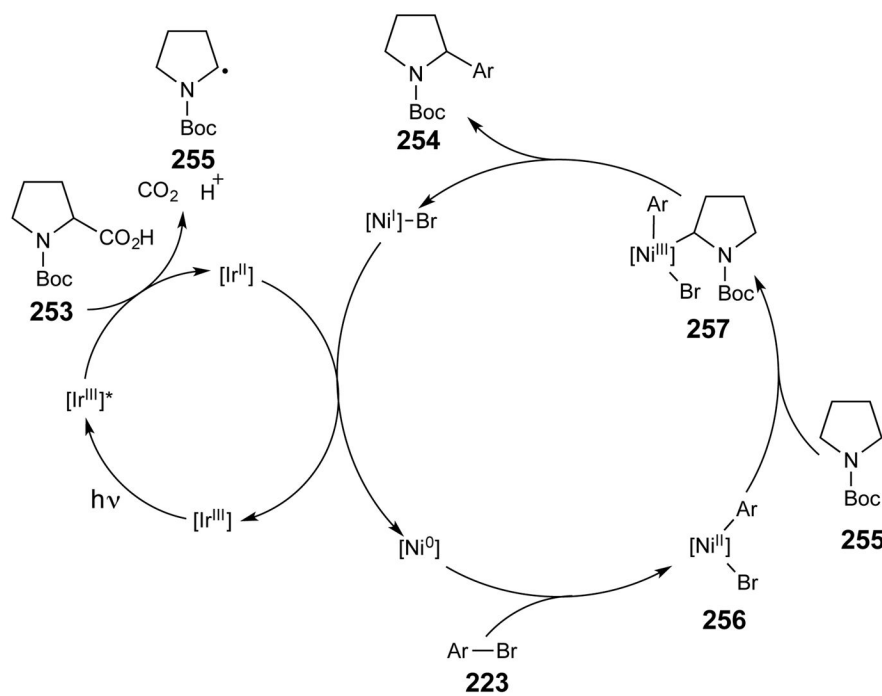
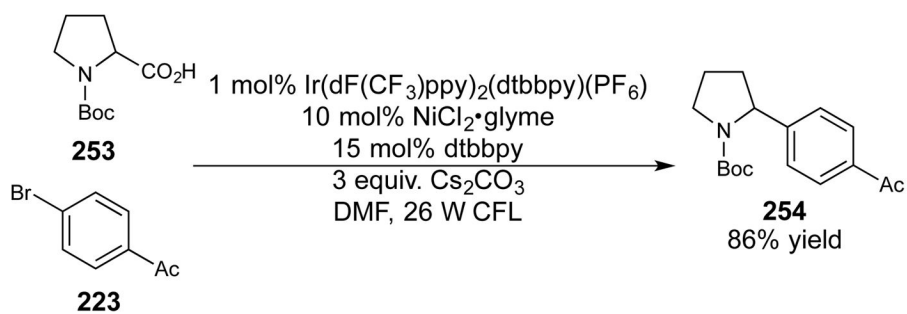
**Scheme 63.**  
Tandem Gold/Photocatalyzed Cyclization/Arylation Reaction



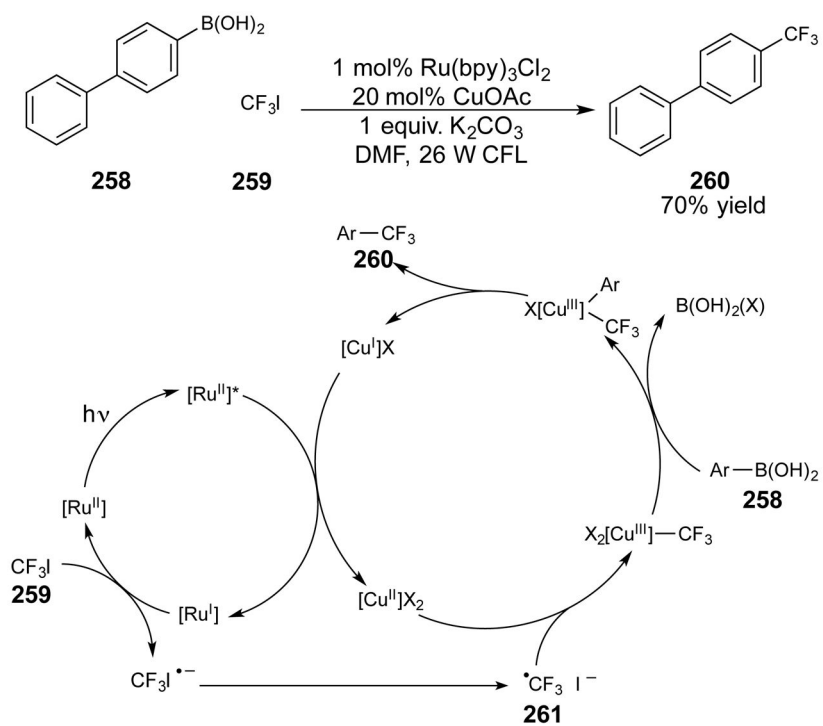
**Scheme 64.**  
Tandem Gold/Photocatalyzed Alkene Functionalization



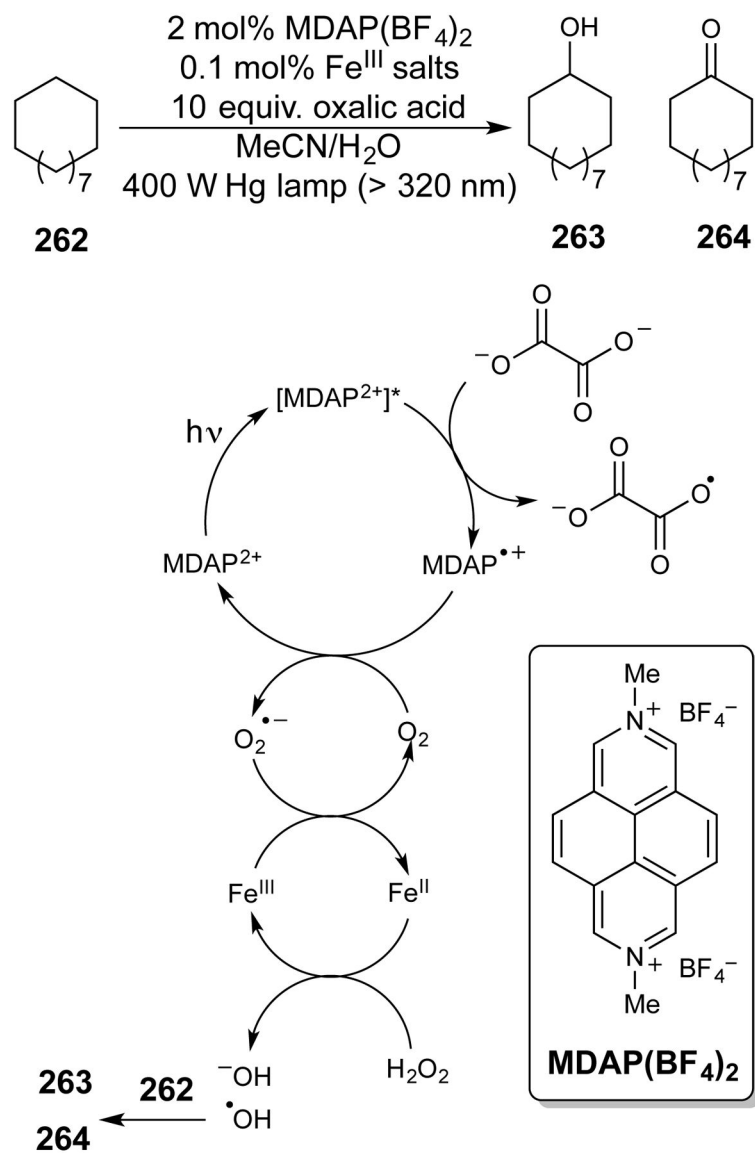
**Scheme 65.**  
Nickel Catalyzed Cross-Coupling Employing Photocatalytically Generated Benzylic Radicals



**Scheme 66.**  
Nickel-Catalyzed Cross Coupling using Photocatalytic Decarboxylation to Generate α-Amino Radicals

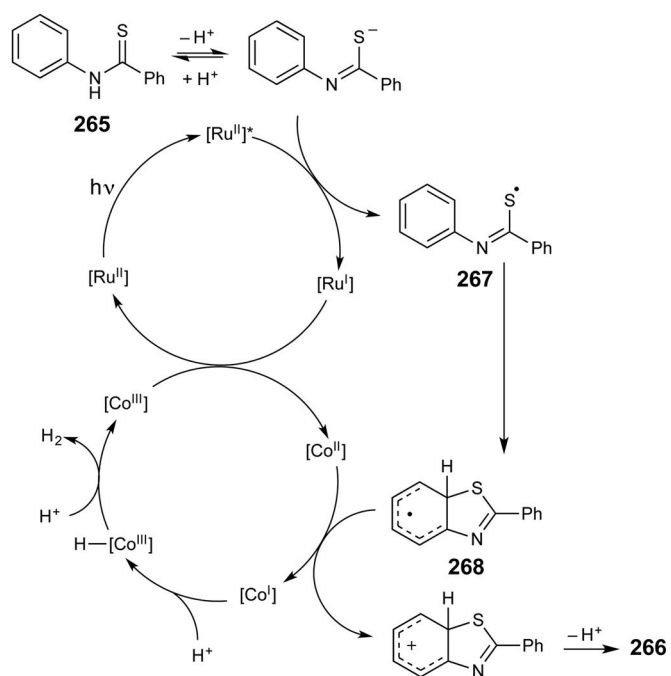
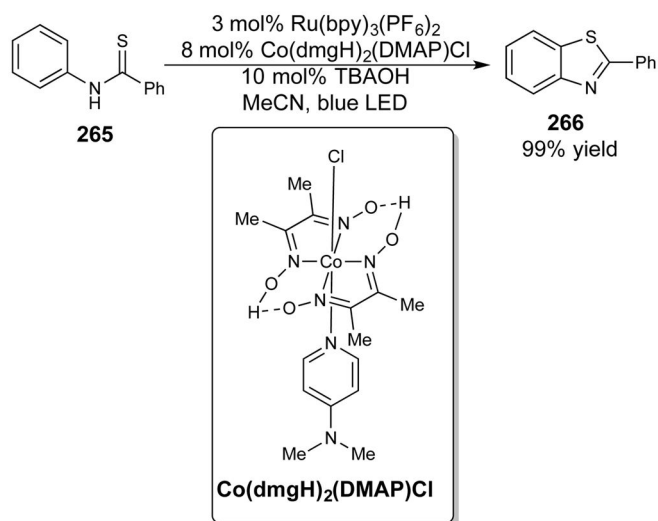


**Scheme 67.**  
Aryl Trifluoromethylation using Tandem Copper/Photocatalysis

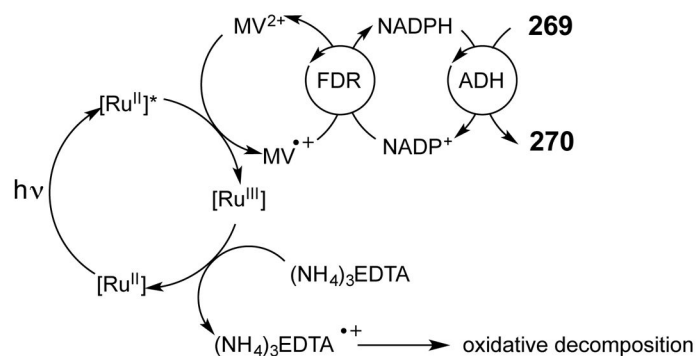
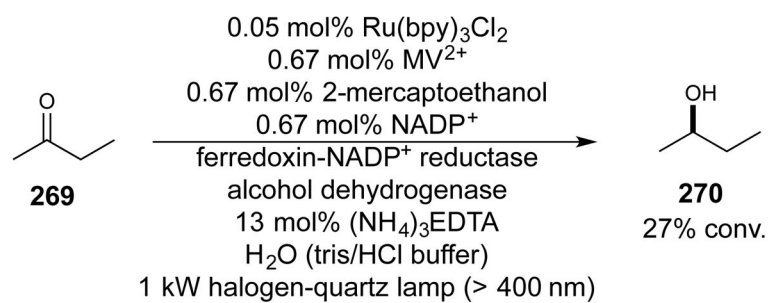


**Scheme 68.**  
Alkane Oxidation by Photogenerated Hydroxyl Radical

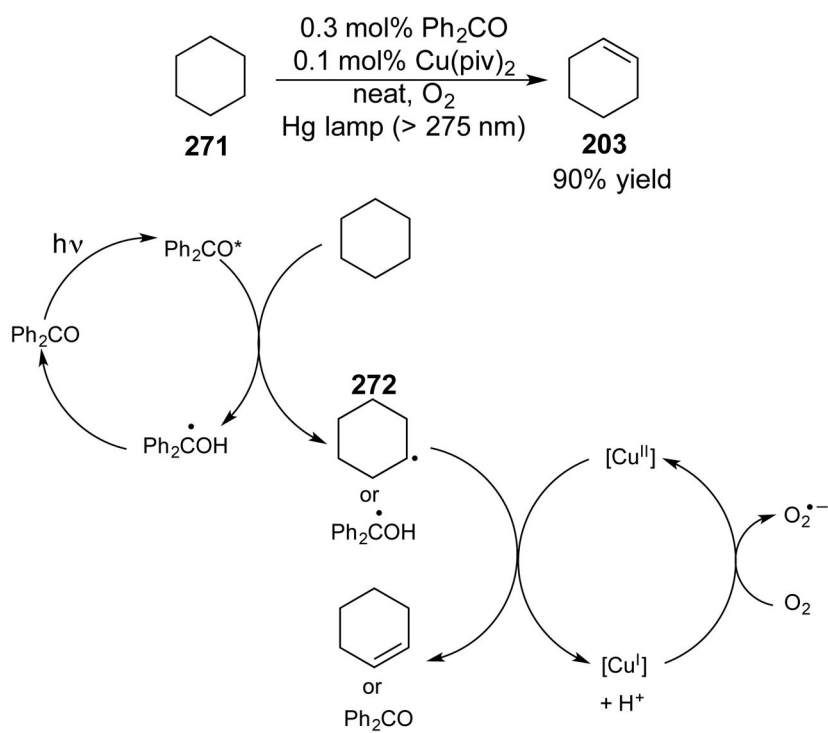




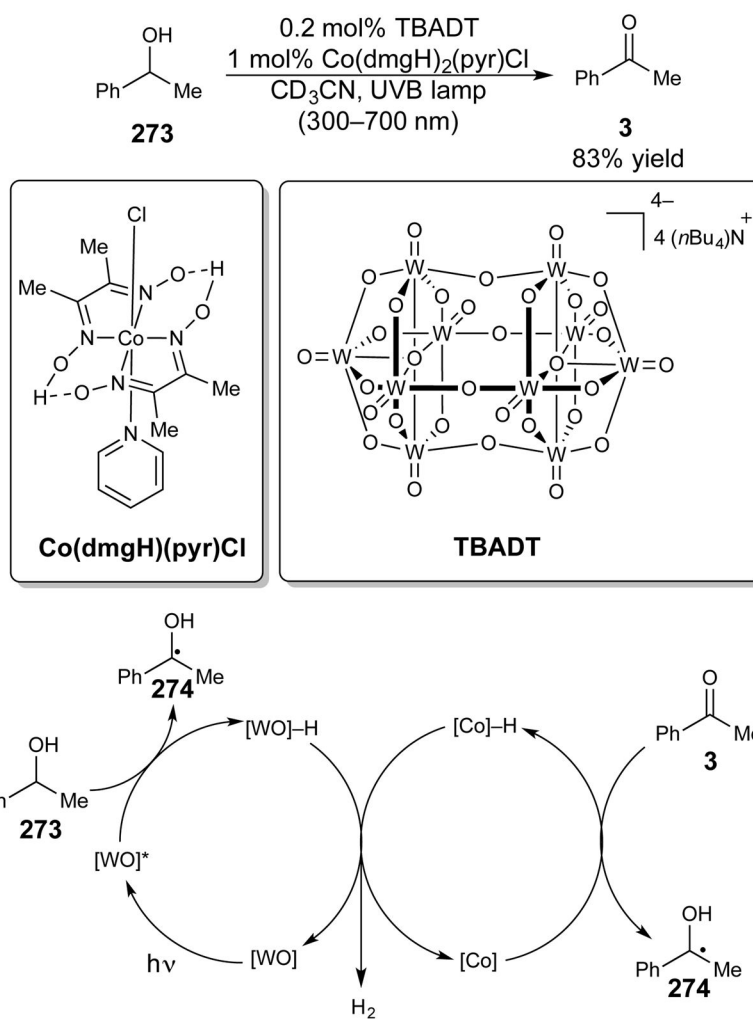
**Scheme 69.**  
Dehydrogenative Cross Coupling using both Cobalt and Photocatalysis



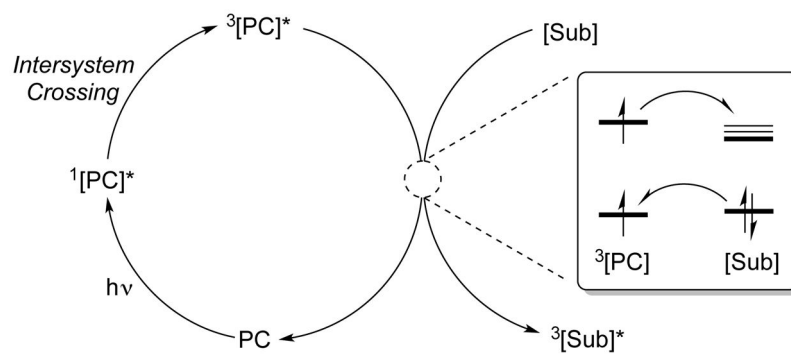
**Scheme 70.**  
Enzymatic/Photocatalytic Ketone Reduction



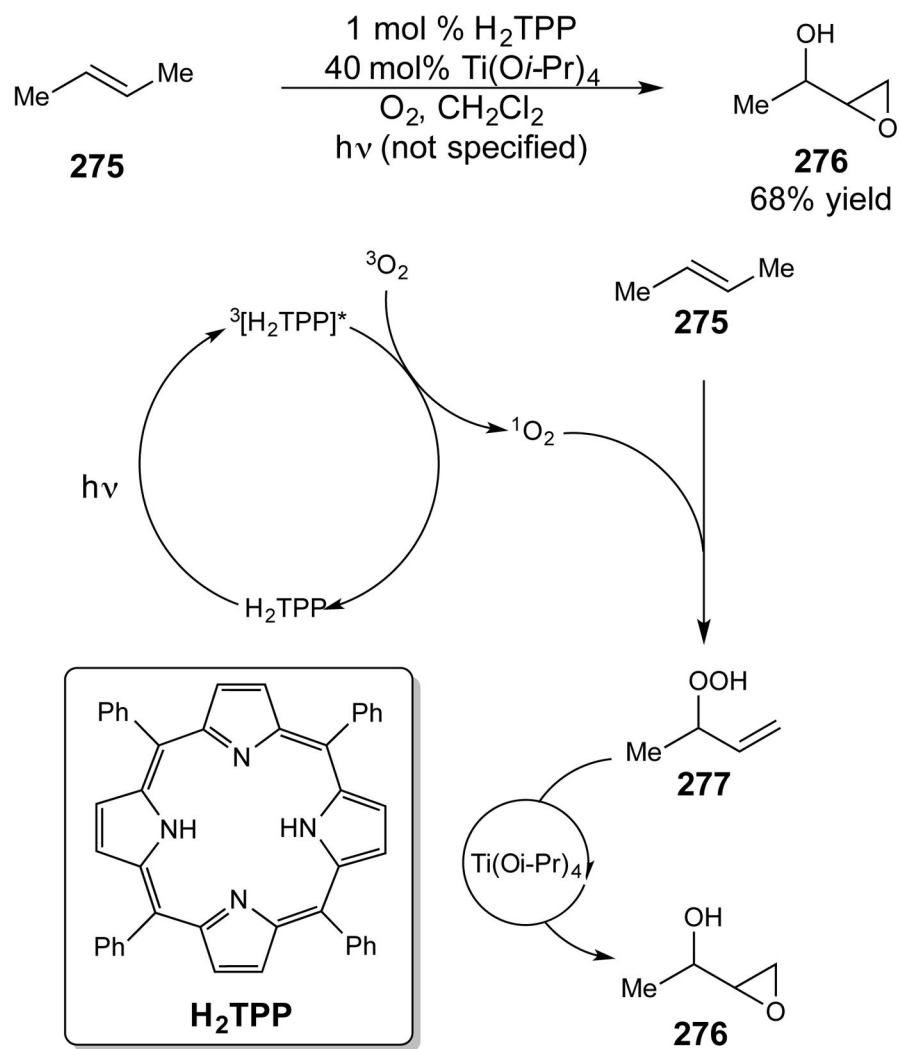
**Scheme 71.**  
Benzophenone/Copper Tandem Catalysis for Alkane Dehydrogenation



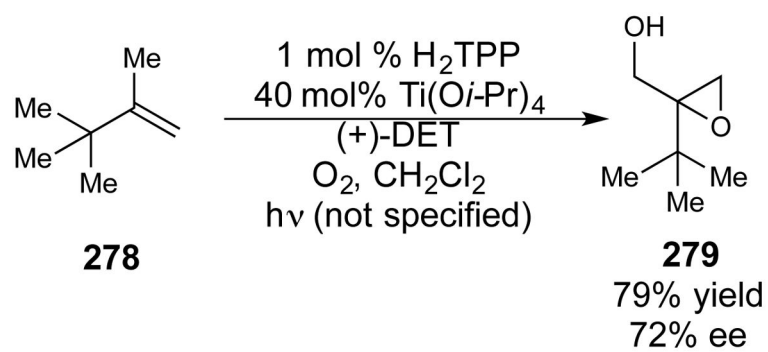
**Scheme 72.**  
Alcohol Dehydrogenation by Tandem Polyoxotungstate and Cobaloxime Catalysis



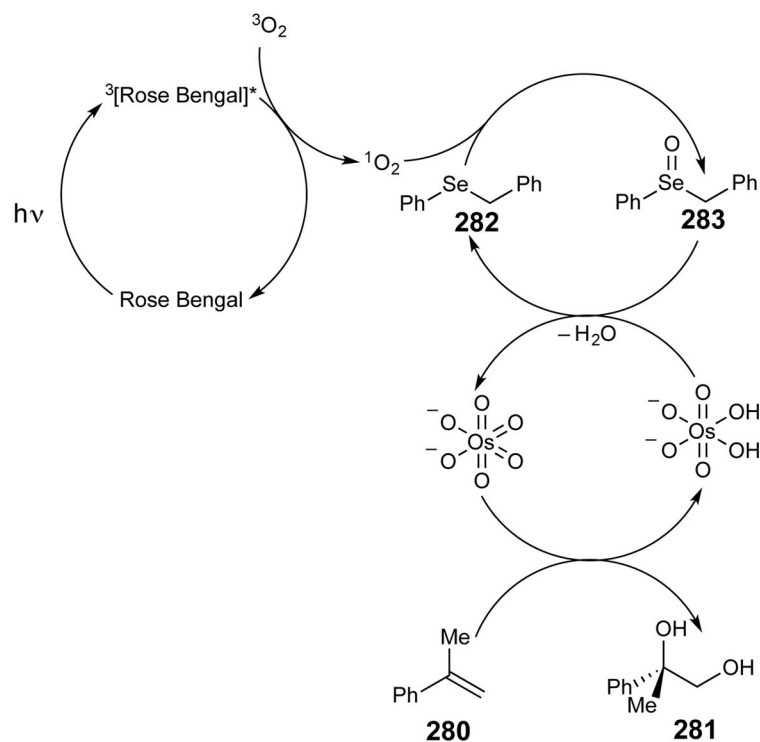
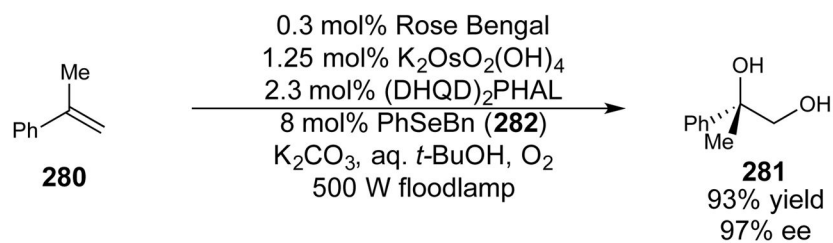
**Scheme 73.**  
The Dexter Mechanism for Triplet Energy Transfer



**Scheme 74.**  
Tandem Allylic Oxidation and Alkene Epoxidation

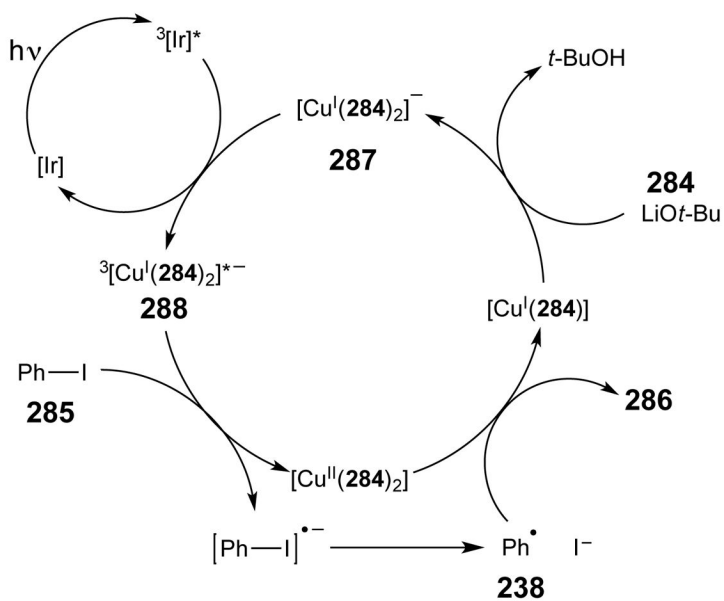
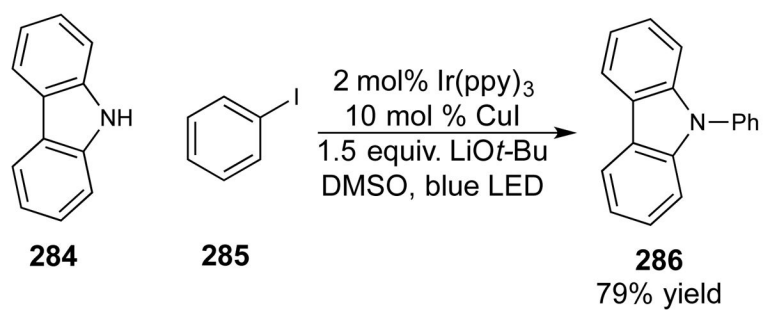
**Scheme 75.**

Asymmetric Epoxidation Applied in Dual Photo/Transition Metal Catalysis

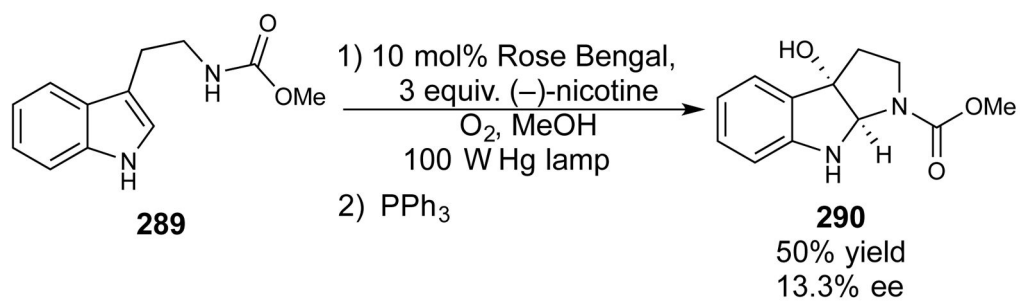


**Scheme 76.**  
Aerobic Alkene Dihydroxylation via Photocatalytic Generation of Selenoxides

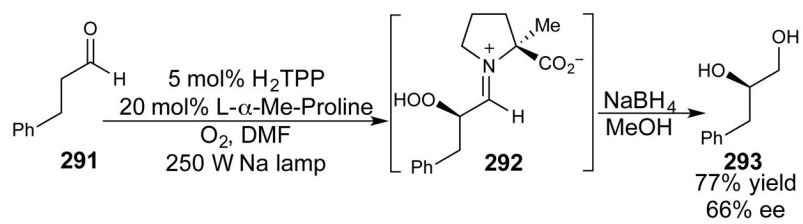




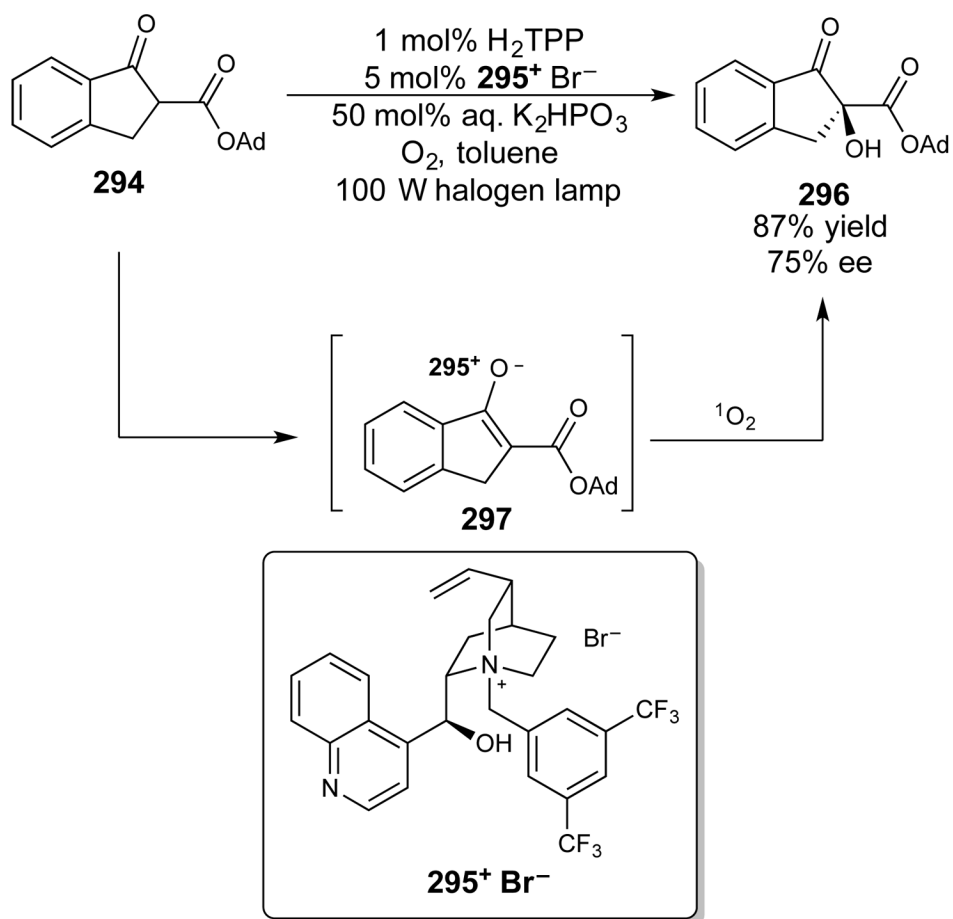
**Scheme 77.**  
Ullmann-Type Coupling using Ir/Cu Dual Catalysis



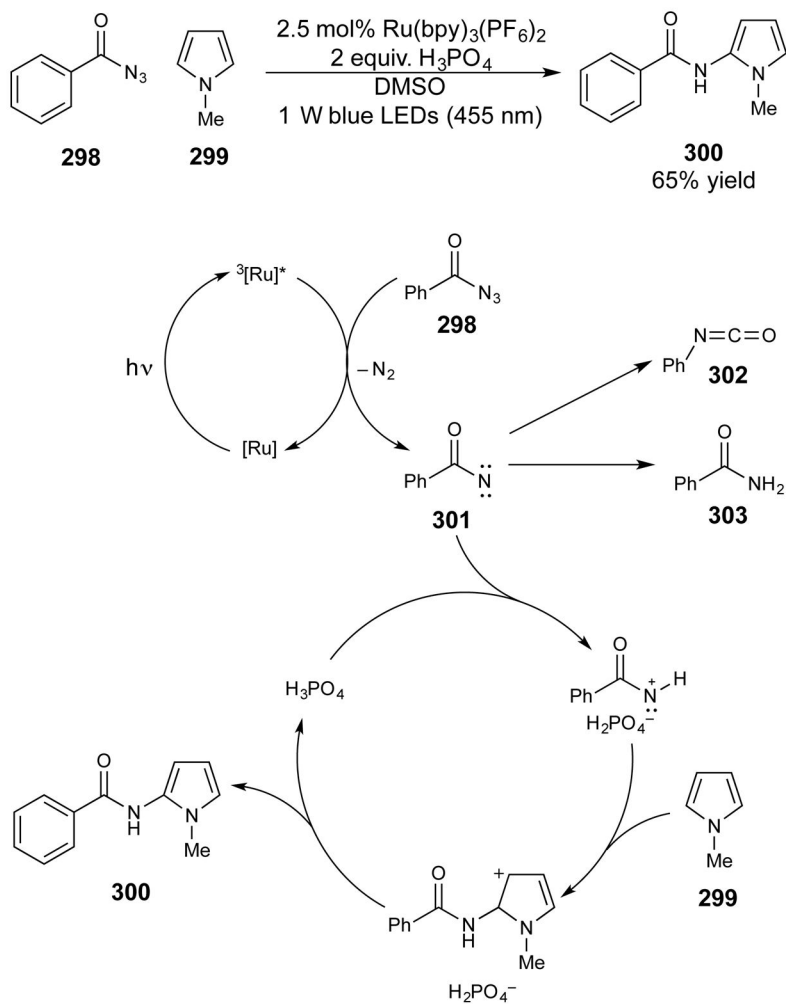
**Scheme 78.**  
Enantioselective photooxygenation of tryptamine



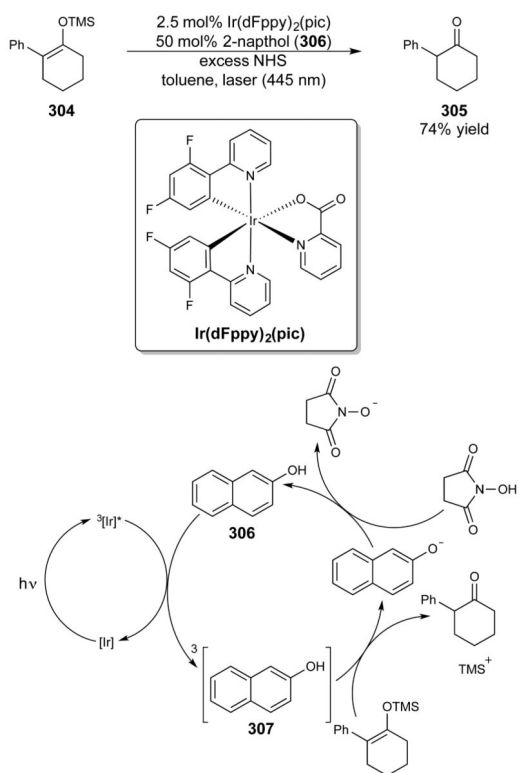
**Scheme 79.**  
Aldehyde  $\alpha$ -Oxygenation by Dual Enamine and Photocatalysis



**Scheme 80.**  
Asymmetric Phase Transfer Co-Catalysis Applied to Photochemical Enolate Oxidation



**Scheme 81.**  
Arene C-H Amination using Triplet Energy Transfer and Brønsted Acid Co-Catalysis



**Scheme 82.**  
Silyl Enol Ether Protonation by Photosensitized Naphthol